UNIVERSITY OF CALIFORNIA
RIVERSIDE

Cortical Processing of Frequency Modulated Sweeps in a Mouse Model of Presbycusis

A Dissertation submitted in partial satisfaction
of the requirements for the degree of

Doctor of Philosophy

in

Neuroscience

by

Michael Scott Trujillo

September 2012

Dissertation Committee:
Dr. Khaleel A. Razak, Chairperson
Dr. Kelly J. Huffman
Dr. Peter W. Hickmott

The Dissertation of Michael Scott Trujillo is approved:

_____

_____

_____

Committee Chairperson

University of California, Riverside

Acknowledgements

I would like to acknowledge my committee for their guidance over the past five years. My success is a tribute to their support and encouragement. Dr. Hickmott and Dr. Huffman, I thank you. I would also like to acknowledge my advisor, Dr. Khaleel Razak, who I consider not only a mentor, but a friend. Thank you Khaleel.

I would also like to thank my parents, James Trujillo and Karyn Thompson. My position in the world is a tribute to their excellent parenting, which continues even to today. Also I acknowledge my wonderful Suegra, Ilean Baltodano. Gracias por toda su ayuda y apoyo!

To my sons Nicolas Ernesto Trujillo and Nathaniel James Trujillo: I thank you both for the inspiration you have provided me. A father cannot ask for better sons. I love you both and write this dissertation for you.

Most importantly, I dedicate this dissertation to my loving wife, Lilette Baltodano. We have been together for 14 years and she has been the biggest supporter of my life. I literally would not have gone this far in my education without her. Throughout my pursuit of this PhD, she has made countless sacrifices that I will never forget. The completion of my dissertation would not have been possible without her love and support. Lilette: You are the greatest wife a man can have. I love you and thank you for your support, encouragement, and sacrifice!

ABSTRACT OF DISSERTATION

Cortical Processing of Frequency Modulated Sweeps in a Mouse Model of Presbycusis

by

Michael Scott Trujillo

Doctor of Philosophy, Graduate Program in Neuroscience
University of California, Riverside, September 2012
Dr. Khaleel Razak, Chairperson

The percentage of humans older than 65 years is rapidly increasing. Presbycusis (age-related hearing loss) is one of the most prevalent age-related disabilities and can impair speech recognition and social-emotional health. Deficits in auditory processing are likely caused by an interaction between changes in the way the brain processes sound and peripheral sensory hearing loss. The purpose of this dissertation was to analyze auditory cortical processing in a mouse model that undergoes hearing loss with age. The focus was on cortical processing frequency modulated (FM) sweeps.

This C57bl/6 mouse undergoes predictable high frequency hearing loss starting ~3 months of age and continuing to profound hearing loss by 12. Three experiments were performed. First, FM sweep response properties were analyzed in the young (1-3 mo old) adult auditory cortex. The main findings of this experiment indicate that the young adult mouse auditory cortex is selective for a narrow range of FM sweep rates (between 0.5 and 3 kHz/msec) and this selectivity is depth-dependent. The second experiment explored the mechanisms that shape FM sweep rate selectivity in young mouse cortex. The main findings of the second experiment were that two mechanisms shape FM sweep rate selectivity in the mouse cortex: duration tuning and sideband inhibition. Sideband

inhibition is the dominant mechanism, shaping FM sweep rate selectivity in approximately 88% of neurons tested. Duration tuning shaped FM sweep rate selectivity in approximately 34% of neurons tested. The third experiment compared direction selectivity, FM rate selectivity, variability, and mechanisms between three age groups, young (1 – 3 months), middle (6-8 months), and old (14 – 20 months). The main findings of the third experiment were that presbycusis resulted in decreased FM selectivity, slowed FM rate selectivity, increased variability and decreased sideband inhibition. Together, these studies establish mechanisms of spectrotemporal processing in a model system which is amenable to genetic manipulation to address relative contributions of genetics and experience-dependent factors in auditory processing. Future studies should compare the results obtained in the presbycusis model with mice strains that do not undergo age-related hearing loss to disambiguate relative contributions of age and hearing loss.

TABLE OF CONTENTS

LIST OF TABLES

LIST OF FIGURES

LIST OF ABBREVIATIONS

A1: Primary auditory cortex

AAF: Anterior auditory field

AP: All-pass selectivity

BR: Best Rate

BP: Band-pass selectivity

C57: C57/bl6 strain of mouse

CF: Characteristic frequency

DFM: Downward sweeping FM sweep

DSI: Direction Selectivity Index

FP: Fast-pass selectivity

HFI: High frequency inhibition

RTI: Rate Tuning Index

SP: Slow-pass selectivity

Chapter 1 - Introduction

As of the year 2005, there were more than 36 million people living in the United States over the age of 65 (He et al. 2005). By U.S. Census Bureau projections, the population over 65 will nearly double in the U.S. and more than double worldwide to 974 million people by 2030. These projections support the notion that the world population is getting older, a fact supported by a prediction that nearly half of the babies born in developed countries after 2009 will live beyond 100 years (Christensen et al. 2009). Aging is associated with cognitive deficits such as progressively degraded ability to understand speech and language. Theories of senescence-related cognitive deficits have existed for nearly a century (Pearl 1928). More recently, the 'speed of processing' and 'noisy processing' theories have been posited (Mahncke et al. 2006a; Mahncke et al. 2006b; Salthouse 1996). Both theories operate on the tenet that age-related deficits in sensory processing underlie deficits in cognitive function. The 'noisy processing' hypothesis posits that weakened, unreliable, and low-fidelity sensory processing impairs cognitive function due to the difficulty in performing cognitive operations on a degraded sensory signal (Mahncke et al. 2006a; Mahncke et al. 2006b). The 'speed of processing' hypothesis posits that a reduction in the speed at which cognitive processing can be carried out impairs an individual's ability to perform cognitive operations (Salthouse 1996).

Impairments in speech comprehension may be due to physiological changes in the brain that decreases the fidelity and speed at which the speech signal is processed. Compounding degradations in central sound processing is sensory degradation at the level of the cochlea (peripheral hearing loss) where the stereocilia that transduce the mechanical energy of sound into electrical neural impulses are lost as a function of age.

1.1 Presbycusis

Age-related hearing impairment is given the term presbycusis (Greek for presbys "elder" + akousis "hearing") and accounts for approximately 80% of all cases of hearing impairment (Davis 1990). Furthermore, 40% of the population over the age of 65 suffers from presbycusis (Ries 1994). While the effects of hearing impairment on speech processing is undoubtedly due to an interaction between changes in the cochlea and changes in the brain, the relative contribution of the cochlea and the brain is contentious (for review see (Gates and Mills 2005). The contentious issue centers on how the types of presbycusis affect central processing of sound. At least four types of presbycusis exist: sensory, neural, metabolic, mechanical and central (Gates and Mills 2005; Schmiedt 2010; Schuknecht 1974). Sensory presbycusis is characterized by the loss of cochlear hair cells and/or supporting cells of the cochlea. Neural presbycusis is characterized by a loss of neurons that innervate the cochlea. Metabolic presbycusis, also known as strial presbycusis, is characterized by atrophy of the stria vascularis, the tissue that contributes to the maintenance of the endocochlear potential. Mechanical presbycusis is characterized by either a stiffening of the basilar membrane and organ of Corti or

stiffening in the ossicles within the inner ear. While Schoknecht (1974) described sensory, neural, metabolic and mechanical presbycusis, central presbycusis was described by (Welsh et al. 1985). Central presbycusis accounts for changes in auditory processing that occur independently of cochlear function and are characterized by age-related deficits in binaural, temporal, and speech and language processing.

Central presbycusis then can be thought of as any age-related impairment in auditory processing. Numerous cognitive auditory processing impairments associated with age. For example, older adults are impaired in discriminating between frequencies and intensities of pure tones (He et al. 1998). More specifically, He at al. (1998) demonstrated an age-related deficit in frequency and intensity discrimination of tonal stimuli where even the deficits in intensity discrimination were frequency dependent. In studies of the aging auditory system, it is difficult to disambiguate peripheral changes (i.e. cochlear hair cell loss) from central changes (i.e. slowed speed or noisy processing). There are two intriguing findings of the He at al. (1998) study. The first was that the aged population in that study had matched audiograms compared to the young subjects. In other words the aged subjects did not, by definition, have sensory presbycusis. The second was that frequency dependent age-related differences were most prominent at low frequencies, with the largest effects seen at 500 Hz. This effect was intriguing because age-related auditory deficits typically occur at higher frequencies, i.e. 8 kHz – 20 kHz (Schuknecht 1974). The fact that age-related deficits are found at lower frequencies in participants who do not have peripheral hearing loss indicates that changes can occur in the brain independent of peripheral sensory changes. Furthermore, high frequency

hearing loss can impact temporal processing in low-frequency channels (Leigh-Paffenroth and Elangovan 2011). Therefore, central auditory processing can change independent of hearing loss, but hearing loss can also have non-specific impacts on auditory processing. This is relevant to this dissertation because the mouse model being explored experiences high frequency hearing loss. While we can establish baseline measures in this mouse model, the changes observed with age may be due to changes independent of hearing loss and/or off-hearing loss channel alterations in auditory processing.

1.2 Age-related changes in auditory perception

Whereas pure tone stimuli are good psychophysical probes for exploring auditory perception, pure tones are rarely encountered in the natural world. Animal vocalizations, including human speech, consist of a spectrotemporal time series that have dynamic changes in frequency. Frequency modulated (FM) sweeps are sounds that change in frequency over time. While human speech and conspecific vocalizations are ideal stimuli to assess auditory processing, FM sweeps provide a context-neutral stimulus to assess auditory perception. FM sweeps have advantages over pure tone stimuli because FM sweeps can be modulated to resemble the rate/direction of frequency changes seen in biologically relevant sounds.

Similar to frequency discrimination, FM detection is also impaired with age and is more profound for a low-frequency carrier frequency (500 Hz) compared to a higher carrier frequency (4 kHz) (He et al. 2007). Again, these deficits were seen in

audiometric-matched aged participants indicating that they did not have hearing loss. Speech understanding degrades as well (Gordon-Salant 2005; Griffiths et al. 1999; Martin and Jerger 2005; Schneider et al. 2002). More specifically, it was reported that age-related deficits in processing of rapid frequency changes in consonants impairs speech processing in older adults, an effect that is compounded by high-frequency hearing loss (Gordon-Salant and Fitzgibbons 2001). At the most fundamental level, speech signals are comprised of a series of rapid transition in frequencies (known as formant transitions) that occur in a specific patterned sequence. There is some indication that peripheral hearing loss degrades a person's ability to extract information from the temporal fine structure, in other words the rapid frequency changes of the speech signal (Moore et al. 2006). Elderly participants have also been shown to perform significantly worse than younger participants in discriminating vowel sounds (Coughlin et al. 1998), confusable speeded word comparisons such as 'DISH-DITCH and 'BEAT-WHEAT' (Gordon-Salant et al. 2006), and identifying tones in a three-tone sequences (Fitzgibbons and Gordon-Salant 2001). Collectively, the literature indicates that speech processing degrades with age, that the degradation in speech processing are likely due to temporal processing deficits, deficits can exist independent of peripheral hearing loss but high frequency hearing loss can exacerbate the consequence of aging.

Two factors make it nearly impossible to disambiguate contributions of central and peripheral hearing loss to age-related auditory processing in humans. The first is that it is unknown how peripheral presbycusis influences central processing of sound. The second is that it is difficult to determine how the physiological response properties in the

brain change with age independent of cochlear hair cell loss. Attempts have been made to tease out hearing loss from aging in psychophysical studies where discrimination performance is compared between hearing impaired and normal hearing adults (Coughlin et al. 1998; Gordon-Salant and Fitzgibbons 2001; Gordon-Salant et al. 2006). These studies are simply descriptive in nature: the mechanisms are unclear. In addition, the cause of hearing loss is not known in the human studies, and some could be genetic and others could experience-induced. Rodent studies have compared the C57 and CBA mouse models and Fischer and Long Evans rat strains (Ouda et al. 2008; Popelar et al. 2006; Spongr et al. 1997; Walton et al. 2008; Walton et al. 1995; Willott et al. 1991). In these studies, the CBA and Long Evans are strains that do not undergo hearing loss with age, but the other two do. These studies are confounded by using different genetic strains, and also suffer from examining very basic processing such as spectral or temporal selectivity. To begin to tease out the effects of peripheral presbycusis of central processing of sound, this dissertation established baseline spectrotemporal response properties in a mouse model of presbycusis at three age groups. The young age group consisted of 1-3 month old mice, a middle age-group consisted of a 6-8 month age group and an old age group consisted of a 14 – 20 month old age group.

1.3 Mouse model of presbycusis

The mouse strain C57bl/6 (C57) is a mouse model of presbycusis that undergoes high frequency hearing loss starting ~3 months of age and continuing to profound hearing loss by 12 months of age (Spongr et al. 1997; Willott et al. 1993; Willott et al. 1991).

There is a progressive loss of both inner hair cells (IHC) and outer hair cells (OHC) of the cochlea (Spongr et al. 1997). The loss of OHC correlates with a frequency-dependent increase in hearing thresholds (Francis et al. 2003). The relative spectral pattern of loss is similar to presbycusis in humans. There is also a reorganization of the tonotopic map of the core auditory cortex where tonotopy reflects the frequency-dependent spectral pattern of hair cell loss (Willott et al. 1993). The core auditory cortex is defined as the primary auditory cortex (A1) and the anterior auditory field (AAF) (Cruikshank et al. 2001).

The C57 mouse has been used in a variety of studies in presbycusis. Typically, the C57 mouse is compared to a mouse strain that maintains robust hearing late into life such as the CBA/caj (CBA) mouse. For example, tuning curves and thresholds of inferior colliculus neurons have been compared between the C57 and CBA strains (Willott et al. 1991). High-frequency inferior colliculus neurons in the aged C57 mouse had higher tone thresholds than the CBA strain, a result present by 6 months of age, suggesting that the hair cell loss that is seen by 6 months (Spongr et al. 1997) results in loss of sensitivity of midbrain auditory neurons. A reorganization of the tonotopic map of the auditory cortex has also been compared between the C57 and CBA strains (Willott et al. 1993). In the young (<3 months) C57 and CBA, there is a tonotopic gradient in the core auditory cortex where characteristic frequency increases in the caudal to rostral extent of A1 and a reversed tonotopy is present in AAF where characteristic frequency decreases caudally to rostrally. Similar to what is seen in the inferior colliculus, by middle age (around 6 months), the tonotopic map of the C57 strain becomes reorganized and is dominated by 12-18 kHz by 12 months of age. Behaviorally, the C57 strain exhibited an enhanced

startle response to low and mid frequency sounds with age while the CBA showed no change, suggesting that central nervous system changes may correlate with behavioral changes to sound evoked startle (Willott et al. 1994).

The cause of the peripheral presbycusis in the C57 strain is a mutation in two genes, the Cdh23 gene and the Sod1 gene (Johnson et al. 2010). The Cdh23 gene codes for the protein cadherin 23 which binds the stereocilia together at the tip links (Kazmierczak et al. 2007). The Sod1 gene codes for the enzyme superoxide dismutase, an important antioxidant that eliminates superoxide radicals from cells. Collectively, these two mutations make the C57 strain susceptible to cochlear hair cell death because of weakened integrity of hair cell bundles and the inability to recover from damage, both mechanical and from free radicals. This mouse strain is a good model for presbycusis due to the known etiology, behavioral manifestation, and predictable time course of peripheral hearing loss.

1.4 Age-related changes in FM sweep processing

In this dissertation, I explore the cortical processing of FM sweeps in the C57 strain mouse. Animal vocalizations consist of upward (increasing in frequency) and downward (decreasing in frequency) FM sweeps with various rates of frequency change (FM sweep rate). FM sweeps are a vital component for discrimination of speech sounds (Stevens and Klatt 1974; Zeng et al. 2005). Aging humans have deficits in identifying and discriminating FM sweeps (He et al. 2007; Moore et al. 2006). Age-related changes in FM processing are seen in the Long Evans rat auditory cortex (Mendelson and Ricketts

2001). Mendelson and Ricketts (2001) reported that young rat cortical neurons responded best to fast FM sweep rates but neurons in the aged rat responded better to the slow FM sweep rates than to fast and medium rates. A comparative analysis of FM sweep rate selectivity with the medial geniculate body of the thalamus and the inferior colliculus indicated that the preference for slower sweep rate was limited to the cortex as no age-related changes were observed subcortically (Mendelson and Lui 2004). These results indicate that age-related changes in FM sweep processing may be a result of changes that occur at the level of the cortex. However, those studies were limited in that they only assessed 3 FM sweep rates, did not attempt to quantify FM sweep rate selectivity, and only assessed young and old rats. More importantly, mechanisms were not studied. Age-related decreases have been reported in parvalbumin containing fast-spiking inhibitory interneurons in the cortex of Fischer 344 rats (Ouda et al. 2008), but not in the inferior colliculus, consistent with the notion that cortex-specific deficits may be present in aging. Collectively, these results indicate that FM sweep rate selectivity and inhibition decrease at the level of the cortex, which provides the rationale for studying FM sweep processing at the level of the cortex in the C57 mouse.

1.6 Mechanisms of FM Rate Selectivity

The relationship between FM sweep rate selectivity and inhibition becomes clear when taking into consideration the contributions of inhibition in shaping FM sweep rate and direction selectivity. The mechanisms that shape FM rate and direction selectivity has been extensively investigated in the pallid bat (Fuzessery et al. 2011; Fuzessery et al.

2006; Razak and Pallas 2005). At least three mechanisms have been shown to shape FM rate selectivity in the bat auditory cortex, with two of the mechanisms relying on a balance between excitation and inhibition (Gordon and O'Neill 1998; Razak and Fuzessery 2008; 2006). The first mechanism, proposed by Suga (1965) suggested that FM sweep selectivity depends on spectrotemporal interactions between excitatory frequencies and sideband inhibition. The second mechanism is duration tuning for tones (Fuzessery et al. 2006). Duration tuning for tones is present in the auditory system across all vertebrate taxa (Brand et al. 2000; Casseday et al. 1994; Ehrlich et al. 1997; Feng et al. 1990; Gooler and Feng 1992). The third mechanism of FM rate selectivity depends on non-linear facilitation. In this mechanism neurons respond poorly to single tones, but show combination sensitive facilitation when two tones are played with a certain delay (Fuzessery et al. 2011; Mittmann and Wenstrup 1995; Razak and Fuzessery 2008; Sadagopan and Wang 2009).

Both duration tuning and sideband inhibition are shaped by an interaction between excitation and inhibition. Two mechanisms have been proposed to explain duration tuning for short duration tones (Casseday et al. 1994; Fuzessery and Hall 1999). The first mechanism, known as the coincidence model posits that three components shape selectivity for short duration tones. The first component is an inhibitory input of short latency that results in an IPSP that lasts the duration of the sound. The second component is a delayed EPSP that is generated by stimulus onset. The third component is that the rebound from inhibition must coincide with the EPSP so that a summation can occur and elicit a response (Casseday et al. 1994). The second mechanism, known as the anti-

coincidence model posits that early inhibition does not contribute to excitation. Conversely, a delayed inhibition lasts the duration of the sound, or at least longer than the EPSP from the excitatory input. The excitatory input arrives later than the early inhibition but has a fixed time course. If the EPSP occurs during the IPSP, they cancel each other out and response to the sound is reduced or eliminated. If the sound duration is short, the IPSP is over before the EPSP arrives to the neuron and a response is elicited. The contribution of inhibition to duration tuning for tones was confirmed by iontophoretic application of bicuculline in the IC of the pallid bat (Fuzessery and Hall 1999). Regardless of the mechanism by which duration tuning is created for tones, it underlies a mechanism that can shape selectivity to FM sweep rate. The FM sweep rate in which the excitatory band spends the same amount as the tone duration that promotes optimal response will elicit the best response for FM sweep rates. For slower FM sweep rates, the amount of time spent in the excitatory bandwidth resembles long tone durations and response would be decreased.

While duration tuned neurons are prevalent in subcortical regions such as the echolocating bat IC (Fuzessery and Hall 1999; Gittelman and Pollak 2011), duration tuning is sparse cortex of the pallid bat (Razak and Fuzessery 2006). Conversely, sideband inhibition is the dominant mechanism in the pallid bat cortex (Razak and Fuzessery 2006), similar to what is reported in the current study. The mechanism governing sideband inhibition was first proposed by Suga (1965) and subsequently supported by Gordon & O'Niell (1998) and Razak & Fuzzessery (2006). For sideband inhibition, either low frequency or high frequency, FM sweeps transverse the inhibitory

sidebands (assuming appropriate direction) prior to traversing the excitatory band. In this mechanism, inhibition is slower to arrive to the neuron then excitation. For fast FM sweep rates, the excitation arrives and elicits a neural response prior to the arrival of inhibition. For slow FM sweep rates, sideband inhibition, which was encountered first, is advantaged in that the excitatory band is delayed. Thus for slow sweep rates, the delayed onset inhibition is able to reach the neuron before the excitation and thus suppressing the response. It is unknown whether the mechanisms shaping FM sweep rate selectivity is a general physiological principle in all animals or if it is limited to echolocating bats that require precise timing in processing their echolocation call. Furthermore, it is unknown if these mechanisms change in presbycusis.

1.7 Hypothesis and predictions

If inhibition shapes FM sweep rate selectivity and inhibition decreases with age, then FM sweep rate selectivity should concomitantly decrease. Indeed it has been shown in the visual cortex of macaque monkeys that iontophoretic application of GABA or muscimol (a GABAa receptor agonist) reversed age-related deficits in orientation and direction selectivity (Leventhal et al. 2003). These results indicate that the loss of cortical selectivity for sensory stimuli with age is likely due to a loss of inhibitory processes.

I propose that the loss of sensory input caused by presbycusis in the C57 mouse will decrease FM sweep rate selectivity by 6 months of age when presbycusis begins to become severe. The decrease in FM sweep rate selectivity will likely be attributed to loss of high frequency inhibitory processes. The reduction in inhibitory processes may be due to decreases in parvalbumin neurons as reported in Ouda et al. (2008) or a reduced drive

to inhibitory neurons due to lack of excitation from high frequency channels in the cochlea. Due to a decrease in inhibition, FM rate selectivity is predicted to change.

Chapter 2: Selectivity for the rate of frequency modulated sweeps in the mouse auditory cortex

The majority of this chapter was published in the Journal of Neurophysiology:

Trujillo M, Measor K, Carrasco MM, and Razak KA. Selectivity for the rate of frequency-modulated sweeps in the mouse auditory cortex. *J Neurophysiol* 106: 2825-2837, 2011.

Kevin Measor provided data for two figures in the publication. His figures, methods and aims are excluded from this chapter. The remainder of this chapter is as published in Journal of Neurophysiology.

Abstract

Frequency modulated (FM) sweeps are common components of vocalizations, including human speech. Both sweep direction and rate influence discrimination of vocalizations. Across species, relatively less is known about FM rate selectivity compared to direction selectivity. Here, FM rate selectivity was studied in the auditory cortex of anesthetized 1-3 month old C57Bl/6 mouse. Neurons were classified as fast-pass, band-pass, slow-pass or all-pass depending on their selectivity for rates between 0.08–20 kHz/msec. Single unit recording (n=223) from A1 and AAF show that the mouse auditory cortex is best poised to detect and discriminate a narrow range of sweep rates between 0.5-3 kHz/msec. Based on recordings obtained at different depths, neurons in the infragranular layers were less rate selective than neurons in the granular layers suggesting FM processing undergoes changes within the cortical column. On average, there was very little direction selectivity in the mouse auditory cortex. There was also no

correlation between characteristic frequency and direction selectivity. The narrow range of rate selectivity in the mouse cortex indicates that FM rate processing is a useful physiological marker for studying contributions of genetic and environmental factors in auditory system development, aging and disease.

Introduction

Frequency modulated (FM) sweeps are common components of animal vocalizations, including human speech. FM sweeps are important in discrimination of speech sounds (Stevens and Klatt 1974; Zeng et al. 2005). Deficits in spectrotemporal processing can lead to speech perception impairments and cognitive training programs that utilize FM sweeps can alleviate some of these impairments (Merzenich et al. 1996; Smith et al. 2009). Presbycusis- or normal aging-related decline in speech processing may be related to a difficulty in processing rapid formant transitions present in consonants. This suggests that deficits in following frequency transitions may cause speech processing decline (Gordon-Salant and Fitzgibbons 2001). The auditory cortex of all species examined contains neurons sensitive to the rate and direction of FM sweeps (Atencio et al. 2007; Brown and Harrison 2009; Godey et al. 2005; Heil et al. 1992a; Nelken and Versnel 2000; Razak and Fuzessery 2006; Suga 1965; Tian and Rauschecker 2004). Furthermore, the mechanisms of FM sweep selectivity have been characterized in the auditory system (Fuzessery et al., 2006; Gittelman et al., 2009; Gordon and O'Neill, 1998; Razak and Fuzessery, 2006; 2008; 2009; Ye et al., 2010; Gittelman and Pollak,

2011). Collectively, these studies suggest that an analysis of FM sweep processing is a useful step in understanding representations of species-specific vocalizations.

The genetic engineering tools currently available make the mouse nervous system a suitable model to study neural dysfunctions caused by genetic disorders and to probe underlying mechanisms. In auditory system research, the mouse holds significant promise in elucidating the mechanisms underlying vocal communication disorders. To provide the foundation for investigating mechanisms of auditory processing dysfunctions, particularly in relation to spectrotemporally complex sounds, the main objective of this study was to determine selectivity for FM sweep in the auditory cortex of the mouse.

FM sweep selectivity has been studied in the mouse inferior colliculus (Hage and Ehret 2003), but not auditory cortex. A comparison of the two areas will provide information on how the representation of spectrotemporally dynamic sounds changes within the ascending auditory system. In mice and across species, relatively less is known about FM sweep rate selectivity compared to direction selectivity. Therefore the first goal of this study was to map FM rate selectivity in both primary auditory cortex (A1) and anterior auditory field (AAF) using a broad range of frequency sweep rates in the mouse (C57bl/6 strain) auditory cortex. Recent studies in the cat auditory cortex suggest that neurons in deeper cortical layers are less selective for stimulus features compared to the granular input layers suggesting hierarchical processing within the cortical column (Atencio et al., 2009; Atencio and Schreiner, 2010). The second aim of this study was to determine if there are cortical depth specific differences in FM rate selectivity in the mouse auditory cortex. The C57 strain of mice was chosen as it forms

the background for various knockout strains used as disease models. The data in this study will therefore serve as control for future investigations of FM sweep processing in transgenic mice.

Methods

The Institutional Animal Care and Use Committee at the University of California, Riverside approved all procedures. Mice (C57bl/6 strain) were obtained from an in-house breeding colony that originated from breeding pairs purchased from Jackson Laboratory (Bar Harbor, Maine). Mice were housed with 2-5 littermates under a 15/9 hour light dark cycle and fed ad libitum. These mice were studied before the onset of accelerated hearing loss (age <3 months).

Surgical procedures

Mice were anesthetized with an i.p. injection of ketamine (150 mg/kg) and xylazine (10 mg/kg) mixture and maintained throughout the experiment via either supplemental dosing with ketamine/xylazine or isoflurane inhalation (0.2–0.5% in air). Anesthetic state was monitored throughout the experiment using the toe-pinch reflex test and supplemental anesthetic was administered or isoflurane concentration was increased as needed. Once an areflexic state of anesthesia was reached, measured by a toe pinch, a scalp incision was made along the midline and the right temporalis muscle was reflexed. The skull was cleaned and then a craniotomy was performed using a dental drill. The auditory cortex was exposed based on skull and vascular landmarks identified in Willot et

al. (1993). Mice were euthanized at the end of the experimental day via an overdose of sodium pentobarbital (125mg/kg).

Acoustic Stimulation

Acoustic stimulation and data acquisition were driven by custom written software (Batlab, developed by Dr. Don Gans, Kent State University) and a Microstar digital signal processing board. Programmable attenuators (PA5, Tucker-Davis Technologies, Florida) allowed control of sound intensities before amplification by a stereo power amplifier (Parasound, HCA1100) or an integrated amplifier (Yamaha AX430). Sounds were delivered through a free field speaker (LCY-K100 ribbon tweeters, Madisound, Wisconsin) located 6 inches and 45° from the left ear, contralateral to physiological recordings. Frequency response of the sound delivery system was measured using a ¼ inch Bruel and Kjaer microphone and measuring amplifier and found to be flat within ± 3 dB for frequencies between 7-40 kHz. Frequencies 5 kHz and below were filtered out (Butterworth, 24dB/octave, Krohn-Hite).

Electrophysiology

Mice were placed in a stereotaxic apparatus (Kopf model 930, Tujunga, CA) and secured in a mouse bite bar adapter (Kopf model 923B, Tujunga, CA). Experiments were conducted in a heated (~80°F), sound-attenuated chamber lined with anechoic foam (Gretch-Ken Industries, Oregon). Electrophysiological recordings were obtained with glass electrodes filled with 1M NaCl (2-10 MΩ impedance). Electrodes were driven

orthogonally into the cortex (with a Kopf direct drive 2660 micropositioner). Single unit recordings were obtained between 100-700 μm depths. For depth measurements, the zero point was marked when the electrode first touches the surface of the cortex (determined by changes in recording trace and audio monitor output). The consistency of the zero point was also verified when the electrode was pulled out from a penetration. Single unit recordings were identified by the constancy of amplitude and waveform displayed on an oscilloscope programmed into the data acquisition software. Poststimulus time histograms were obtained relative to stimulus onset. Action potentials that occurred within 300 msec of stimulus onset were included in the poststimulus time histograms. The number of spikes that were elicited over 20 stimulus repetitions was used for quantification.

Data acquisition

The primary auditory cortex of the C57 mouse can be identified via vascular landmarks (Willott et al. 1991) and increasing characteristic frequencies (CF) in a caudal to rostral direction (Stiebler et al. 1997). The AAF is located immediately rostral to A1, and exhibits a CF reversal relative to A1. The focus of this study was to determine FM sweep selectivity in A1 and AAF. Other areas such as AII and ultrasonic field, while also present in young C57 mice (Willot et al., 1993; Bandyopadhyay et al., 2010) were not sampled. The excitatory tuning curve was determined by presenting pure tones varying in frequency and intensity. The tone duration used was optimized to maximize response to tones as neurons show duration selectivity (Razak, unpublished observations, Brand et

al., 2000). The range of durations used was between 2-50 msec (1 msec rise/fall time). The CF was defined as the frequency at which spikes were generated for at least 5 successive stimulus presentations at the lowest intensity (threshold). The excitatory tuning curve was determined by stepping frequency up and down between 5-50 kHz until no response was observed. After the low and high frequency edge at a given intensity was determined, intensity was decreased in 10 dB steps and the procedure repeated until threshold and CF were determined.

FM rate selectivity

The first step in determining rate selectivity was to present an FM sweep of fixed bandwidth at different durations. The sweep rate (in kHz/msec) of the stimulus was obtained by dividing the FM bandwidth (in kHz) by the duration (in msec). It is important to present sweeps that not only stimulate the excitatory frequencies, but also extend beyond the edges of the tuning curve because rate selectivity is at least partially shaped by inhibitory sidebands (Razak and Fuzessery, 2006). Rate selectivity of a neuron will be different for sweeps that include the sideband compared to sweeps that do not (Razak and Fuzessery, 2006). Therefore, FM sweep bandwidths were adapted according to the CF and tuning width. Once the excitatory tuning curve was obtained, linear FM sweeps centered approximately at CF were presented at 10-20 dB above threshold. The sweep bandwidths exceeded the bandwidth of the tuning curve at that intensity by at least 5 kHz. More typically, the sweeps extended outside the tuning curve by at least 10 kHz. Data from the pallid bat auditory cortex (Razak and Fuzessery, 2006) and unpublished

data from the C57 mouse cortex show that inhibitory sidebands, if present, typically abut the edges of the excitatory tuning curve. Thus our procedure of extending the sweeps outside the tuning curve will capture at least a part of the putative sidebands. FM rates between 0.08 – 20 kHz/msec were tested. These sweep rates were generated using bandwidths between 15 kHz (e.g., 20→5 kHz sweep) and 60 kHz (e.g., 65→5 kHz sweep) and durations between 3-200 msec.

Neurons were classified as all pass (AP), band pass (BP), fast pass (FP) or slow pass (SP) according to FM rate selectivity (Poon et al., 1991; Mendelson et al., 1993; Tian and Rauschecker, 1994; Felsheim and Ostwald, 1996; Ricketts et al., 1998; Razak and Fuzessery, 2006). It must be noted that this classification applies to the range of FM rates (0.08-20 kHz/msec) tested here. The classification may change if other ranges of FM rates were used. AP neurons responded within 50% of maximum response at all rates tested. BP neurons were selective for a range of rates, with responses decreasing below 50% of maximum for slower and faster rates. FP neurons' responses decreased below 50% of maximum as rates were decreased. SP neurons' responses decreased below 50% of maximum as FM rates were increased.

The 50% cutoff rate, defined as the FM rate at which the response declines to 50% of maximum response was measured for FP and BP neurons. For BP neurons, two such rates exist. Only the 50% cutoff for decreasing rate was quantified here. For BP neurons, the best rate (BR) was determined as the sum of the product of the number of spikes elicited by each FM sweep rate divided by the total spikes elicited by all FM sweep rates (Brown and Harris 2009, Atencio et al. 2007):

$$BR = [\sum (Spikes \times FM\ Rate)]/(\sum (Spikes))$$

To quantify the degree of rate selectivity, the rate tuning index (RTI) was calculated for each neuron as follows:

$$RTI = (n/n\text{-}1) \times [1 - (mean/max)]$$

where n = the number of FM sweep rates assessed, mean is the average response across all rates tested and max is the maximum response. This measure is called 'speed tuning' in the literature (Atencio et al. 2007; Brown and Harris 2009).

FM Direction Selectivity

To assess a preference for upward or downward FM sweeps of the same bandwidths and rates, a direction selectivity index (DSI) was calculated as follows:

$$DSI = (D-U)/(D+U)$$

where D and U are the trapezoidal area under the curve for downward and upward FM sweeps (modified from O'Neill and Brimijoin 2002, Razak and Fuzessery 2006). DSI values near 1 indicate a preference for DFM and values near -1 indicate preferences for UFM. DSI was assessed at three different ranges of FM rate: 0.1-1 kHz/msec, 1.1 – 3 kHz/msec, and 3.1 – 10 kHz/msec.

Results

Single unit recordings: classification of FM rate selectivity

FM rate selectivity was determined in 223 neurons in both A1 and AAF with CF between 7-35 kHz. In 90 of these neurons, rate selectivity was studied using both upward

and downward sweeps. In the remaining only downward sweeps were used. FM rate selectivity was determined by first measuring FM duration selectivity with sweeps of a fixed bandwidth and differing durations. In 102/223 neurons, FM duration selectivity was measured with at least two different FM bandwidths. Multiple FM bandwidth tests facilitate differentiating between FM rate selectivity and sound duration/bandwidth tuning (Razak and Fuzessery, 2006; Fuzessery et al., 2006). Figure 2.1A, C, E shows examples of FM duration selectivity in which two different sweep bandwidths were tested. Note that the selectivity changes with FM bandwidth. When FM sweep rates (in kHz/msec) were calculated by dividing the FM bandwidth by duration and the responses were re-plotted against FM sweep rate (Figures 2.1B, D, F), it can be seen that the neuron's rate selectivity is similar regardless of the sweep bandwidth. This indicates that the neuron was indeed selective for FM sweep rates, and not the duration/bandwidth of the sound used.

Figure 2.1G shows the 50% cutoff rates for FP, BP and SP neurons obtained with a narrow bandwidth and broad bandwidth sweep. In the vast majority (87/102, 85%) of these neurons, the 50% cutoff was within 1 kHz/msec of each other for the two bandwidths. This suggests that these neurons were selective for sweep rate, and not tuned to the sound duration/bandwidth.

Figure 2.1C, D also addresses another important methodological issue in studying FM sweep selectivity. Short duration sweeps (<10 msec) were used to generate rapid FM rates. Such short duration sweeps may appear as clicks and not really test FM processing. However, Figure 2.1C shows that the neuron can distinguish a 3 msec sweep

with a 45 kHz bandwidth (50→5 kHz sweep) and a 3 msec sweep with a 15 kHz (20→5 kHz sweep). The important parameter for this neuron's response was FM rate. The fact that it responded better to a 7 kHz/msec sweep than to the faster 10 kHz/msec sweep also precludes the possibility that these sounds were processed as clicks because of the rapid rates used.

Figure 2.2 shows examples of the four types of FM rate selectivity (AP, BP, FP and SP) along with sample PSTHs. The FM rate tuning type was similar regardless of whether total number of spikes or peak firing rate was used calculate response magnitude in 70% of AP, 82% of BP, 89% FP and 78% SP neurons. In all subsequent figures and analyses, response magnitude was measured as the 'number of spikes'.

Mouse cortical neurons are selective for a narrow range of FM rates

FM selective neurons in A1 and AAF exhibit a narrow range of selectivity for FM sweep rates (Figures 2.3A-D). The narrow range of selectivity was striking given that a broad range of FM sweep rates (0.08 - 20 kHz/msec) were tested. For FP neurons (Figure 2.3A), ~70% of neurons had a 50% cutoff rate between 0.5-2 kHz/msec for both upward sweeps (11/16 neurons) and downward sweeps (23/33 neurons). For SP neurons (Figure 2.3B), the 50% cutoff of the majority of neurons was between 0.5 - 2 kHz/msec. No difference was observed between upward and downward sweep 50% cutoff rates for FP and SP neurons (One-way Anova, $p = 0.17$).

Band pass neurons were selective for a narrow range of FM sweep rates. BP neurons have two different 50% cutoff rates, one as sweep rate is decreased (Figure 2.3C)

and one as sweep rate is increased (Figure 2.3D). The 50% cutoff rate-slow was between 0.5 – 2 kHz/msec in 74% (31/42) of neurons tested with upward sweeps and 87% (76/87) of neurons tested with downward sweeps. No difference was observed between up and down sweep 50% cutoff rates for BP neurons. The 50% cutoff rate-fast (Figure 2.3D) was more evenly distributed across the rates tested, with ~80% of neurons exhibiting cutoff rates <12 kHz/msec. The best rate of BP neurons also showed a narrow range with best-rates between 1-3 kHz/msec in 47% of neurons tested with upward sweeps and for 71% of neurons tested with downward sweeps (Figure 2.3E). Almost all BP neurons tested have best rates between 1-7 kHz/msec. These data show that the vast majority of FP neurons will respond best for FM rates faster than ~1-2 kHz/msec and that the sweep rates over which maximum firing rate change occurs in FP neurons is ~1 kHz/msec. Likewise, the majority of SP neurons will respond best to rates slower than ~1-2 kHz/msec, and the maximal change in their firing rate occurs for rates ~1-2 kHz/msec. The majority of BP cells will respond best to rates ~1-4 kHz/msec.

Rate tuning index is a quantitative measure that shows the degree to which a neuron is selective for a given FM sweep rate (Brown and Harris 2009, Atencio et al. 2007). The rate tuning index is useful in making comparisons of rate selectivity across species. Table 4.1 shows the mean (± s.e.) RTI for the different types of neurons and for the two sweep directions. As expected, the all pass neurons had the lowest average RTI.

Effect of anesthetic type

In the presentation above, data obtained from mice anesthetized with ketamine/xylazine (KX) for both induction and maintenance were combined with data from ketamine/xylazine (induction) and isoflurane (maintenance, KXI). The justification for combining data was that no differences were found between the two anesthetic groups in terms of 50% cut-off for fast pass neurons (n=25 with KX, n=8 with KXI, t-test, p=0.75) or RTI (p=0.64). Likewise, for band pass neurons (n=76 with KX, n=11 with KXI) no difference was found for 50% cut-off rate (t-test, p=0.71), RTI (p=0.32) or best rate (p=0.71).

Comparison of 1-2 month old cortical data with 2-3 month old data

The C57 strain undergoes early onset presbycusis, with high-frequency hearing loss starting ~3 months. Cochlear function and auditory responses in the C57 strain are comparable to the CBA strain ~2 months of age. We compared rate selectivity between 1-2 (30-60 days) and 2-3 (61-89 days) month old mice to determine if there are differences which may suggest abnormal processing in the latter group. A t-test between the two age groups of RTI showed no difference in BP ($t=1.69$, $p>0.05$), FP ($t=-1.45$, $p>0.05$) and SP ($t=-0.99$, $p>0.05$) neurons. A t-test between the age groups of 50% cut-off rates in BP ($t=-0.53$, $p>0.05$), FP ($t=-1.14$, $p>0.05$) and SP neurons ($t=-1.4$, $p>0.05$) showed no difference. Finally, a comparison of best rate of BP neurons also showed no difference ($t = -0.4484$, $p>0.05$). These data indicate that the narrow range of rate

selectivity observed in the C57 mouse cortex was unlikely to be influenced by early onset presbycusis.

FM direction selectivity

FM direction selectivity was studied in 90 neurons in A1 and AAF. Upward and downward sweeps with the same bandwidth were varied in duration to obtain FM rate selectivity functions. Direction selectivity was quantified using the direction selectivity index (DSI). Because direction selectivity can vary with the sweep rate of the stimulus, DSI was measured at three different sweep rate ranges: 0.1 – 1 kHz/msec, 1.1-3 kHz/msec and 3.1-10 kHz/msec.

Figure 2.4A shows an example of a direction selective neuron which preferred downward sweeps. The DSI values at different sweep rate ranges are shown within the panel, Figure 2.4B shows a neuron which responded similarly to the two sweep directions. On average, there was very little direction selectivity in the mouse auditory cortex (Figure 2.5). The average DSI was ~0 regardless of the sweep rate range (2.5A). A one-way ANOVA of FM rate range by DSI revealed no effect of rate range ($F(2,269) = 1.13$, $p = 0.3234$). Fewer than 20% of neurons showed a DSI values greater than 0.33 or less than -0.33 (twice the response to one direction compared to the other). There was no relationship between DSI and CF at any of the three sweep rates ($p>0.05$, Figure 2.5B-D). Finally, in ~86% (77/90) of neurons, there was no difference in the FM rate selectivity type for upward and downward sweeps.

Effects of cortical depth on FM rate selectivity

The FM rate selectivity measures from single unit recordings presented above were obtained at depths between 100 -700μm. A one-way Anova of FM tuning type x depth revealed a significant main effect of depth on FM tuning type ($F(3, 197) = 3.57$, $p < 0.05$). AP neurons were found deeper than BP and FP neurons (Figure 2.6). This suggested a depth (cortical layer) effect on FM rate tuning.

To assess this directly, FM rate properties were measured at multiple depths in penetrations made orthogonal to the cortical surface. This was accomplished in 46 penetrations in both A1 and AAF. In each of these penetrations, FM rate selectivity was measured for a neuron isolated between 250-400 μm (mean depth 289 +/- 63μm) and compared with a neuron isolated deeper than 400 μm (mean depth 504 +/- 91μm). For the penetration shown in Figure 2.7A, the neuron found at 356 μm was BP tuned. A second neuron isolated in the same penetration at 552 μm responded with greater number of spikes, and also responded similarly at all rates tested (all pass). The neurons shown in Figure 2.7B exhibited similar maximum responses, but the rate selectivity changed from BP to AP with depth. In 38/46 penetrations, rate selectivity changed type with a BP to AP change occurring in 14 penetrations, FP To AP change occurring in 7 penetrations and a BP to FP change occurring in 7 penetrations. In 8/46 penetrations, there was no change in rate selectivity type with depth. The neurons shown in Figure 2.7C exhibited similar rate selectivity functions independent of their depth. Across the population, a paired t-test revealed that neurons at shallow cortical depths had a significantly ($t=5.8$,

$p<0.0001$) higher RTI value than more deeply located neurons (Figure 2.7D). These results indicate FM rate selectivity decreases with cortical depth.

Discussion

This study examined the cortical organization of FM sweep rate selectivity in the mouse. Two patterns of organization were discovered. First, there are cortical depth-specific differences, with the dominant trend being a decline in FM rate selectivity with depth. In the mouse cortex, depths between 250-450 µm correspond approximately to deep layer III and layer IV (granular layers, Anderson et al., 2009). Layers deeper than 450 µm correspond to infragranular layers. These data suggest that granular and infragranular layers differ in FM selectivity as seen in the cat (Atencio and Schreiner 2010) and support a hierarchical model for processing within a cortical column. Second, and perhaps the most striking finding, is the narrow range of FM rate selectivity exhibited by cortical neurons. Most of the band pass neurons responded best to a narrow range of FM rates (~1-3 kHz/msec) and most fast pass and slow pass neurons exhibited 50% cutoff rates between 0.5-2 kHz/msec.

FM sweep direction selectivity

Less than 20% of neurons in the mouse A1 and AAF show DSI values > +0.3 or < -0.3 at the FM sweep rate ranges tested. This is in contrast to that reported in the mouse inferior colliculus (IC), in which nearly half the neurons exhibited direction selectivity according to the above criterion (Hage and Ehret, 2003). Both studies used similar anesthetics (ketamine/xylazine), linear FM sweeps and FM rates. The direction

selectivity reported here is also lower than those found in the auditory cortex of other species (44% in rats: Ricketts et al., 1998, 45% in cats: Mendelson et al., 1993). There was also no correlation between CF and DSI in our dataset. Such correlations have been reported in rat and squirrel monkey A1 (Zhang et al., 2003; Godey et al., 2005), but not in the mouse IC (Hage and Ehret, 2003), owl monkey and cat A1 (Heil et al. 1992; Mendelson et al. 1993; Atencio et al. 2007). These differences are likely explained by the under-sampling of neurons with CF<5 kHz and CF>30 kHz in our study. In the rat and squirrel monkey A1, high DSI values were typically found at the low or high end of the CF range sampled, particularly at frequencies near the beginning or the end of the fixed bandwidth FM sweeps used to study sweep selectivity. A clearer picture of FM direction selectivity in the mouse cortex requires a broader sampling of CF range. But for regions of A1 and AAF with CF in the 7-30 kHz range, very little direction selectivity or correlation with CF is seen in the mouse.

Depth dependent changes in FM rate selectivity

Cortical penetrations in which multiple neurons were isolated at different depths revealed a significant depth dependent change in FM rate selectivity. FM rate tuning declined significantly with depth (250-400 μm versus >450 μm), with the most prominent change being fast pass/band pass to all pass. These changes can occur with or without changes in maximal firing rates. The finding that FM rate selectivity declines from the granular to infragranular layers is consistent with findings in the cat A1 based on spectrotemporal receptive field analysis that the infragranular layers are less feature-

selective and fire with less temporal precision than granular layers (Atencio et al., 2009). Thus while properties such as CF and binaural interaction are similar at different depths (Abeles and Goldstein, 1970, Imig and Adrian, 1977), responses to dynamic stimuli may undergo significant changes across cortical layers. This may reflect differences in intracortical interactions shaping FM rate selectivity at different depths (Kaur et al., 2004; Happel et al., 2010). This may also reflect laminar differences in intrinsic properties in the mouse auditory cortex (Huggenberger et al., 2009).

Narrow range of response selectivity for FM rate in the mouse auditory cortex

For the range of FM rates tested in this study (0.08–20 kHz/msec), most slow pass and fast pass neurons had their 50% cutoff ~0.5-2 kHz/msec. The slow rate cutoff of most band pass neurons was also in the 0.5–2 kHz/msec range. The 50% cutoff is approximately the center of FM rates across which the neuron shows maximum change in response magnitude. This range is therefore where maximum information is likely to be available (Harper and McAlpine, 2004; Jazayeri and Movshon, 2006). These data suggest that rates ~0.5-2 kHz/msec are best discriminated by the mouse auditory cortex. The majority of band pass neurons in A1/AAF responded best to rates between 1-3 kHz/msec, indicating that band pass neurons best detect this narrow range of rates. The best FM rates reported for the mouse is considerably faster than those reported in the owl and squirrel monkey A1 (Godey et al., 2005; Atencio et al., 2007). While this may reflect species differences, it must be noted that we only report best rate for band pass neurons. The monkey A1 papers report best rate (‘speed’) for all classes of neurons. Thus, if slow

pass neurons, which dominate A1 of the mouse, were included, the best rate will be much lower in the mouse cortex as well. Likewise the best rates reported here are also faster than those reported in chinchilla A1 (Brown and Harrison, 2009). However, in the chinchilla only rates <1 kHz/msec were studied.

The functional significance of the selectivity for a narrow range of FM rates in the mouse auditory cortex is unclear. It is possible that these neurons discriminate sweep rates present in the rich repertoire of vocalizations emitted by mice. On the other hand, the narrow range of selectivity may reflect fundamental constraints on the mechanisms underlying FM rate selectivity. Most of these vocalizations have spectral energy in the 60-110 kHz range (Holy and Guo 2005; Panksepp et al., 2007; Grimsley et al., 2011), whereas the neurons recorded here had CF (and tuning) between 5-40 kHz. It has been suggested that neurons with this range of CF in the ICc indeed respond to very high frequency vocalizations based on the distortion products with energy in the neurons' lower frequency tuning curve (Portfors et al. 2009; Holmstrom et al., 2010). This is true for both the tonal and FM components of vocalizations which have different FM sweep rates. An examination of published sonograms of mouse vocalizations does indicate that there are a number of vocalizations with sweep rates between 0.5-2 kHz/msec (Liu et al., 2003; Portfors, 2007; Grimsley et al., 2011). In the C57 mice, three of the four dominant call types include FM sweeps (Panksepp et al., 2007). The FM rates of these sweeps are between 0.8 – 1.2 kHz/msec, which falls within the narrow range of cortical rate selectivity observed in this study. Thus the range of cortical rate selectivity may be relevant for processing vocalizations. Neurons with CF extending into 50-80 kHz range

have been reported in the mouse cortex, in a region termed the ultrasonic field (UF, Stiebler et al., 1997). These neurons may play a role in processing vocalizations as well.

Methodological considerations

The C57bl6 strain of mouse was studied at ages <3 months. This strain has been studied as a model for early onset presbycusis, and the data from this study serves as baseline for future work on how FM processing changes in presbycusis. However, the question arises whether the data shown here for young mice may be influenced by early onset hearing loss. Previous electrophysiological studies show that the C57 mice develop high-frequency loss from 3-6 months (Mikaelian, 1979; Henry and Chole, 1980; Willott, 1986; Hunter and Willott, 1987) with a loss of outer hair cells in the basal 20% of the cochlea present from 3 months of age (Spongr et al., 1997). Comparison of cochlear morphology, ABR and DPOAE responses show that the C57 strain is similar to the CBA/CaJ strain at 1 month, and begins to deviate at 3 months (Park et al., 2010). Auditory cortical responses and gross tonotopy appear to be normal in the young C57 mice (Bandyopadhyay et al., 2010) and start to show plasticity from 3 months of age (Willot et al., 1993). Taberner and Liberman (2005, J. Neurophysiol.) compared auditory nerve fiber responses between C57 (~4 month) and CBA strains (age between 2-4 month) and found no differences in spontaneous rates, tuning curves, rate versus level functions, dynamic range, response adaptation, phase-locking, and the relation between spontaneous rate and response properties. The only difference found in the 4 month old C57 mice was the expected elevation in high-frequency hearing at that age. Taken together, these

studies show most changes in the C57 auditory system compared to the CBA strain begins to happen around 3 months of age and becomes more pronounced between 3-6 months. These studies also suggest that the 2 month old C57 mouse is comparable to the CBA strain. Our comparison of data from 1-2 month old and 2-3 month old cortex shows no significant differences in sweep rate selectivity measures. Thus we conclude that early onset-presbycusis had minimal influence on the data and suggest that the narrow range of rate selectivity is likely to be typical of mouse cortex.

Conclusions:

Speech recognition declines with ageing and presbycusis. FM sweeps play an important role in speech processing (Zeng et al., 2007). Cortical FM sweep selectivity changes with age (Mendelson and Ricketts, 2001). Thus FM rate selectivity may serve as a useful physiological probe to develop a model system in which contributions of both genetic and experience-dependent factors in auditory cortex aging and disease can be evaluated. The cortical mechanisms underlying FM sweep selectivity are known based on studies in bats and rodents (Razak and Fuzessery, 2006; Ye et al., 2010). Preliminary data suggest similar mechanisms are operational in the mouse auditory cortex as well. Ongoing studies address if and how cortical FM rate selectivity is altered by aging and presbycusis.

Figures:

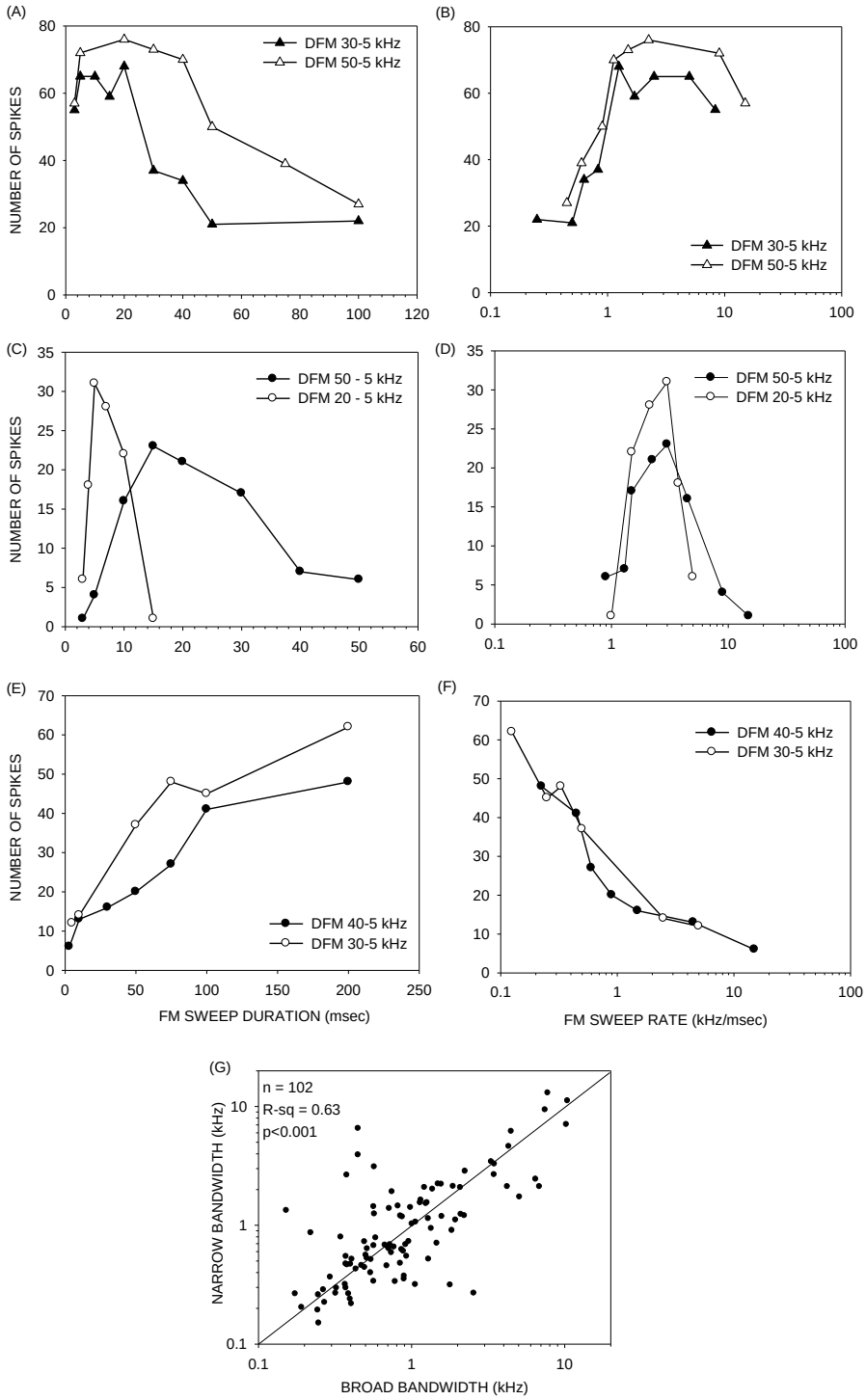
(A)
NUMBER OF SPIKES
DFM 30-5 kHz
DFM 50-5 kHz
(B)
DFM 30-5 kHz
DFM 50-5 kHz
(C)
NUMBER OF SPIKES
DFM 50 - 5 kHz
DFM 20 - 5 kHz
(D)
DFM 50-5 kHz
DFM 20-5 kHz
(E)
NUMBER OF SPIKES
DFM 40-5 kHz
DFM 30-5 kHz
FM SWEEP DURATION (msec)
(F)
DFM 40-5 kHz
DFM 30-5 kHz
FM SWEEP RATE (kHz/msec)
(G)
n = 102
R-sq = 0.63
p<0.001
NARROW BANDWIDTH (kHz)
BROAD BANDWIDTH (kHz)

Figure 2.1: Rate selectivity functions (B, D, F) were plotted from duration selectivity functions **(A, C, E)** wherein the bandwidth of the FM sweep (in kHz) is divided by the duration of the FM sweep (in msec) to obtain the FM sweep rate in kHz/msec. These neurons were not selective for sound duration or bandwidth, but were selective for FM rate. DFM: downward frequency modulated sweep. **(G)** A scatter plot of the 50% cutoff at multiple bandwidths for band pass, fast pass and slow pass neurons. The x-axis represents the 50% cutoff for broad bandwidth FM sweeps. The y-axis represents the 50% cutoff for narrow bandwidths. The diagonal line represents equal 50% cutoff rates for the two different bandwidths used.

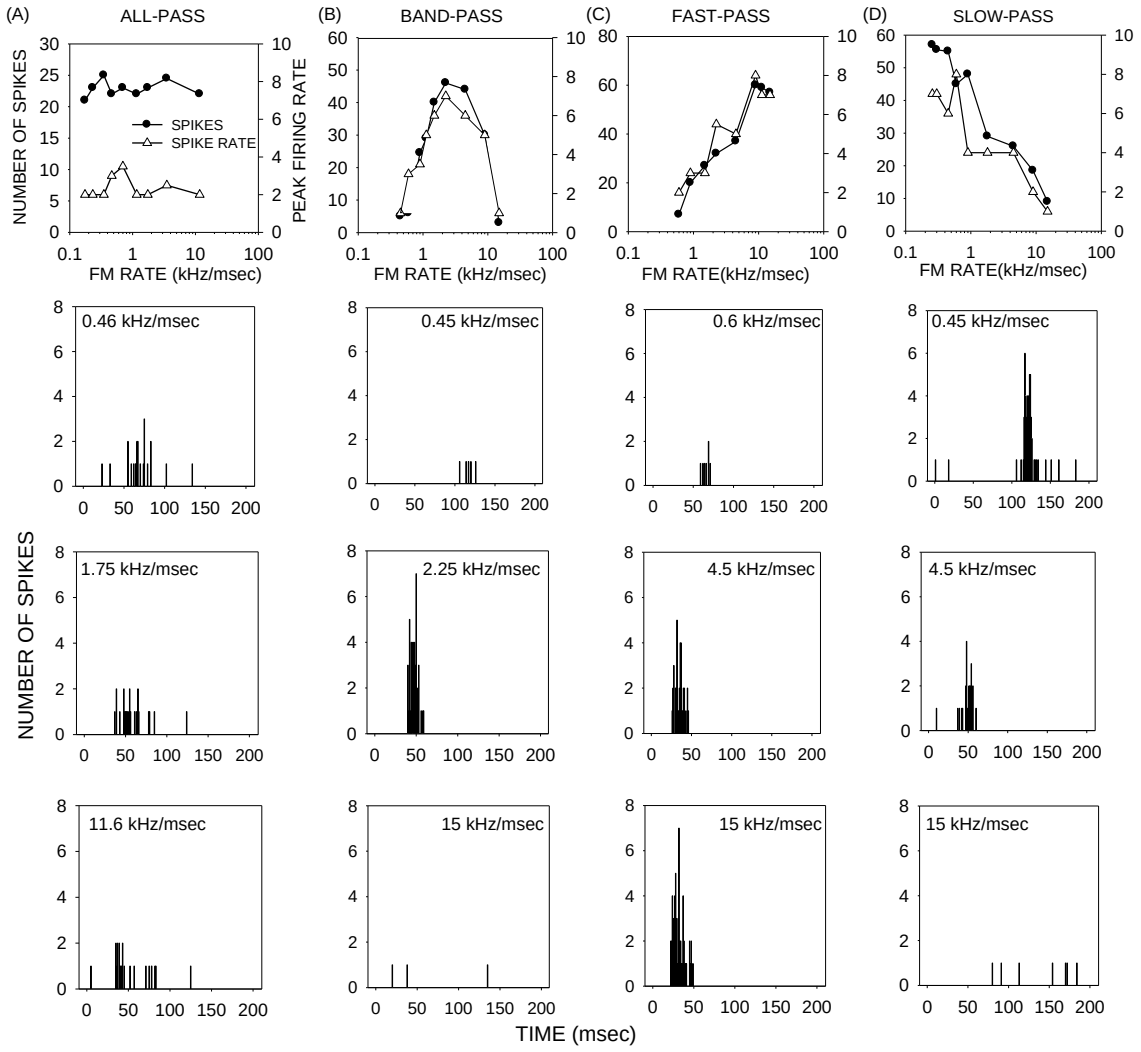

Figure 2.2: Examples of FM rate selectivity functions (A – D) to illustrate the rate selectivity type classification. Example PSTHS for each type of neuron are shown below each graph. (A) All pass, (B) band pass, (C) Fast pass and (D) Slow pass.

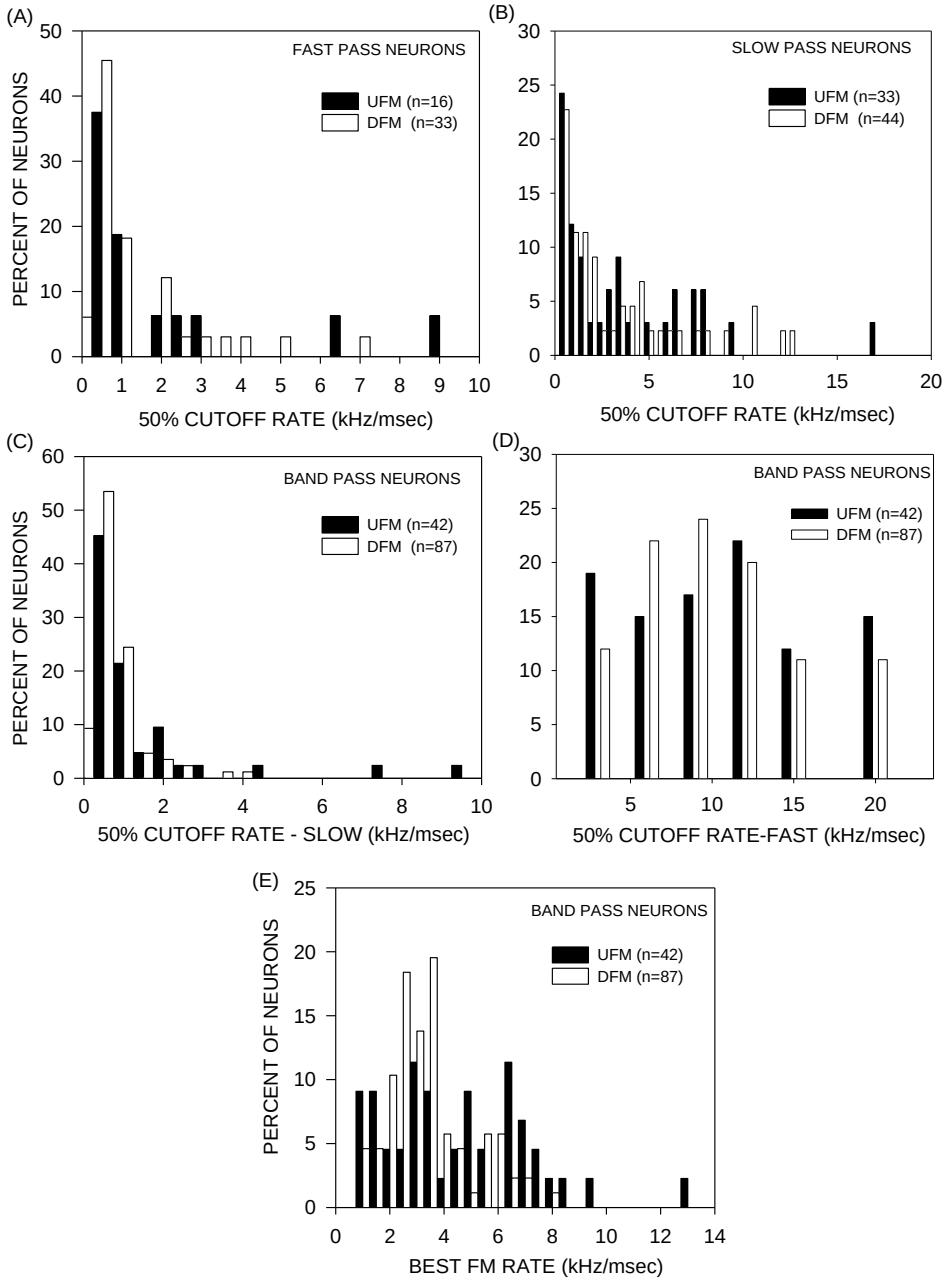

Figure 2.3: (A) Distribution of 50% cutoff rate for fast pass neurons. These neurons respond at better than 50% of maximum response for rates faster than the cutoff. **(B)** Distribution of 50% cutoff rates for slow pass neurons. These neurons respond at better than 50% of maximum response at rates slower than the cutoff. **(C, D)** Band pass neurons have two 50% cutoff rates, one as sweep rate is decreased (C) and one as sweep rate is increased (D). **(E)** The distribution of best rate in band pass neurons. DFM: downward sweeps; UFM: upward sweeps. No significant differences were found between upward and downward sweep 50% cutoff rates.

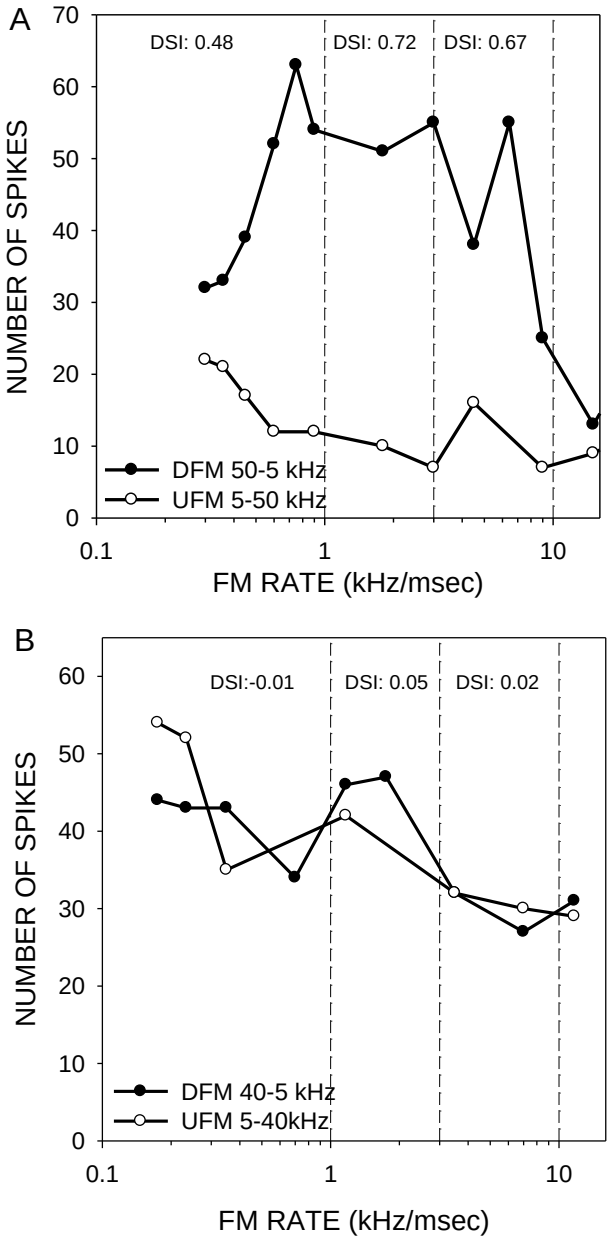

Figure 2.4: FM direction selectivity in the mouse auditory cortex. (A) An example of a direction selective neuron. **(B)** An example of a non-selective neuron. DFM – downward FM; UFM – upward FM sweep. DSI – direction selective index

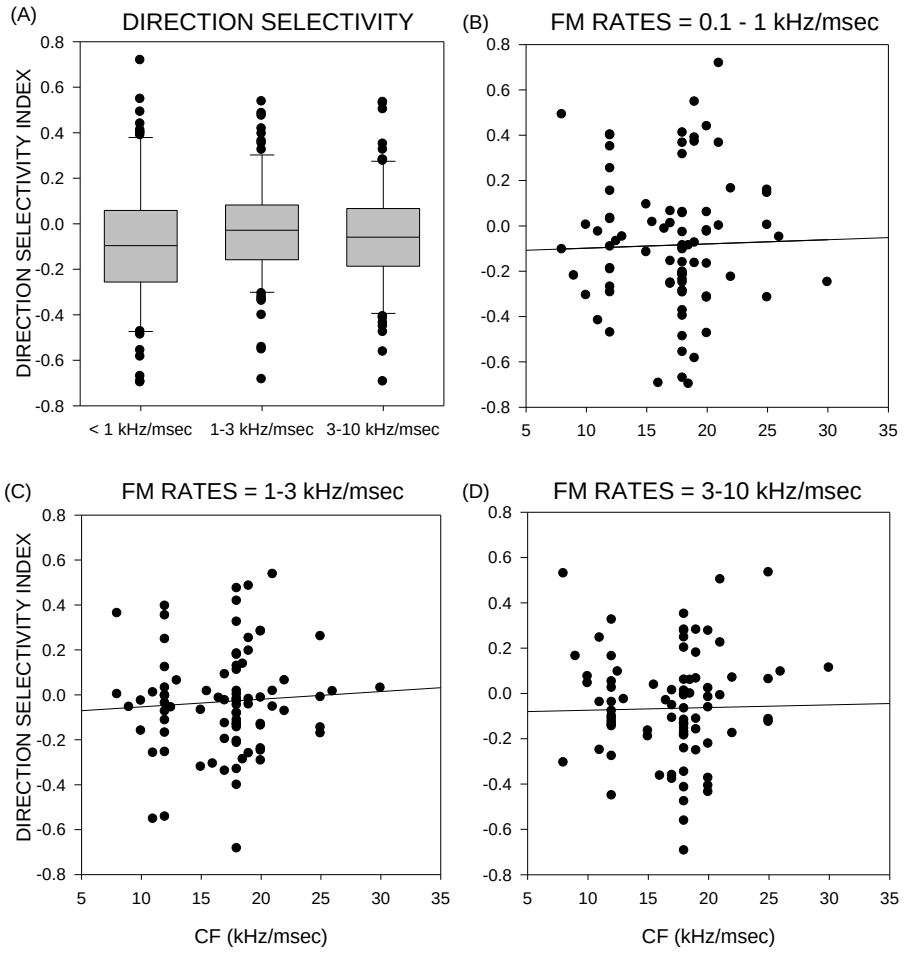

Figure 2.5: Direction selectivity (A) The distribution of direction selectivity index (DSI) values measured at three different ranges of FM sweep rates. **(B-D)** There was no correlation between CF and DSI at any of the three rate ranges tested. Positive DSI values indicate downward FM selectivity. Negative DSI values indicate upward sweep selectivity.

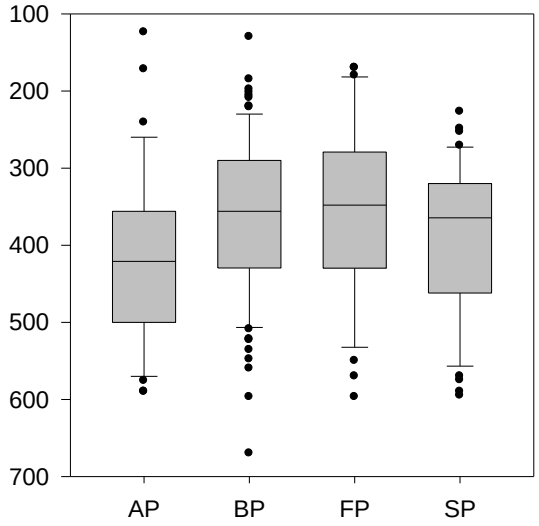

Figure 2.6: Distribution of the depths at which neurons with different FM rate selectivity types were found across A1 and AAF based on the single unit recordings. The boxes represent the 25th and 75th percentile. The horizontal line within the boxes represents the median and the vertical lines represent the standard deviation around the mean. The dots represent the 5th and 95th percentile.

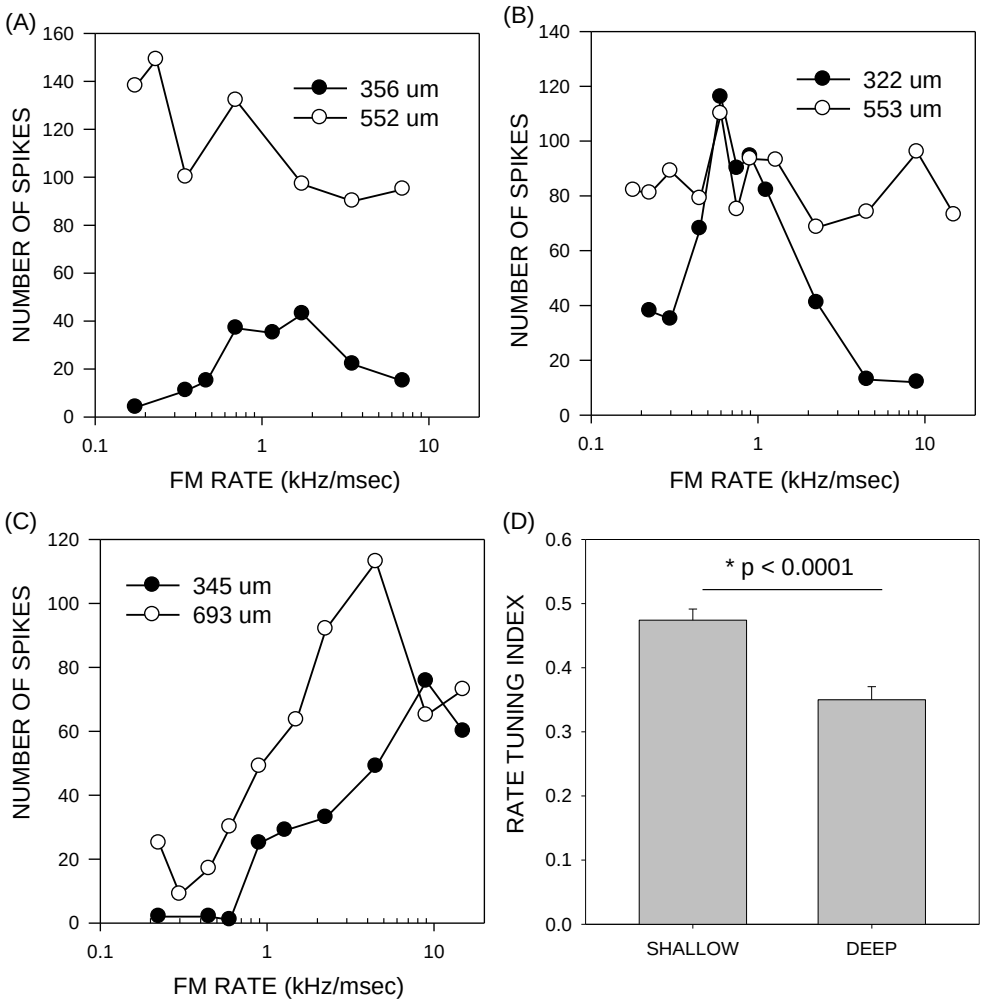

Figure 2.7: (A-C) Representative FM rate selectivity functions from two different depths in orthogonal penetrations indicating depth-dependent changes in rate selectivity. (A) A penetration in which response magnitude increased with depth and selectivity type changed from BP to AP. (B) A penetration in which selectivity changed from BP to FP with depth without an increase in response magnitude. (C) A penetration in which the rate selectivity type did not change with depth. (D) Mean (± sem) rate tuning index of neurons found in shallow versus deeper layers in 28 penetrations.

Chapter 3: Mechanisms underlying selectivity for the rate of frequency modulated sweeps in the core auditory cortex of the mouse

As of the writing of this dissertation, this chapter has been submitted for review to the Journal of Neurophysiology. Dr. Maria Magdalena Carrasco contributed 12 neurons to this manuscript. Her data are included in this chapter because they form a small percentage of the number of neurons I analyzed.

ABSTRACT

The rate and direction of frequency modulated (FM) sweeps are relevant cues in vocalization processing. As in every species examined, the mouse auditory cortex contains FM sweep selective neurons. Particularly noteworthy is the selectivity for a narrow range of sweep rates. This study focused on the mechanisms underlying rate selectivity in the auditory cortex of anesthetized C57bl/6 mice. Linear downward FM sweeps with rates between 0.08–20 kHz/msec were tested. At least two different mechanisms shape FM rate selectivity in the mouse auditory cortex: sideband inhibition and duration tuning. Sideband inhibition was determined using the two-tone inhibition paradigm in which excitatory and inhibitory tones are presented with different delays. The frequency-delay combinations producing inhibition served to map out the sideband. Sideband inhibition was present in the vast majority (84%, n=58) of neurons. The spectrotemporal properties of sideband inhibition predicted rate selectivity and the removal of sidebands from the sweep reduced/eliminated rate tuning. The second mechanism was duration tuning. If a neuron is selective for the duration that a sweep

spends in the excitatory frequency tuning curve, then rate selectivity will ensue. Duration tuning for excitatory tones was present in ~30% of neurons (n=104). In these neurons, properties of duration tuning predicted FM rate tuning. Both mechanisms predicted rate selectivity equally well, but sideband was present in a larger percentage of neurons suggesting that sideband inhibition is the dominant mechanism in the mouse auditory cortex. Similar mechanisms shape sweep selectivity in the auditory system and movement-velocity selectivity in the visual system suggesting similar solutions to analogous problems across sensory systems.

Introduction

Animal vocalizations, including human speech, consist of upward and downward frequency modulated (FM) sweeps with various rates of frequency change. FM sweeps are important components for discrimination of speech (Stevens and Klatt 1974; Zeng et al. 2005). Moreover, FM sweeps are relatively simple sounds that can serve as probes to understand fundamental mechanisms of spectrotemporal processing in the auditory system. The auditory cortex of all species examined contain neurons selective for the rate and/or direction of FM sweeps (Atencio et al. 2007; Brown and Harrison 2009; Godey et al. 2005; Hall et al. 2000; Heil et al. 1992b; Mendelson and Cynader 1985; Nelken and Versnel 2000; Razak and Fuzessery 2006; Suga 1965; Tian and Rauschecker 1994; 2004; Washington and Kanwal 2008). FM sweep selectivity is present in the mouse auditory cortex as well, with the dominant feature being selectivity for a narrow

range of FM sweep rates (Trujillo et al. 2011). The present study focused on the mechanisms underlying such selectivity.

The mouse is a useful model system to study sensory processing due to the available genetic engineering tools (Barkat et al. 2011; Linden et al. 2003; Linden and Schreiner 2003; Liu 2006; Mataga et al. 2001; Morishita et al. 2010; O'Connor et al. 2009; Portfors 2007; Portfors et al. 2009; Sugiyama et al. 2008). The strong selectivity for FM sweep rates in the mouse auditory cortex can serve as a physiological tool to study basic circuitry, development and disease models of auditory processing. An understanding of the mechanisms underlying FM rate selectivity in the mouse auditory cortex will facilitate inquiries of not just whether selectivity changes during development or because of genetic disorders, but will also provide insights on underlying cellular substrates. Another motivation for studying mechanisms of FM rate selectivity in the mouse is that almost all of the published work on this topic is based on work in the bat auditory system (Gittelman and Li 2011; Gittelman and Pollak 2011; Gordon and O'Neill 1998; Razak and Fuzessery 2008; 2006; Suga 1965). It remains unclear if bat auditory systems are specialized to process the fast FM sweep rates present in echolocation calls, or if the mechanisms inform about general principles guiding spectrotemporal processing in the auditory system. Therefore, this study focused on the mechanisms of FM rate selectivity in the auditory cortex of the C57bl/6 mouse, a strain commonly used to study genetic disorders with auditory communication implications including presbycusis (Erway et al. 1993; Johnson et al. 1997; Johnson et al. 2000; Noben-Trauth et al. 2003) and Fragile X syndrome (Michalon et al. 2012).

At least three different mechanisms shape FM sweep rate selectivity in bat cortex (Gordon and O'Neill 1998; Razak and Fuzessery 2008; 2006). Suga (1965) suggested that FM sweep selectivity depends on spectrotemporal interactions between excitatory frequencies and sideband inhibition. This mechanism has been explored in detail in the auditory system of the pallid bat. Using the two-tone inhibition paradigm in which excitatory and inhibitory tones are presented with various delays, the spectral and temporal properties of sideband inhibition can be determined (Brosch and Schreiner 1997; Calford and Semple 1995; Fuzessery et al. 2006; Razak and Fuzessery 2006). A delayed high-frequency sideband inhibition (inhibition near the high-frequency edge of the tuning curve) shaped rate selectivity for downward FM sweeps in the auditory cortex of the pallid bat (Razak and Fuzessery, 2006). Downward sweeps with fast sweep rates can reach the excitatory frequencies before the delayed inhibition arrives, eliciting neural response. For slow downward sweeps, the delayed inhibition has sufficient time to arrive to the neuron simultaneously or before the excitation and reduces responses. The timing and bandwidth of high-frequency inhibition predicted rate selectivity for downward sweeps.

The second mechanism underlying FM rate selectivity is duration tuning (Fuzessery et al. 2006). Duration tuning for tones is present in the auditory system across all vertebrate taxa (Brand et al. 2000; Casseday et al. 1994; Ehrlich et al. 1997; Feng et al. 1990; Gooler and Feng 1992). Fuzessery et al., (2006) showed that duration tuning plays a role in spectrotemporal processing underlying FM rate selectivity. Sweeps of different rates spend different durations within the excitatory frequency tuning curve. If a

neuron is tuned to the duration of excitatory tones, then sweeps of different rates will elicit different responses. The best sweep rate will be the one that spends the optimal duration within the tuning curve. In the pallid bat inferior colliculus (IC), duration tuning predicted rate selectivity in nearly 50% of the neurons (Fuzessery et al. 2006). However, this mechanism was absent in the auditory cortex (Razak and Fuzessery 2006).

The third mechanism of FM rate selectivity depends on non-linear facilitation. In this mechanism neurons respond poorly to single tones, but show combination sensitive facilitation when two tones are played with a certain delay (Fuzessery et al. 2011; Mittmann and Wenstrup 1995; Razak and Fuzessery 2008; Sadagopan and Wang 2009). The differences in frequency between the two tones and the delay that elicited optimal facilitation co-varied, and their ratio predicted FM rate selectivity.

The primary aim of this study was to determine the relative contributions of these three mechanisms to FM rate selectivity observed in the mouse auditory cortex. Both primary auditory cortex (A1) and anterior auditory field (AAF) were studied. We show that the primary mechanism shaping rate selectivity in the core fields of the mouse auditory cortex is sideband inhibition. Duration tuning is important in a minority of neurons. A small number of neurons exhibited both mechanisms. The facilitation mechanism was mostly absent.

Methods

Mice (C57bl/6 strain, age 30-83 days, n=59 of either sex) were obtained from an in-house breeding colony that originated from Jackson Laboratory (Bar Harbor, Maine). Two to five littermates were housed in each cage under a 12/12 light/dark cycle and fed

ad libitum. This mouse strain shows accelerated age-related hearing loss (Henry and Chole 1980; Hunter and Willott 1987; Mikaelian 1979; Spongr et al. 1997; Willott 1986). This can begin as early as 2 months of age, although audiometric evidence of hearing loss appears ~3 months. Taberner and Liberman (2005) compared auditory nerve fiber responses between C57bl/6 (~4 month) and CBA strains (age between 2-4 month) and found no differences in spontaneous rates, tuning curves, rate versus level functions, dynamic range, response adaptation, phase-locking, and the relation between spontaneous rate and response properties. Trujillo et al. (2011) showed no differences in FM sweep selectivity between 1-2 mo old mice and 2-3 mo old mice. Therefore, the data from ages between 30-83 days were pooled. All procedures were approved by The Institutional Animal Care and Use Committee at the University of California, Riverside.

Surgical Procedures

A combination of ketamine (150 mg/kg) and xylazine (10 mg/kg) was injected (i.p.) to induce anesthesia for surgery. Anesthesia was maintained throughout the experiment by either supplemental dosage of ketamine-xylazine or isoflurane inhalation (0.2–0.5% in air). Anesthetic state was assessed via the toe-pinch reflex test throughout the experiment and supplemental anesthetic was administered as needed. After an areflexic state of anesthesia was reached, a midline scalp incision was made and the right temporalis muscle was reflected. A dental drill was used to perform a craniotomy to expose the auditory cortex. At the end of electrophysiological recording, mice were euthanized with pentobarbital sodium (125 mg/kg).

Acoustic Stimulation

Acoustic stimuli were driven and data were acquired by custom software (Batlab, Dr. Don Gans, Kent State University, Kent, OH). Sound intensities were controlled with programmable attenuators (PA5; Tucker-Davis Technologies, Gainesville, FL) prior to amplification by a stereo amplifier (Parasound HCA1100) or an integrated amplifier (Yamaha AX430). Sounds were delivered through a free-field ribbon tweeter (LCY-K100, Madisound,Wisconsin) located 6 inches and 45° from the left ear, contralateral to physiological recordings. Frequency response of the acoustic stimuli system was flat within ± 3dB for frequencies between 7-40 kHz as measured by a ¼ inch Bruel and Kjaer microphone and measuring amplifier. A Krohn-Hite filter (Brockton, MA) was used to filter out frequencies below 5 kHz (Butterworth, 24dB/octave).

Electrophysiology

A stereotaxic apparatus (Kopf model 930, California) and bite bar (Kopf model 923B) were used to secure mice for electrophysiological recordings. Experiments were conducted in a sound-attenuated chamber lined with anechoic foam (Gretch-Ken Industries, Oregon). Neurophysiological recordings were acquired using glass microelectrodes filled with 1M NaCl (2 – 10 MΩ impedance). Electrodes were driven into the cortex with a Kopf direct drive 2660 micropositioner. Single-unit recordings were obtained between depths of 200 and 560 μm (mean = 358 ± 87.9 μm). Single-unit responses were identified by constancy of amplitude and waveform as displayed on an

oscilloscope and were isolated using a window discriminator. Data quantification consisted of counting the number of spikes elicited over 20 stimulus repetitions. Poststimulus time histograms (PSTHs) were obtained over a 300 msec window relative to stimulus onset. There is typically no spontaneous activity in the anesthetized mouse auditory cortex.

Data Acquisition

The primary auditory cortex (A1) of the C57 mouse can be identified by vascular landmarks (Willott et al. 1993) as well increasing characteristic frequency (CF) in the caudal to rostral direction (Stiebler et al. 1997; Trujillo et al. 2011). The anterior auditory field (AAF) is located immediately rostral to A1 and exhibits a reversed tonotopy relative to A1. Both A1 and AAF are considered core auditory cortex (Cruikshank et al. 2001). The purpose of the present study was to determine the mechanisms that govern FM sweep selectivity in the core auditory cortex; so both A1 and AAF neurons were studied. These neurons can be distinguished from 'non-core' neurons based on robust tone responses, narrow tuning and short response latencies. The goal was not to determine if A1 and AAF differed in FM rate mechanisms; therefore, no effort was made to identify the location of neurons within these two fields. Pure tones (5-50 kHz, 1 msec rise/fall times and 2-30 msec duration), broadband noise and up/down sweeps were used as search stimuli to isolate single neurons. Upon isolation, tone response properties were acquired. Pure tones with frequencies between 5-50 kHz (1-5 kHz resolution, 2-30 msec duration, 1 msec rise/fall time) were presented to determine excitatory frequency tuning curves. The

CF was noted as the frequency at which the neuron responded to at least five consecutive presentations at the lowest sound intensity tested. The excitatory frequency tuning at 10, 20 and 30 dB above the minimum threshold was then determined by increasing intensity in 10 dB steps and changing frequencies with 1 kHz resolution.

Frequency modulated (FM) sweep rate selectivity

The vast majority of neurons in the mouse core auditory cortex respond similarly to upward and downward sweeps (Trujillo et al. 2011). Therefore, this study focused on identifying mechanisms of rate selectivity only for downward FM sweeps. Sweep rate selectivity was determined by presenting linear downward FM sweeps of fixed bandwidth and different durations. The sweep rate, defined as the rate of change in kHz/msec, was determined by dividing the FM bandwidth (in kHz) by the duration (in msec). FM sweeps that were approximately centered on the CF were presented at a single intensity, 10-20 dB above CF threshold. Unless noted otherwise, the FM sweep bandwidth extended at least 10 kHz outside the tuning curve. This ensures that putative high-frequency inhibitory sidebands, which abut the excitatory tuning curve in A1 (Razak and Fuzessery 2006; Wu et al. 2008), were included in the downward FM sweep. Sweep durations between 2 and 200 msec (rise/fall time 1 msec) were used. This allowed FM rates between 0.08 - 20 kHz/msec to be presented. This range covers the rates present in various mouse vocalizations (Grimsley et al. 2011; Liu et al. 2003; Portfors 2007; Rotschafer et al. 2012). We have shown previously that core cortical neurons in the mouse respond selectively to FM sweep rate and not to sweep duration or sweep

bandwidth (Trujillo et al. 2011). Also, neurons respond selectively to sweep rates even at the very short durations used.

Neurons were classified (e.g., Figure 3.1) as all-pass (AP), band-pass (BP), fast-pass (FP), or slow-pass (SP) according to FM rate selectivity (Felsheim and Ostwald 1996; Mendelson et al. 1993; Poon et al. 1991; Razak and Fuzessery 2006; Ricketts et al. 1998; Tian and Rauschecker 1994; Trujillo et al. 2011). AP neurons respond above 50% of maximum response for all rates tested (e.g., Figure 3.1A). These are non-selective neurons and were not studied further. SP neurons were selective for slow FM sweep rates and responses decreased below 50% of maximal response as FM sweep rate was increased (Figure 3.1D). Relatively few SP neurons were found in this study, thus mechanisms were not explored in SP neurons. BP neurons were selective for a range of rates, with responses dropping below 50% of maximal response as FM sweep rate was decreased or increased beyond that range (e.g., Figure 3.1B). FP neurons were selective for fast FM sweep rates and responses decreased below 50% of maximal response as FM sweep rate was decreased (e.g., Figure 3.1C). This study focused on identifying mechanisms underlying FP and BP rate selectivity.

Neurons were further quantified using the 50% cutoff rate, best rate and rate tuning index (RTI). The 50% cutoff rate was defined as the rate at which response fell to 50% of maximum response. FP neurons have one value of 50% cut-off rate. BP neurons have two such values, one at fast rates (‘50% cut-off – fast’) and one at slow rates (‘50% cutoff – slow’). Best rate (BR) was quantified for BP neurons as center of the range of FM rates that produced >80% of maximum response.

Rate tuning index (RTI) was used to quantify the degree of rate selectivity (Atencio et al. 2007; Brown and Harrison 2009; Trujillo et al. 2011) and is calculated as follows:

$$RTI = (n/n-1) \times [1- (mean/max)]$$

where n = the number of FM sweep rates assessed, 'mean' is the average response across all rates tested and 'max' is the maximum response.

Mechanisms

Following identification of neurons with BP or FP rate selectivity, the contributions of sideband inhibition, duration tuning and facilitation as underlying mechanisms were assessed as follows:

Sideband Inhibition

The bandwidth and arrival time of high-frequency inhibitory (HFI) sidebands were quantified using a two-tone inhibition paradigm (Brosch and Schreiner 1997; Calford and Semple 1995; Gordon and O'Neill 1998; Razak and Fuzessery 2006). The focus was only on the high-frequency sideband because downward sweeps traverse this sideband before entering the excitatory tuning curve. In the two-tone inhibition paradigm, an excitatory (at the CF) tone and a second tone were presented with different delays between them. The intensities of both tones were the same, 10-20 dB above CF threshold. The CF tone was 5 msec in duration and the second tone was 10 msec in duration (rise/fall times of both tones were 1 msec). To identify inhibitory frequencies,

the two tones were presented with delays of -2 to +10 msec between them. Zero delay indicates simultaneous onset, positive delays indicate delayed CF tone relative to the second tone and negative delays indicate that the CF tone was presented first (e.g., Figure 3.2A, B).

A qualitative-quantitative sequence was used to identify the HFI sideband. The frequency of the second tone was roved between the highest excitatory frequency of the neuron and 50 kHz with 1-5 kHz resolution. Preliminary data indicated that inhibitory sidebands in most neurons lie just outside the excitatory tuning curve (consistent with Razak and Fuzessery, 2006; Wu et al., 2008). Therefore, the frequency of second tone was varied with 1 kHz resolution near the high-frequency edge of the tuning curve, and with 5 kHz resolution further away. The frequency-delay combinations of the two tones that resulted in a clear decrease in response compared to CF tone alone were qualitatively noted as inhibitory. The arrival time of HFI was then quantified by holding the frequency of the second tone at the center of this range of inhibitory frequencies and varying the delay between the two tones (e.g., Figure 3.2A, B). The 'arrival time of inhibition' was defined as the delay between the two tones at which the response declined below 50% of response to CF tone alone (vertical arrow in Figure 3.2B). The bandwidth of inhibition was then quantified by holding the delay constant at the delay of maximum inhibition and varying the inhibitory tone frequency in 0.5 kHz steps (Figure 3.2C). The range of frequencies of the second tone that reduced responses by at least 50% of CF response was noted as the bandwidth of HFI.

Duration Tuning

The response of neurons to the CF tone with durations between 2-200 msec was recorded to determine duration tuning. Neurons were classified (e.g., in Figure 3.4) according to duration tuning for CF tones as all-pass-DT, band-pass-DT, short-pass-DT, or long-pass-DT (Fuzessery and Hall 1999; Fuzessery et al. 2006; Razak and Fuzessery 2006). 'DT' is used in this paper to distinguish similar classification scheme for FM rate selectivity functions. All-pass-DT neurons responded within 50% of maximum for all durations. Band-pass-DT neurons demonstrated at least 50% decline from maximum for durations shorter or longer than a preferred duration. The response of short-pass-DT neurons decreased below 50% of maximal response as durations increased. The response of long-pass-DT neurons fell below 50% of maximal response as tone durations decreased.

Facilitation

Neurons that depend on facilitation for rate selectivity respond poorly or not at all to single tones, but show strong two-tone facilitation and robust responses to FM sweeps (Razak and Fuzessery 2008). Therefore, the first step in analyzing this mechanism was to identify neurons that respond well to sweeps, but not to individual tones within the sweep. Only four neurons were found in the core mouse auditory cortex that showed this property. Therefore, it was not possible to further analyze facilitation mechanism in this study. We interpret the scarcity of two-tone facilitation to mean that this mechanism does not contribute significantly to FM sweep rate selectivity in the mouse cortex.

Critical tests for sideband inhibition and duration tuning in shaping FM rate selectivity

If HFI shapes downward FM sweep rate selectivity, then removing the HFI from the sweep should reduce or eliminate rate selectivity. A downward FM sweep will exclude the HFI sideband if the sweep starts inside the high-frequency edge of the tuning curve. The rate tuning index (RTI) can be used to compare rate selectivity for FM sweeps that include and exclude the HFI. The degree to which RTI declines with the exclusion of HFI indicates the necessity of HFI in shaping rate selectivity.

The duration tuning mechanism is based on the interactions between excitation and inhibition generated by individual tones (Casseday et al. 2000; Casseday et al. 1994; Fuzessery and Hall 1999). Therefore, if this mechanism was acting alone, the exclusion of putative sideband inhibition should not influence rate tuning. Therefore, the RTI values for downward FM sweeps that include or exclude sideband inhibition should be similar if duration tuning was the mechanism. Based on these conceptual grounds, the RTI was compared for sweeps that included and excluded HFI to determine whether sideband inhibition or duration tuning was involved in shaping rate selectivity. The abbreviation 'RTI-out' denotes that RTI was calculated for sweeps that started outside the tuning curve and, therefore, included putative high-frequency sideband. The abbreviation 'RTI-in' indicates that the sweep excluded putative HFI sidebands by starting inside the tuning curve.

RESULTS

The main aim of this study was to determine mechanisms underlying FM rate selectivity in the core auditory cortex (A1/AAF) of the mouse. The focus was only on downward sweeps as most neurons in the mouse auditory cortex respond similarly to up/down sweeps (Trujillo et al. 2011). The focus was also only on band-pass (BP) and fast-pass (FP) neurons in terms of mechanisms. Non-linear facilitation was found in only 4 of these neurons. This mechanism appears to play a minor role in shaping FM rate selectivity in A1/AAF of the mouse. Therefore, the rest of the manuscript describes how sideband inhibition and duration tuning mechanisms shape BP and FP selectivity for downward FM sweeps. Whether HFI sideband shaped rate tuning was tested in 53 neurons. Whether duration tuning shaped rate tuning was tested in 97 neurons (71 BP and 26 FP).

Sideband inhibition

HFI sideband explained downward FM rate selectivity in 47/53 (88.8%) neurons tested. Figure 3.2 shows an example. Figure 3.2A is a schematic of the two-tone inhibition paradigm. Figure 3.2B shows that this neuron exhibited a maximal decline in response when the CF tone (16 kHz) was delayed by 2 msec relative to the inhibitory tone (23 kHz). The arrival time, defined as the delay at which response declined to 50% of response to CF tone alone, was ~0.44 msec (Figure 3.2B). Figures 3.2C – 3.2F shows PSTHs for the arrival time function depicted in Figure 3.2B. The bandwidth of inhibition was obtained by keeping the delay between the two tones constant (at the delay of

maximum inhibition, 2 msec for this neuron) and varying the frequency of the inhibitory tone. The range of frequencies that inhibit the response to at least 50% of CF response was noted. Frequencies between 21.5-23.5 kHz satisfied the 50% inhibition criterion in this neuron (Figure 3.2G). The interaction between HFI bandwidth and arrival time can predict rate selectivity (Razak and Fuzessery 2006). The 50% cut-off rate is predicted by the following formula:

Predicted 50% cut-off rate = [HIF - HEF] / arrival time (unit kHz/msec)

where, HIF is the highest inhibitory frequency and HEF is the highest excitatory frequency The excitatory tuning curve of the neuron in Figure 3.2 at the intensity at which two-tone inhibition was measured was 9 – 22 kHz. Therefore, the spectral difference between HIF (23.5 kHz) and HEF (22 kHz) was 1.5 kHz. Given the arrival time of 0.44 kHz/msec, the predicted 50% cutoff was 3.41 kHz/msec (1.5 kHz/0.44 msec). Figure 3.2H shows the actual FM rate selectivity function for this neuron. When the sweep included the HFI (the 50-5 kHz sweep) the actual 50% cut-off rate was 3.41 kHz/msec, the same as the predicted value. When the sweep excluded the HFI by starting inside the excitatory tuning curve (the 20-5 kHz sweep), the neuron lost rate selectivity (Figure 3.2H) indicating that the HFI was necessary for rate selectivity in this neuron.

Figure 3.3 shows a FP neuron which depended on HFI sideband to shape rate selectivity. The HFI arrival time (3.5 msec, Figure 3.3A) and bandwidth (5 kHz) in this neuron predicted a 50% arrival time of 1.42 kHz/msec. The observed 50% cut-off rate was 1.4 kHz/msec (Figure 3.3B). When the HFI was excluded from the sweep, the

neuron lost rate selectivity indicating that the HFI shaped rate selectivity in this FP neuron.

HFI was quantified using the two-tone inhibition paradigm in 53 neurons that were BP or FP rate selective. The criterion for 50% inhibition (e.g., Figures 3.2B, 3.3A) was met in 47 (88.8%) neurons, indicating HFI was present in the majority of neurons in the core auditory cortex of the mouse. The mean arrival time and bandwidth of HFI were 2.62 ± 2.2 msec and 4.26 ± 2.4 kHz, respectively (n=47). In these neurons, the actual FM rate selectivity functions were also recorded facilitating a comparison of predicted and observed rate selectivity. There was a strong correlation between the predicted and observed 50% cut-off rate (Figure 3.6A, Pearson correlation, $r = 0.73$, $p < 0.001$). The regression line lies close to the unity slope line indicating the accuracy with which sideband properties predicted rate selectivity. In 36/47 neurons with identified HFI, the critical test for the contribution of sideband inhibition to rate selectivity was performed. That is, rate selectivity index for sweeps that included the HFI (RTI-out) was compared with rate selectivity index when HFI was excluded (RTI-in). The mean RTI-in was significantly lower than the mean RTI-out (Figure 3.7A, paired t-test, $t= 9.22$, $p < 0.001$, $\eta^2 = 0.84$) indicating that exclusion of HFI from the sweep significantly reduced rate tuning in these neurons. Together, these data indicate that HFI was present in the majority of BP/FP neurons, the properties of HFI predicted rate selectivity and exclusion of HFI reduces/eliminates rate selectivity.

Duration Tuning

Duration tuning for CF tones was examined in 97 neurons. Figure 3.4 provides examples and associated PSTHs for the four different types of duration tuning observed in this study. All neurons recorded in this study responded to the onset of the tones in a manner similar to that depicted in the PSTHs in Figure 3.5. No offset responders were found. Figure 3.4E shows the distribution of the different duration tuning types. The vast majority of neurons were all-pass-DT (non-selective for tone duration). A third of the population (33/97) of neurons exhibited short-pass-DT or band-pass-DT in the core auditory cortex of the mouse. Figure 3.5 depicts a neuron in which short-pass duration tuning predicted FM sweep rate selectivity. The neuron was strongly selective for the duration of the CF tone, with a best duration of ~2.2 msec. The 50% cut-off duration was 7 msec (vertical arrow in Figure 3.5A) indicating tone durations longer than 7 msec elicited less than 50% of maximum response from this neuron. The excitatory tuning bandwidth of this neuron at the intensity at which duration tuning was determined was 9 – 20 kHz (excitatory bandwidth of 11 kHz). Using the method of Fuzessery et al. (2006), the 50% cutoff sweep rate and best sweep rate for DFM can be predicted as follows:

Predicted 50% cutoff = [Excitatory Bandwidth/50% cutoff duration for pure tones]

Predicted Best Rate = [Excitatory Bandwidth/best duration for pure tones]

For the neuron in Figure 3.5, the predicted 50% cutoff was 1.57 kHz/msec (11 kHz/7 msec, dashed arrow in 5B). The predicted best rate was 4.98 kHz/msec (11 kHz/2.2 msec). The observed 50% cutoff and best rate for the neuron depicted were 0.8

kHz/msec and 3.08 kHz/msec respectively. Whether HFI was also present in this neuron was not evaluated. However, exclusion of putative HFI by starting the sweep inside the tuning curve (the 20-5 kHz/msec sweep), did not reduce rate tuning (the RTI-in and RTI-out were similar, Figure 3.5B). This indicates that mechanisms within the excitatory tuning curve, and not HFI, shaped FM sweep rate tuning in this neuron. The prediction data suggest that duration tuning is the likely underlying mechanism.

In 33 short-pass-DT and band-pass-DT neurons, excitatory frequency tuning curves and actual FM rate selectivity curves were also recorded, facilitating a comparison of predicted and observed FM rate selectivity. Figure 3.6B demonstrates that predicted 50% cut-off rate based on duration tuning is correlated with observed 50% cut-off rate ($r = 0.53$, $p < 0.01$), Figure 3.6C demonstrates that the predicted and observed best rate of band-pass neurons were also correlated ($r = 0.39$, $p < 0.05$). We predicted that the RTI-out and RTI-in of neurons that depend on duration tuning for rate selectivity will be similar (e.g., Figure 3.5). However, in the 21 short-pass duration tuned neurons in which RTI-in and RTI-out were also determined, there was a reduction in RTI when the sweep started inside the tuning curve (Figure 3.7A, $t = 2.92$, $p < 0.01$, $\eta^2 = 0.56$). This suggests that HFI may contribute to rate selectivity in these neurons as well. A comparison of effect size reveals that the reduction in RTI-in compared to RTI-out is greater for neurons that depended on HFI for rate tuning than for neurons that depended on duration tuning ($\eta^2 = 0.84$ vs. $\eta^2 = 0.56$). Figure 3.7B provides further support for this assessment. The difference in RTI (RTI-out – RTI-in) was compared between HFI and duration tuned neurons. The reduction in RTI in duration tuned neurons was significantly smaller than in

the neurons with HFI (Figure 3.7B, two-sample t-test, $t = 2.56$, $p < 0.05$). The RTI-out *versus* RTI-in comparison shows that even in duration tuned neurons, putative HFI sidebands contribute to rate selectivity. These data also indicate that FM rate selectivity is more dependent on sweep bandwidth in neurons that depend on the HFI mechanism than those that depend on duration tuning.

Prediction accuracy was quantified using the following equation as a measure of how close the predicted and observed 50% cut-off rates were:

Prediction Accuracy = $\left|$(observed 50% cutoff - predicted 50% cutoff)$\right|$ / observed 50% cutoff.

The prediction accuracy did not depend on which mechanism shaped rate selectivity (Figure 3.6D. $t = 1.21$, $p = 0.23$) indicating that when present either mechanism predicted rate selectivity similarly. Even though both mechanisms predict rate selectivity, we interpret that sideband was the dominant mechanism simply because HFI was present in a larger percentage of neurons (~89%) than duration tuning (33%). The distribution of these two mechanisms is not CF- dependent. A t-test between the CF of duration tuned neurons and neurons that HFI revealed no significant difference ($t = -1.2$, $p = 0.23$). Therefore, these mechanisms are likely to be found anywhere along the tonotopic axis. However, neurons with HFI and duration tuning exhibited significantly different 50% cut-off rates. The 50 % cutoff rate was significantly slower for duration tuned neurons then for HFI neurons (Figure 3.6E, two-sample t-test, $t = 2.57$, $p < 0.05$). This indicates differences in response selectivity shaped by each mechanism.

A minority of neurons exhibited both HFI and duration tuning

Whether both mechanisms were present in the same neuron was assessed in 32 neurons that had HFI. Ten (~31%) of these neurons were also duration tuned. This level of duration tuning is consistent with the ~30% duration tuning found in the overall population. The presence of both mechanisms in the same neurons raises the question of whether these mechanisms independently predict observed rate selectivity or if they add to each other in some manner. Figure 3.8 shows a representative neuron with both mechanisms in which either mechanism independently predicts observed rate selectivity. This neuron was duration tuned to the CF tone (Figure 3.8A) with a best duration ~ 3 msec. The neuron also exhibited HFI, with arrival time of 1.6 msec and a bandwidth of 5 kHz (Figure 3.8B). The neuron was BP selective for FM sweep rates (Figure 3.8C). The predicted 50% cutoff using duration tuning (2.6 kHz/msec) or using HFI (3.2 kHz/msec) were similar to the observed 50% cutoff rate (4.1 kHz/msec). An analysis of prediction accuracy for the 10 neurons using each mechanism showed that HFI and duration tuning individually predict similar rate selectivity in these neurons (Figure 3.8D, paired t-test, $t = -1.73$, $p = 0.12$).

DISCUSSION

At least two different mechanisms shape rate selectivity in the core auditory cortex of the young C57 mouse: sideband inhibition and duration tuning. Although both mechanisms predicted rate selectivity equally well, sideband inhibition was found in more neurons tested (~89%) than duration tuning (33%). Facilitation mechanism was

rarely seen in the core auditory cortex. On average, neurons that depend on duration tuning for rate selectivity exhibited a slower 50% cut-off rate compared to neurons that depended on HFI (Figure 3.6E). The 50% cut-off rate is approximately in the middle of the range of rates that produce maximal change in response magnitude in a neuron. Therefore, it is the rate around which the neuron provides maximal information (Harper and McAlpine 2004). This suggests that the two mechanisms result in maximum information about FM sweep rates over different, but overlapping, ranges of rates. In addition, the sweep bandwidth influenced rate tuning to a greater degree in neurons that depended on HFI compared to neurons that depended on duration tuning for rate tuning (Figure 3.7). Thus the two mechanisms produced different rate selectivity properties.

Duration tuning for tones in the auditory system

The relative scarcity of band- and short-pass duration tuning in the mouse A1 is consistent with similar findings in the mouse and chinchilla IC (Brand et al. 2000; Chen 1998), the pallid bat A1 (Razak and Fuzessery 2006) and the cat cortical dorsal zone (He et al. 1997). This differs from findings in little brown bat A1 (Galazyuk and Feng 1997), pallid bat and big brown bat IC (Casseday et al. 1994; Fuzessery et al. 2006) in which ~50-60% of neurons exhibit short- and band-pass duration tuning. Thus, comparative data in general point to more duration tuning in the midbrain of bats compared to auditory cortex across species, although the little brown bat data serve as an exception to this generalization.

Duration tuning has been typically proposed as a temporal feature detector for conspecific vocalizations (Brand et al. 2000; Feng et al. 1990; Gooler and Feng 1992). In frogs for example, neurons in the auditory midbrain have been postulated to code for durations of mating calls or the amplitude modulations contained within them (Feng et al. 1990; Gooler and Feng 1992). Fuzessery et al. (2006) suggested an additional role for duration tuning. Duration tuning for tones in the pallid bat IC shapes spectrotemporal integration relevant to FM rate selectivity. According to this model, sweeps with rates that causes the excitatory tuning curve to be stimulated at the optimal duration will elicit maximum response. For slower and faster sweeps, the excitatory tuning curve is stimulated over non-optimal durations, and thus such rates elicit reduced responses. This was found to be the case in the mouse auditory cortex as well in which CF duration tuning and width of excitatory tuning curve predicted FM rate selectivity in ~33% of neurons. Thus, duration tuning in the auditory system may serve to establish both temporal and spectrotemporal filters across taxa.

Two mechanisms have been proposed to explain duration tuning for short duration tones (Casseday et al. 1994; Fuzessery and Hall 1999). The first mechanism, known as the coincidence model explains selectivity in short- and band-pass neurons. The first component in this model is a short latency IPSP that lasts for the duration of the tone. The second component is a delayed EPSP generated by tone onset. At the optimal duration, rebound from the IPSP will coincide with the delayed EPSP to elicit robust responses (Casseday et al. 1994). At other delays, coincidence will be absent or sub-optimal. This model predicts selectivity in offset neurons in which response latency is

tied to stimulus offset. Since none of the neurons in the mouse auditory cortex in this study exhibited offset responses, it is unlikely that the coincidence mechanism is involved.

The second mechanism, known as the anti-coincidence mechanism explains short-pass duration tuning in onset neurons (Fuzessery and Hall 1996). In this model, an onset-triggered IPSP lasts the duration of the sound. The second component is an onset-triggered, but delayed, EPSP. The EPSP latency is at least as long as the optimal sound duration. Thus optimal, short duration tones will generate IPSP that is over before the EPSP occurs. For longer, non-optimal durations, the IPSP will overlap with the EPSP and thus reduce responses. Because all neurons in this study responded to stimulus onset, duration tuning in the mouse auditory cortex is likely explained by the anti-coincidence mechanism.

Sideband inhibition in the auditory system

Sideband inhibition is common in auditory system across species (Brosch and Schreiner 1997; Calford and Semple 1995; Razak and Fuzessery 2006; Sutter and Loftus 2003; Wu et al. 2008; Zhang et al. 2003). Suga (1965) proposed that sideband inhibition properties may explain FM sweep selectivity. This mechanism was investigated in detail in the auditory system of bats (Gordon and O'Neill, 1988; Fuzessery et al. 2006, Razak and Fuzessery, 2006). In these studies, it was shown that the spectrotemporal interactions between excitatory tuning curve and inhibitory sidebands shaped FM sweep selectivity. In the pallid bat A1, this was the dominant mechanism of sweep selectivity. The present

data on mouse cortex indicates that similar mechanisms shape selectivity across auditory generalists (mice) and specialists (pallid bat). This study was limited to mechanisms shaping rate selectivity for downward sweeps and therefore focused on the HFI sideband. Most neurons in the mouse auditory cortex respond similarly to up and down sweeps (Trujillo et al. 2011). Therefore, it is predicted that the properties of sideband on the low-frequency side are similar to those on the high-frequency side. In direction selective cells, asymmetries in properties of sidebands may be present (Razak and Fuzessery, 2006). Wu et al., (2008) suggested that sideband inhibition is shaped by rapid spiking interneurons commonly identified as Parvalbumin positive. These neurons are known to be involved in shaping selectivity for rapid temporal features of sound (Atencio and Schreiner 2008), consistent with the notion proposed here that sideband inhibition shapes selectivity for fast or medium sweep rates.

Origins of mechanism

It is unclear if these mechanisms are computed at the level of the cortex or whether the selectivity is inherited from subcortical computations. In aging rats, FM sweep selectivity is reduced in the auditory cortex but not in the midbrain or thalamus (Lee et al. 2002; Mendelson and Lui 2004; Mendelson and Ricketts 2001). This suggests that at least some of the mechanisms shaping sweep selectivity in rodent A1 are local. Iontophoretic application of GABAA receptor antagonists have shown that sideband inhibition is shaped at the level of the IC (Fuzessery and Hall 1996) as well as in A1 (Razak and Fuzessery 2009). This indicates that FM sweep selectivity may be first

shaped in the midbrain and refined at the level of the cortex. There is a high degree of convergence in the midbrain-thalamus-cortex pathway that may smear cortical selectivity necessitating refinement in the cortex using local inhibitory circuits (McMullen and de Venecia 1993; Middlebrooks and Zook 1983). This is consistent with data from Miller et al. (2001) who showed that excitatory properties are more faithfully transmitted from thalamus to A1 compared to inhibitory properties.

Comparison to previous studies of auditory and other sensory systems

In the bat auditory system, sideband inhibition, facilitation and duration tuning shape FM rate selectivity (Gordon and O'Neill 1998; Razak and Fuzessery 2006). Other mechanisms such as relative amplitudes of inhibitory/excitatory conductance (of already selective inputs) and spike threshold also contribute (Gittelman and Pollak 2011). Properties of sideband inhibition have also been shown to play a role in FM sweep direction selectivity in the rat A1 (Sadagopan and Wang 2010; Zhang et al. 2003). The mouse auditory cortex is similar to the pallid bat A1 in that sideband inhibition is the dominant mechanism. However, these two systems differ in that facilitation, but not duration tuning, was the second most common mechanism in the pallid bat cortex. Less than 8% of neurons were duration tuned, and even in these neurons, duration tuning did not predict rate selectivity. In the mouse auditory cortex, facilitation was largely absent. Both sideband inhibition and facilitation shape relatively similar rate selectivity in the pallid bat A1 and this may reflect tuning of mechanisms to respond selectivity to the very narrow range of rates present in the echolocation calls of the pallid bat. In the mouse,

sideband inhibition and duration tuning shape selectivity for different ranges of rates and this may reflect the broader range of rates relevant to an auditory generalist.

Selectivity for FM sweep rate is analogous to movement velocity selectivity in the visual system. Three mechanisms have been proposed to underlie velocity selectivity that are fundamentally similar to those in the auditory system. These are spatiotemporal asymmetries in lateral inhibition (superior colliculus-(Razak and Pallas 2005); visual cortex-(Duysens et al. 1985a; Duysens et al. 1985b; Patel and Sillito 1978)), facilitation (Duysens et al. 1985a) and tuning for the duration that a stimulus spends in the receptive field (Duysens et al. 1996). These similarities across auditory systems and other sensory systems indicate that multiple, but similar, solutions are used to solve analogous problems.

Methodological Considerations

These data have to be interpreted within the context of certain methodological issues. The first is that mechanisms were assessed under ketamine/xylazine/isoflurane anesthesia. Ketamine is widely used as an anesthetic in auditory neurophysiology. In the auditory cortex, ketamine reduces spontaneous activity and evoked neuronal spiking to auditory stimuli (Syka et al. 2005; Zurita et al. 1994). Thus it is likely that response magnitudes reported in this study are under-estimates relative to responses from awake animals. It is also possible that mechanisms related to sound-driven inhibition not related to two-tone inhibition may have been missed in this study (Galindo-Leon et al., 2009). Whether these anesthetics influence duration tuning and/or the arrival time and

bandwidth properties of sideband inhibition has not been systematically evaluated and cannot be commented on. The second issue is the use of linear FM sweeps as stimuli. (Nelken and Versnel 2000) compared ferret A1 responses to linear and logarithmic sweeps and found that FM rate selectivity did not differ based on the type of sweep, suggesting the sweep trajectory will not have had a bearing on the results reported here. The present study was also limited in scope. Focus was on mechanisms underlying FP and BP selectivity for downward sweeps. It is likely that additional mechanisms exist to shape slow-pass FM rate selectivity.

Conclusions

These data show that neural selectivity for a relatively simple sound can be predicted based on linear interactions between two tones (sideband) or temporal selectivity for individual excitatory tones (duration tuning). This is consistent with data from the pallid bat auditory system. The non-linear facilitation mechanism was largely absent in the mouse cortex. How selectivity for FM sweeps then translates to representation of complex vocalizations remains to be explored. Mouse ultrasonic vocalizations contain FM sweeps with rates between 0.5 and 3 kHz/msec (Grimsley et al. 2011; Liu et al. 2003; Portfors 2007; Rotschafer et al. 2012). Either the 50% cut-off rate or best rate of most neurons in the core auditory cortex of the mouse are present in the range of rates present in vocalizations (Trujillo et al. 2011), and thus may be involved in vocalization processing. However, one caveat with this interpretation, and a paradox with mouse vocalizations in general, is that most neurons in the central IC and core auditory

cortex have CFs below 50 kHz, while most adult vocalizations are in the 60-110 kHz range (Portfors et al. 2009). Portfors and colleagues suggested one possible resolution in that low-CF neurons may respond to distortion products in the high-frequency vocalizations (Holmstrom et al. 2010; Portfors et al. 2009). It remains to be seen if such distortion products maintain sweep rates to which most low-CF neurons are selective for.

While both duration tuning and sideband inhibition depend on interactions between excitation and inhibition, they differ in one fundamental way. According to the scheme of (Happel et al. 2010) duration tuning can be thought of as arising due to on-CF and near-CF interactions between excitation and inhibition. Sidebands can be thought of as arising from non-CF and on-CF interactions. Some of these non-CF inputs are inhibitory and generate the sideband (Kaur et al. 2005). In presbycusis, the loss of response to high-frequencies suggest that the HFI-based mechanism will be more susceptible to aging and hearing loss and underlie altered selectivity for FM sweeps in the cortex (Lee et al. 2002; Mendelson and Lui 2004; Mendelson and Ricketts 2001). This may explain reduction in speech processing in quite and in noise with aging and hearing loss. The general reduction in inhibition with aging may also impact duration tuning-related selectivity. The extent to which these two mechanisms are differentially plastic in presbycusis is currently being investigated. An understanding of the mechanisms of spectrotemporal processing in the mouse cortex will facilitate studies of cellular mechanisms of experience-dependent auditory system plasticity.

Figures

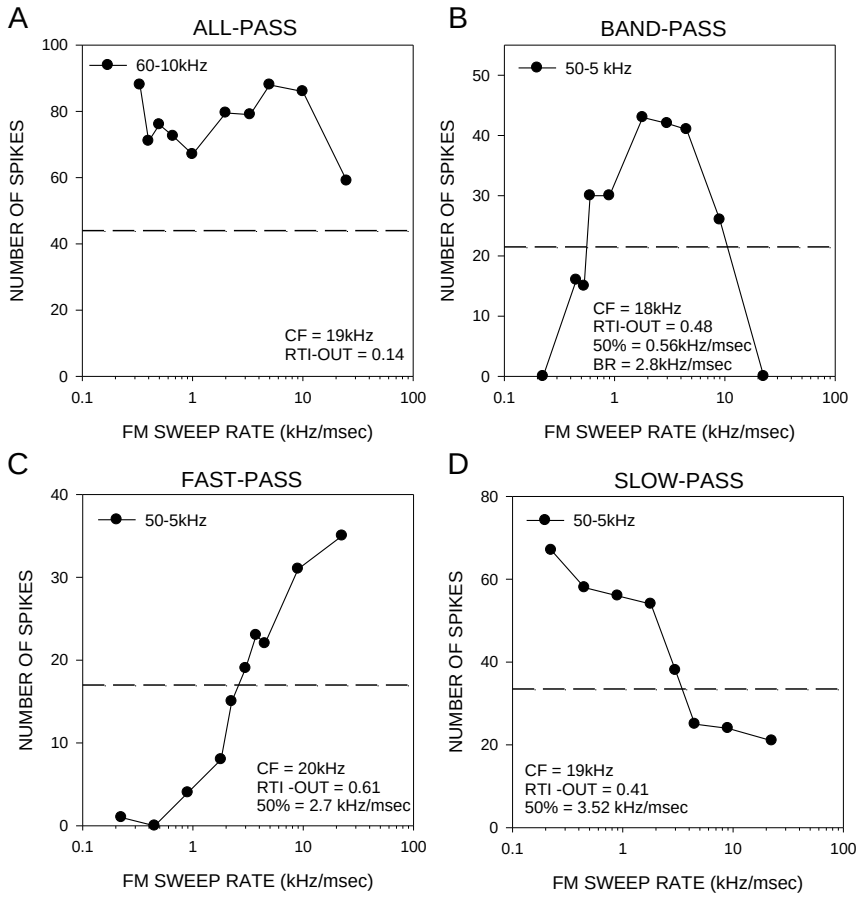

Figure 3.1: Classification of FM sweep rate tuning. (A) All-pass (B) Band-pass (C) Fast-pass (D) Slow-pass. The dashed line in each panel marks 50% of maximum response. The 'number of spikes' on the y-axis in this and all subsequent graphs are in response to 20 repetitions of each stimulus. The bandwidth of sweep used is indicated in each panel. CF: characteristic frequency, RTI-out: rate tuning index calculated for sweeps with bandwidths that extended well outside the excitatory tuning curve, BR: best rate for the band-pass neuron, 50%: the 50% cut-off rate for fast-pass and band-pass neurons.

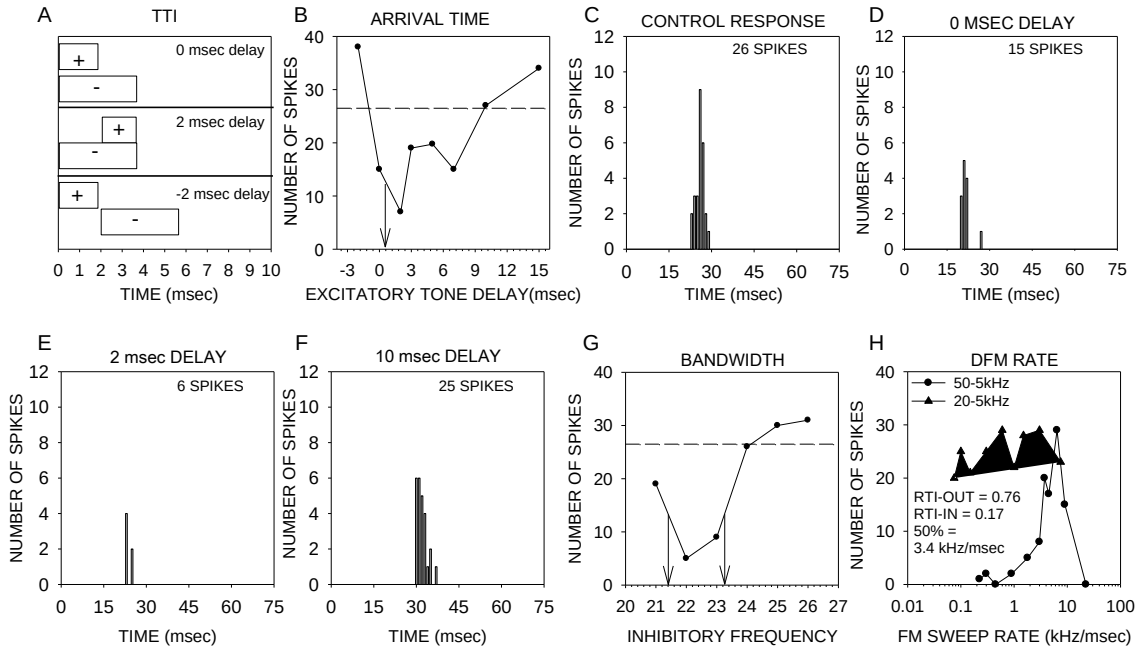

Figure 3.2: An example of delayed HFI shaping downward FM rate selectivity. (A) Schematic for the temporal relationships between excitatory and inhibitory tones used in the two-tone inhibition paradigm. Positive delays indicate that the excitatory (+) tone was delayed relative to the inhibitory (-) tone. Negative delays show the excitatory tone was advanced. Zero delay indicates simultaneous onset of both tones. (B) The two-tone inhibition plot for a HFI tone (23 kHz, 10 msec duration) and an excitatory CF tone (16 kHz, 5 msec duration). The dashed line marks the response to the CF tone presented alone. The vertical arrow shows the delay between the two tones at which response decreases to 50% of CF tone response. This delay, termed 'arrival time of inhibition', was ~ 0.44msec in this neuron. The PSTHs at selected delays (C-F) show the time course of two-tone inhibition. Sound onset is at 0 msec. (G) The bandwidth of HFI was determined by changing the frequency of the inhibitory tone while the delay between the two tones was fixed at the best delay (2 msec) identified in (B). The frequency range that suppressed response of the neuron by at least 50% of CF-alone response was considered bandwidth of HFI. The HFI bandwidth of this neuron (indicated by the vertical arrows) was 2 kHz. (H) The neuron was strongly rate selective (RTI-out = 0.76) when the sweep bandwidth included the HFI (the 50-5 kHz sweep). The neuron lost rate selectivity (RTI –in = 0.17) when the sweep excluded HFI (the 20-5 kHz sweep).

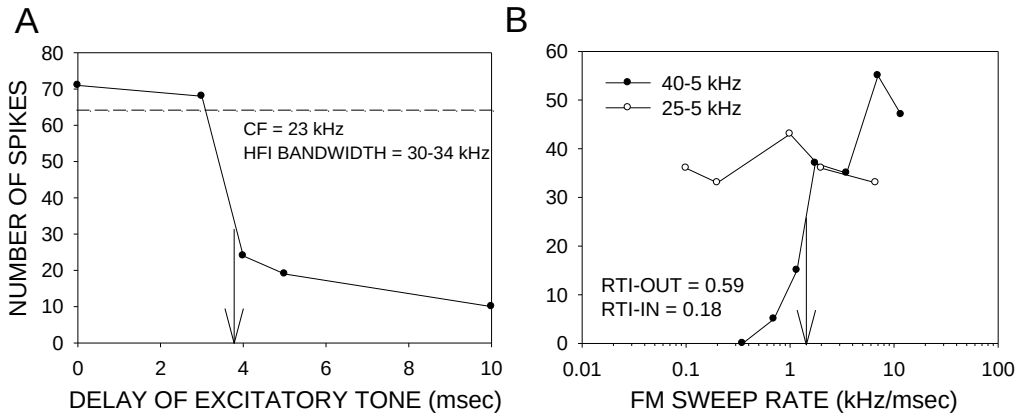

FIGURE 3.3: A second example of delayed HFI shaping downward FM rate selectivity in a FP neuron. (A) The two-tone inhibition plot for a HFI tone (32 kHz, 10 msec duration) and a CF tone (23 kHz, 5 msec duration). The dashed line marks the response to the CF tone presented alone. The vertical arrow shows the arrival time of inhibition (3.5 msec). The bandwidth of HFI inhibition was 30-34 kHz. (B) When the downward FM sweep included the HFI (the 40-5 kHz sweep), the neuron was rate selective, with an RTI-out of 0.59. When the sweep excluded the HFI, the neuron lost sweep selectivity and the RTI-in was 0.18 (the 25-5 kHz sweep).

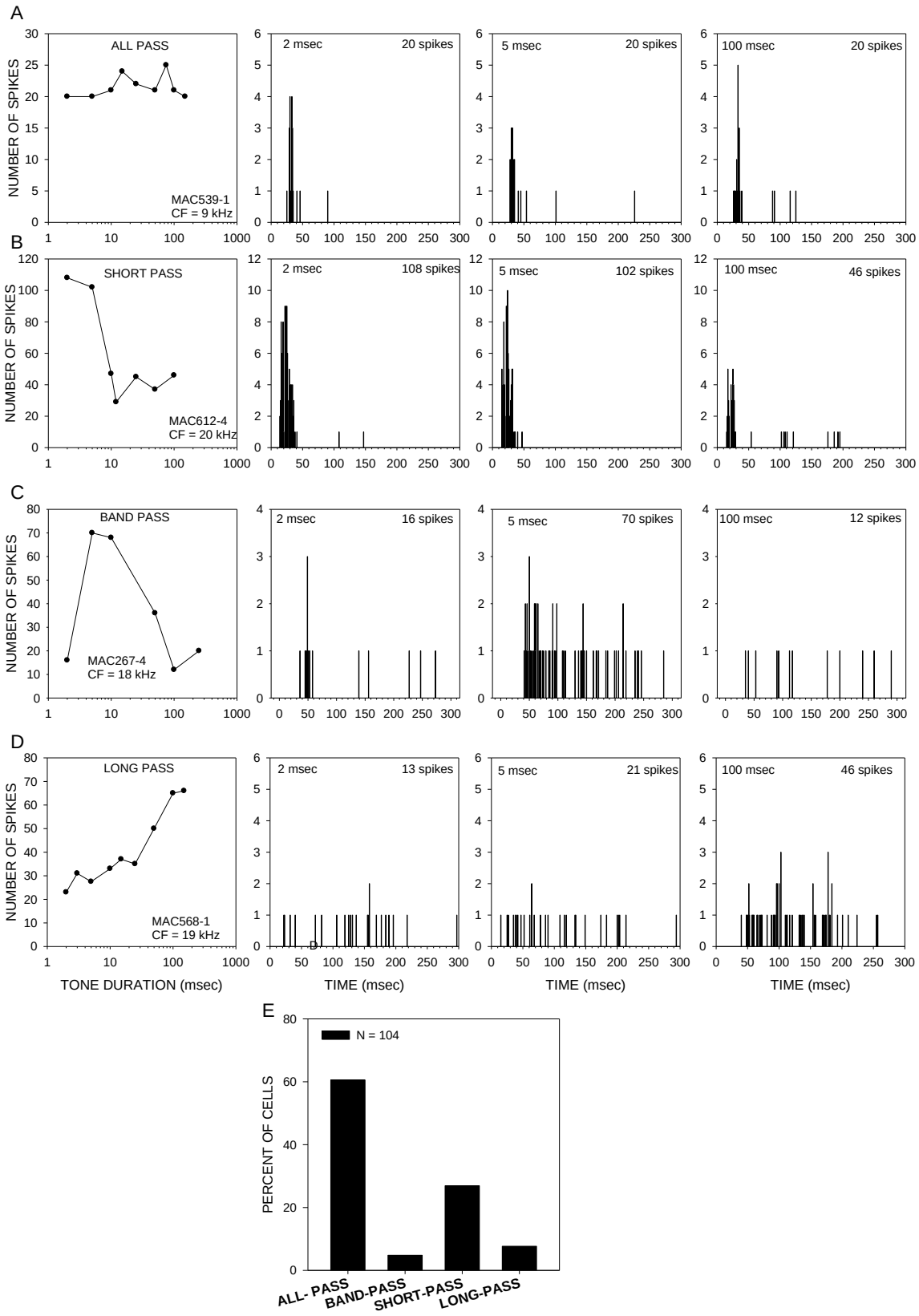
A
ALL PASS
MAC539-1
CF = 9 kHz
2 msec
20 spikes
5 msec
20 spikes
100 msec
20 spikes
B
SHORT PASS
MAC612-4
CF = 20 kHz
2 msec
108 spikes
5 msec
102 spikes
100 msec
46 spikes
C
BAND PASS
MAC267-4
CF = 18 kHz
2 msec
16 spikes
5 msec
70 spikes
100 msec
12 spikes
D
LONG PASS
MAC568-1
CF = 19 kHz
2 msec
13 spikes
5 msec
21 spikes
100 msec
46 spikes
NUMBER OF SPIKES
TONE DURATION (msec)
TIME (msec)
E
N = 104
PERCENT OF CELLS
ALL- PASS
BAND-PASS
SHORT-PASS
LONG-PASS

Figure 3.4: Classification of duration tuning type in response to CF tone (A) All-pass-DT (B) Short-pass-DT (C) Band-pass-DT (D) Long-Pass-DT. Selected PSTHs are also shown. Tone onset is at 0 msec. (E) The distribution of duration tuning types.

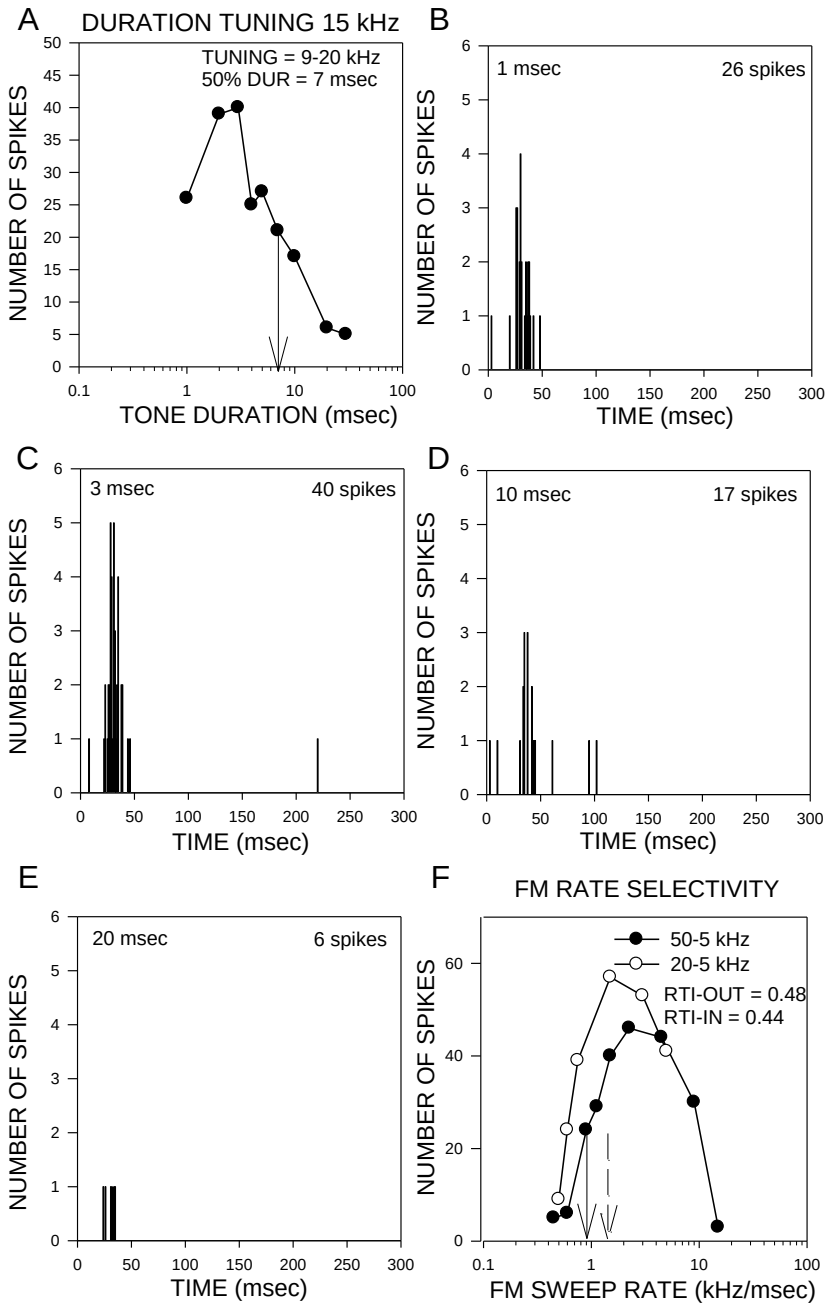

FIGURE 3.5: A neuron that depended on duration tuning for FM rate selectivity. (A) This neuron was tuned to the CF tone (15 kHz) duration with strong responses to durations between 2-3 msec. The vertical arrow depicts the duration at which response decline to 50% of maximum. Duration tuning was tested at 15 dB above CF threshold in this neuron. The excitatory tuning of this neuron at this intensity was 9-20 kHz. (B – E) Select PSTHs for the duration tuning function depicted in (A). (F) When tested with downward FM sweeps, that started well outside the excitatory tuning curve (the 50-5 kHz

sweep), the neuron was BP rate selectivity, with preference for rates ~3 kHz/msec. The rate tuning index for sweeps starting outside the tuning curve (RTI-out) was 0.48. When the sweep started inside the tuning curve (the 20-5 kHz sweep), and thus excluded putative sidebands, the neuron was still BP tuned with a best rate ~2 kHz/msec. The rate tuning index for the sweep starting inside the tuning curve (RTI-in) was 0.44, similar to the RTI-out. This indicates that the contribution of putative HFI to rate selectivity was relatively minor in this neuron. The solid arrow depicts the observed 50% cutoff rate of 0.8 kHz/msec and the dashed arrow depicts the predicted 50% cutoff rate of 1.57 kHz/msec. The predicted best rate was 4.9 kHz/msec and the observed best rate was 3.08 kHz/msec.

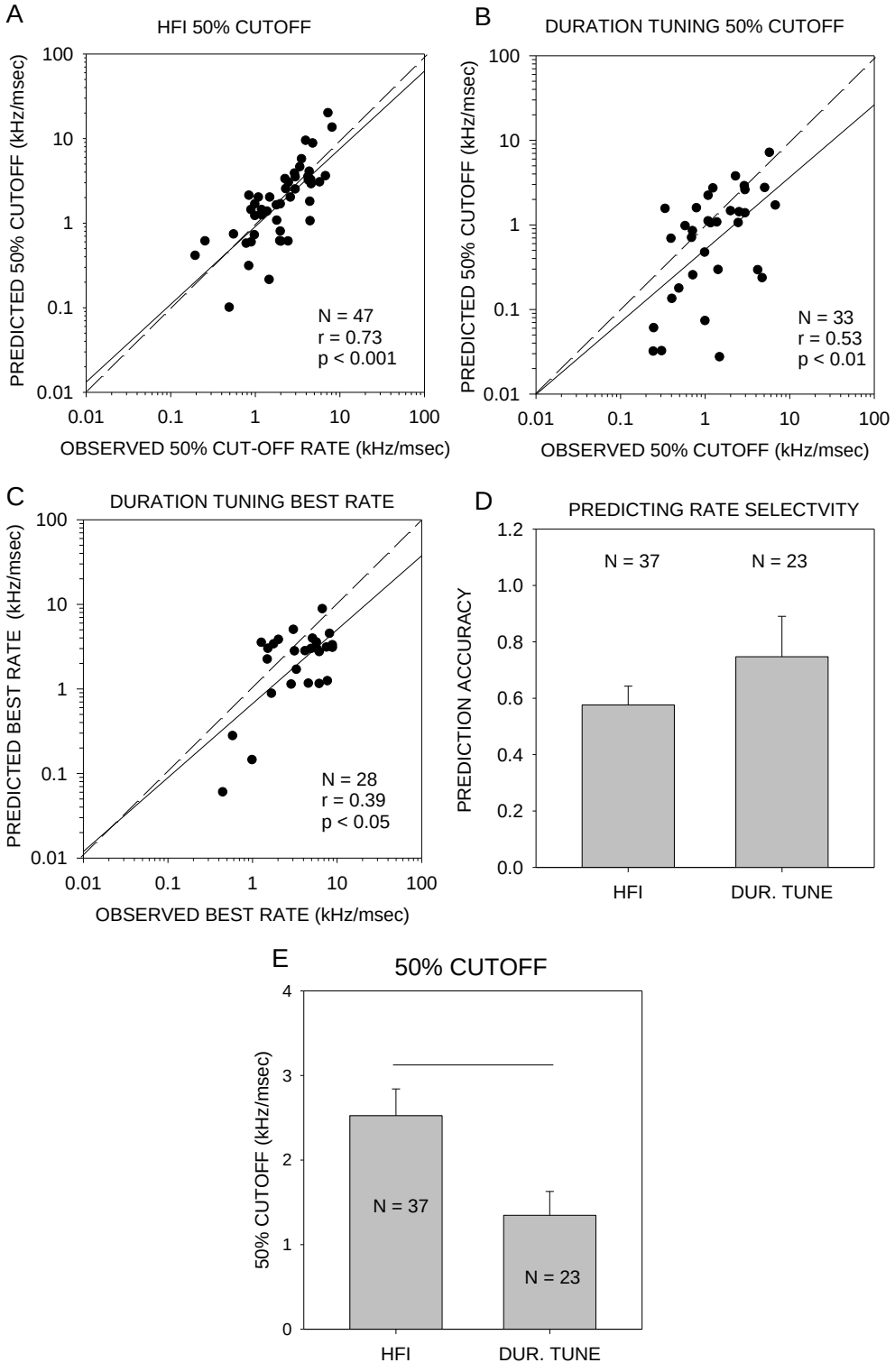
A
HFI 50% CUTOFF
PREDICTED 50% CUTOFF (kHz/msec)
OBSERVED 50% CUT-OFF RATE (kHz/msec)
N = 47
r = 0.73
p < 0.001
B
DURATION TUNING 50% CUTOFF
PREDICTED 50% CUTOFF (kHz/msec)
OBSERVED 50% CUTOFF (kHz/msec)
N = 33
r = 0.53
p < 0.01
C
DURATION TUNING BEST RATE
PREDICTED BEST RATE (kHz/msec)
OBSERVED BEST RATE (kHz/msec)
N = 28
r = 0.39
p < 0.05
D
PREDICTING RATE SELECTVITY
PREDICTION ACCURACY
N = 37
N = 23
HFI
DUR. TUNE
E
50% CUTOFF
50% CUTOFF (kHz/msec)
N = 37
N = 23
HFI
DUR. TUNE

FIGURE 3.6: Predicting Rate Selectivity. (A) Properties of HFI bandwidth and arrival time predicts 50% cutoff rate for FP and BP rate tuned neurons. A Pearson correlation revealed a significant correlation ($r = 0.73$, $p < 0.001$). The diagonal line represents the regression line. The diagonal dashed line represents the unity slope line. (B) An interaction between the 50% cutoff duration for Short-Pass–DT neurons and the excitatory tuning bandwidth predicts 50% cutoff in FP and BP neurons. A Pearson correlation revealed a significant correlation ($r = 0.53$, $p < 0.01$). The diagonal dashed line represents unity slope. (C) An interaction between the best duration and tuning bandwidth predicts the best rate for BP neurons. A Pearson correlation revealed that the correlation was significant ($r = 0.39$, $p < 0.05$). The diagonal dashed line represents the unity slope line. (D) Mean ± SEM for prediction accuracy. The bar titled "HFI" represents neurons where HFI was present and the bar titled "DUR. TUNE" represents neurons where short-pass duration tuning was present. Prediction accuracy did not differ between HFI and duration tuned neurons ($t = -1.21$, $p = 0.23$) indicating that duration tuning and HFI predict 50% cutoff equally well. (E) Mean ± SEM for the 50% cutoff rate for FP and BP neurons. A two-sample t-test revealed that duration tuned neurons have a significantly slower 50% cutoff rate compared to HFI neurons ($t = 2.57$, $p < 0.05$).

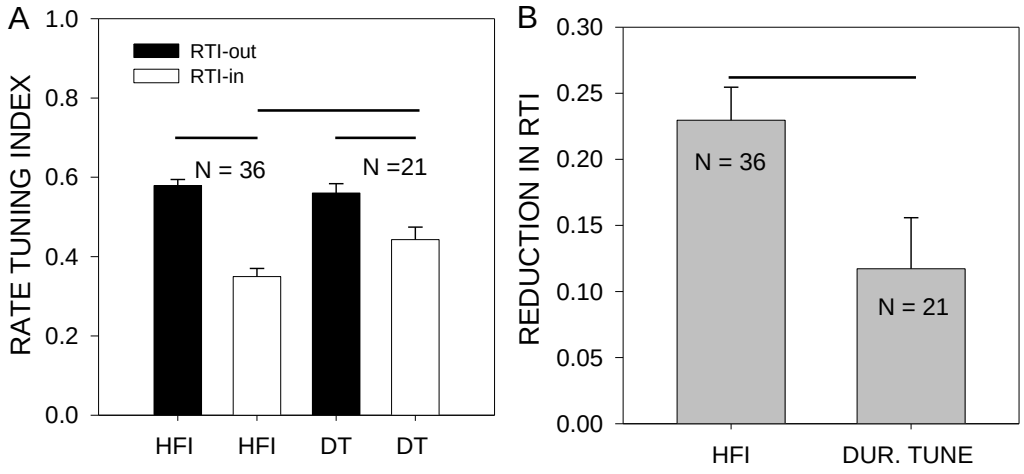

Figure 3.7: RTI is influenced by sweep bandwidth to different degrees in neurons with HFI *versus* duration tuned neurons (A) The mean ± SEM for RTI for sweeps that start outside the excitatory tuning curve (black bars) vs. inside the tuning curve (white bars). Reduction in RTI-in compared to RTI-out would indicate that the neuron is sensitive to sweep bandwidth as a result of sideband inhibition. The horizontal bars represent comparisons for which a t-test revealed significant difference ($p < 0.05$). A paired t-test revealed that RTI was significantly reduced for sweeps starting inside the tuning curve for neurons with HFI ($t = 9.22$, $p < 0.001$, $\eta^2 = 0.84$). RTI-in was also smaller than RTI-out for duration tuned neurons ($t = 2.92$, $p < 0.01$, $\eta^2 = 0.56$), but the reduction in duration tuned neurons was significantly smaller than the reduction seen in neurons with HFI (comparison of effect sizes: $\eta^2 = 0.84$ *versus* $\eta^2 = 0.56$). (B) Mean ± SEM reduction of RTI (RTI Out – RTI In) for the neurons represented in (A). A two-sample t-test revealed that RTI-in is reduced compared to RTI-out to a significantly greater extent in neurons with HFI relative to duration tuned neurons ($t = 2.56$, $p < 0.05$).

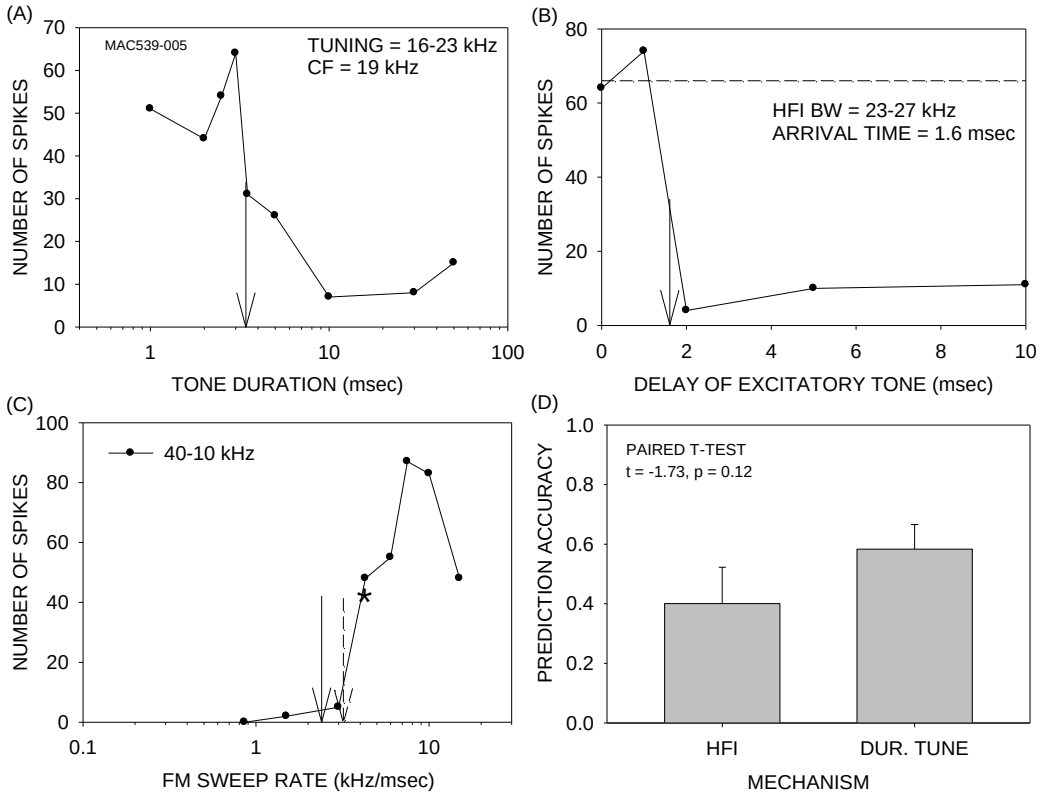

Figure 3.8: Neurons in which both mechanisms are present. (A–C) An example neuron in which both duration tuning and HFI were present. (A) shows the duration tuning function for this neuron. The 50% duration was 3.2 msec and the tuning curve bandwidth was 16-23 kHz, predicting a 50% cutoff of 2.5 kHz/msec (solid arrow in C). (B) shows the arrival time of inhibition (1.6 msec). The bandwidth of inhibition was 5 kHz, predicting a 50% cutoff of 3.1 kHz/msec (dashed arrow in C). The observed 50 % cutoff was 4.1 kHz/msec (asterisk in C). (C) shows the actual rate selectivity function of this neuron. (D) represents prediction accuracy for the 10 neurons in which both mechanisms were present. The bar titled 'HFI' used HFI to predict the 50% cutoff and the bar titled 'DUR. TUNE' used duration tuning to predict. A paired t-test revealed no significant difference between the two predictions ($t = -1.73$, $p = 0.12$) indicating that both mechanisms can independently predict rate tuning.

Chapter 4: Cortical processing of frequency modulated sweeps in a mouse model of presbycusis

Abstract

Presbycusis (age-related hearing loss) is one of the most prevalent disabilities associated with age and can impair speech understanding and social and emotional well-being. How presbycusis impacts spectrotemporal processing in the central auditory system remains unclear. The focus of this study was to compare frequency modulated (FM) sweep processing and underlying mechanisms across three age groups (1-3 months, 6-8 months, and 14-20 months) in a mouse model of presbycusis (C57bl/6 strain). Changes in selectivity and response variability to linear sweeps of either direction (up/down) and different rates (0.8-20 kHz/msec) were quantified. There are four main findings in this study. First, there is a presbycusis-related reduction in FM rate selectivity. Second, there is a presbycusis-related slowing of the sweep rates at which neurons are likely to provide best detection and discrimination of sweep rates. Third, there is a presbycusis-related increase in trial-to-trial variability in the number of spikes and inter-spike intervals. Fourth, there is a reduction in the percentage of neurons exhibiting sideband inhibition as a function of presbycusis. In the young mouse, high frequency inhibition (HFI) shapes FM sweep rate selectivity in 80% of neurons, but only 34% in the middle age and 12% in the old age exhibited HFI. Collectively these results suggest that FM sweep processing becomes both slow and noisy with presbycusis, a finding that may explain speech processing deficits with age-related hearing loss.

Introduction

Human auditory processing abilities deteriorate with age. Age-related deficits are seen in pure tone discrimination, frequency modulated (FM) sweep detection, phoneme discrimination, and word recognition (Fitzgibbons and Gordon-Salant 2001; Gordon-Salant et al. 2006; He et al. 1998; He et al. 2007). Age-related deficits are further compounded by hearing loss. Presbycusis (age-related hearing loss) affects ~35% of humans older than sixty-five and ~45% of humans older than seventy-five years (Gates and Mills 2005). It is the most prevalent form of hearing impairment and contributes to speech processing deficits, social isolation, depression and may contribute to cognitive impairment in the aged (Frisina and Frisina 1997; Gates and Mills 2005; Lopez-Torres Hidalgo et al. 2009; Weinstein and Ventry 1982).

Behavioral studies in humans with presbycusis have shown both spectrotemporal and temporal processing deficits (Fitzgibbons and Gordon-Salant 2004; 2001; Fitzgibbons et al. 2006; Gordon-Salant and Fitzgibbons 1999; 1993; Gordon-Salant et al. 2006; He et al. 1998; He et al. 2007). While physiological studies in animal models of presbycusis have examined temporal processing (Walton et al. 2008; Walton 2010; Walton et al. 1995) with gap detection (Walton et al. 2008) and amplitude modulations (Walton 2010), very little is known about spectrotemporal processing deficits and the underlying mechanisms. Presbycusis in humans and rodents begins with high-frequency hearing loss and spreads to affect lower-frequency channels with age. The fundamental question is how hearing loss at high-frequencies affects neural responses to broadband stimuli. Cortical response selectivity is expected to change profoundly based on the

breadth of spectral and temporal integration cortical neurons perform (Happel et al. 2010; Kaur et al. 2005; Nelken et al. 2003; Razak and Fuzessery 2006; Sadagopan and Wang 2009; Ulanovsky et al. 2004), but the nature of these changes remain unclear.

The purpose of the present study was to determine if and how spectrotemporal processing in auditory cortex changes because of presbycusis. At the outset it must be noted that the purpose was not to disambiguate effects of age versus hearing loss but to quantify the combined effect on spectrotemporal processing. The C57bl/6 mouse strain (C57) is a model of presbycusis and undergoes high frequency hearing loss beginning ~3 months of age and continuing to profound hearing loss by 12 months (Spongr et al. 1997; Willott et al. 1993; Willott et al. 1994; Willott et al. 1991). In this study we focused on response selectivity for FM sweeps in the core auditory cortex of C57 mice to determine the effects of presbycusis. FM sweeps are relatively simple sounds to examine spectrotemporal processing in the auditory system. In addition, mechanisms underlying FM sweep selectivity are known (Gordon and O'Neill 1998; Razak and Fuzessery 2006) facilitating inquiries of not just whether selectivity changes with presbycusis, but also how. FM sweeps are important components for discrimination of speech (Stevens and Klatt 1974; Zeng et al. 2005) and are common components of animal vocalizations. The auditory cortex of all species examined contain neurons selective for the rate (change in frequency over time) and/or direction (upward or downward) of FM sweeps (Atencio et al. 2007; Brown and Harrison 2009; Godey et al. 2005; Hall et al. 2000; Heil et al. 1992b; Mendelson and Cynader 1985; Nelken and Versnel 2000; Razak and Fuzessery 2006; Suga 1965; Tian and Rauschecker 1994; 2004b; Washington and Kanwal 2008). In the

young adult mouse auditory cortex, neurons are selective for a narrow range of FM sweep rates (Trujillo et al. 2011).

We examined FM rate and direction selectivity, variability of response magnitude, first spike latency and inter-spike interval for repeated presentations of FM sweep stimuli, duration tuning to tones and sideband inhibition. The latter two response properties are known to shape FM sweep selectivity in both bats and mice (Godey et al. 2005; Razak and Fuzessery 2006; Trujillo et al. 2012). Three age groups of C57 mice were studied: young ('Y', 1-3 mo old), middle-age ('M', 6-8 mo old) and old ('O', 14-20 mo old). We report that presbycusis results in reduced FM sweep rate selectivity, selectivity for slower sweeps and increased response variability. We also report decreased sideband inhibition as a mechanism shaping FM sweep rate selectivity and increased duration tuning.

Methods

All procedures were approved by The Institutional Animal Care and Use Committee at the University of California, Riverside. Mice were obtained from an in-house breeding colony that originated from Jackson Laboratory (Bar Harbor, Maine). Two to five littermates were housed in each cage under a 12/12 light/dark cycle and fed *ad libitum*. The C57 mice show accelerated age-related hearing loss with a predictable time course (Henry and Chole 1980; Hunter and Willott 1987; Mikaelian 1979; Spongr et al. 1997; Willott 1986). Three age groups were tested in this study. Mice of either sex were used. The young age group consisted of ages between 1 – 3 months (N = 48 mice),

the middle age group consisted of ages between 6 – 8 months (N = 31 mice), and the old group consisted of 14 – 20 months (N = 34 mice). These age ranges were chosen to study periods of relatively little hearing loss to moderate to profound loss (Ison et al. 2007; Willott et al. 1993; Willott et al. 1994; Willott et al. 1991).

Surgical Procedure

A combination of ketamine (150 mg/kg) and xylazine (10 mg/kg) was injected (i.p.) to induce anesthesia for surgery and electrophysiology. Anesthesia was maintained throughout the experiment by either supplemental dosage of ketamine-xylazine or isoflurane inhalation (0.2–0.5% in air). Anesthetic state was assessed via the toe-pinch reflex test throughout the experiment and supplemental anesthetic was administered as needed. After an areflexic state of anesthesia was reached, a midline scalp incision was made and the right temporalis muscle was reflexed. A dental drill was used to perform a craniotomy to expose the auditory cortex. At the end of electrophysiological recording, mice were euthanized with pentobarbital sodium (125 mg/kg).

Acoustic Stimulation

It is important to note that the FM sweep and tonal stimuli used in this study were all presented at 10-20 dB above response threshold, and therefore there was not a detectability issue in studies of 'M' and 'O' mice recordings. Acoustic stimuli were driven and data were acquired by custom software (Batlab, Dr. Don Gans, Kent State University, Kent, OH). Sound intensities were controlled with programmable attenuators

(PA5; Tucker-David Technologies, Gainesville, FL) prior to amplification by a stereo amplifier (Parasound HCA1100) or an integrated amplifier (Yamaha AX430). Sounds were delivered through a free-field ribbon tweeter (LCY-K100, Madisound,Wisconsin) located 6 inches and 45° from the left ear, contralateral to physiological recordings. Frequency response of the acoustic stimuli system was flat within ± 3dB for frequencies between 7-40 kHz as measured by a ¼ inch Bruel and Kjaer microphone and measuring amplifier. A Krohn-Hite filter (Brockton, MA) was used to filter out frequencies below 5 kHz (Butterworth, 24dB/octave). Experiments were conducted in a sound-attenuated chamber lined with anechoic foam (Gretch-Ken Industries, Oregon).

Auditory Brainstem Response

Auditory brainstem responses (ABR) were acquired in a subset of mice (14 young, 22 middle, and 20 old) to quantify variability in hearing loss within age groups. Electrodes were placed subdermally along the midline of the scalp (active electrode), the left cheek (reference) and the tail (ground) (Zheng et al. 1999). Pure tones were presented from 7 – 50 kHz (5 msec duration, 0.5 msec rise/fall time, 10 Hz repetition rate, 256 repetitions) in 3-5 kHz increments. Evoked ABR waveforms were acquired in a 7.5 msec window relative to stimulus onset. Threshold at each frequency was obtained by stepping up attenuation from 10 dB. The threshold was defined as the maximum attenuation (minimum intensity) that produced at least three distinct peaks within 7.5 msec.

Electrophysiology

A stereotaxic apparatus (Kopf model 930, California) and bite bar (Kopf model 923B) were used to secure mice for electrophysiological recordings. Neurophysiological recordings were acquired using glass microelectrodes filled with 1M NaCl (2 – 10 MΩ impedance). Electrodes were driven into the cortex with a Kopf direct drive 2660 micropositioner. Single-unit recording were obtained between depths of 124 μm and 728 μm (mean = 402 ± 114) for 'Y', between 111 μm and 714 μm (mean = 405 ± 125) in 'M', and between 102 μm and 724 μm (mean = 399 ± 116) in 'O'. Single-unit responses were identified by constancy of amplitude and waveform as displayed on an oscilloscope and were isolated using a window discriminator. Data quantification consisted of counting the number of spikes elicited over 20 stimulus repetitions. Poststimulus time histograms (PSTHs) were obtained over a 300 msec window relative to stimulus onset.

Data Acquisition

The primary auditory cortex (A1) of the C57 mouse can be identified by vascular landmarks (Willott et al. 1993) as well increasing characteristic frequency (CF) in the caudal to rostral direction (Stiebler et al. 1997; Trujillo et al. 2011). The anterior auditory field (AAF) is located immediately rostral to A1 and exhibits a reversed tonotopy relative to A1. Both A1 and AAF are considered core auditory cortex (Cruikshank et al. 2001). Single neurons were isolated using pure tones (5-50 kHz, 1 msec rise/fall times and 2-30 msec duration), broadband noise and up/down sweeps were used as search stimuli. Upon isolation, tone response properties were acquired. Pure tones with frequencies between

5-50 kHz (1-5 kHz resolution, 2-30 msec duration, 1 msec rise/fall time) were presented to determine excitatory frequency tuning curves. The CF was noted as the frequency at which the neuron responded to at least five consecutive presentations at the lowest sound intensity tested. The excitatory frequency tuning at 10 and 20 dB above the minimum threshold was then determined by increasing intensity in 10 dB steps and changing frequencies with 1 kHz resolution.

Frequency modulated (FM) sweep rate selectivity

Sweep rate selectivity was determined by presenting linear downward and upward FM sweeps of fixed bandwidth and different durations. The sweep rate, defined as the rate of change in kHz/msec, was determined by dividing the FM bandwidth (in kHz) by the duration (in msec). FM sweeps that were approximately centered around the CF were presented at a single intensity, 10-20 dB above CF threshold. FM sweep bandwidth extended at least 3-5 kHz outside the tuning curve. This ensures that putative inhibitory sidebands, which abut the excitatory tuning curve in A1 (Razak and Fuzessery 2006; Wu et al. 2008, also, see chapter 3), were included in the FM sweeps. Sweep durations between 2 and 200 msec (rise/fall time 1 msec) were used. This allowed FM rates between 0.08 - 20 kHz/msec to be presented. This range covers the rates present in various mouse vocalizations (Grimsley et al. 2011; Liu et al. 2003; Portfors 2007; Rotschafer et al. 2012). We have shown previously that core cortical neurons in the mouse respond selectively to FM sweep rate and not to sweep duration or sweep bandwidth (Trujillo et al. 2011).

Classifying FM sweep rate selectivity

Neurons were classified (Figure 4.1) as all-pass (AP), band-pass (BP), fast-pass (FP), or slow-pass (SP) according to FM rate selectivity (Felsheim and Ostwald 1996; Mendelson et al. 1993; Poon et al. 1991; Razak and Fuzessery 2006; Ricketts et al. 1998; Tian and Rauschecker 1994; Trujillo et al. 2011). AP neurons respond above 50% of maximum response for all rates tested (Figure 4.1A). BP neurons were selective for a range of rates; with responses dropping below 50% of maximal response as FM sweep rate was decreased or increased beyond that range (Figure 4.2B). FP neurons were selective for fast FM sweep rates and responses decreased below 50% of maximal response as FM sweep rate was decreased (Figure 4.2C). SP neurons were selective for slow FM sweep rates and responses decreased below 50% of maximal response as FM sweep rate was increased (Figure 4.2D).

FM sweep direction selectivity

To assess the degree to which neurons prefer upward or downward FM sweeps, direction selectivity index (DSI) was calculated as follows:

$$DSI = (D - U)/(D + U)$$

Where D and U are the trapezoidal area under the curve for downward and upward FM sweeps respectively. Positive DSI values indicates a preference for downward sweeping FMs and negative values indicate a preference for upward sweeping FMs. DSI was

assessed at three different ranges of FM rate: 0.1 – 1 kHz/msec, 1.1 – 3 kHz/msec, and 3.1 – 10 kHz/msec.

FM sweep rate selectivity

In the young mouse cortex, the vast majority of neurons are not direction selective (Trujillo et al. 2011). Initial data indicated this was true in 'M' and 'O' mice as well (see Results). Therefore, for sweep rate selectivity measures we chose to focus only on downward FM sweeps. The degree of selectivity was quantified using the rate tuning index (RTI) and is calculated as follows:

$$RTI = (n/n-1) \times [1- (mean/max)]$$

where n = the number of FM sweep rates assessed, 'mean' is the average response across all rates tested and 'max' is the maximum response. This measure is a common indicator of the degree of selectivity of single neurons in the auditory cortex (Atencio et al. 2007; Brown and Harrison 2009; Trujillo et al. 2011).

In addition to RTI, the 50% cutoff rate, defined as the rate at which the response declined to 50% of maximum response was quantified for fast-pass, band-pass, and slow-pass neurons. For band-pass neurons, the best rate was quantified as (Atencio et al. 2007; Brown and Harris 2009, Trujillo et al. 2011):

$$BR = \Sigma(Spikes \times FM\ rate)/ \Sigma\ (spikes)$$

In Figure 4.1B –C, the solid arrows point to the 50% cutoff rates and the dashed arrow in Figure 4.1B points to the best rate.

Mechanisms shaping selectivity

In a subset of neurons, the mechanism shaping FM rate selectivity was determined. Two prominent mechanisms, sideband inhibition and duration tuning for tones have been shown to shape FM sweep rate selectivity in the auditory cortex (Razak and Fuzessery 2006; also see chapter 3)

Sideband Inhibition

The bandwidth and arrival time of high-frequency inhibitory (HFI) sidebands were quantified using a two-tone inhibition paradigm (Brosch and Schreiner 1997; Calford and Semple 1995; Gordon and O'Neill 1998; Razak and Fuzessery 2006). The focus was only on the high-frequency sideband because downward sweeps traverse this sideband before entering the excitatory tuning curve. In the two-tone inhibition paradigm, an excitatory (at the CF) tone and a second tone were presented with different delays between them. The intensities of both tones were the same, 10-20 dB above CF threshold. The CF tone was 5 msec in duration and the second tone was 10 msec in duration (rise/fall times of both tones were 1 msec). To identify inhibitory frequencies, the two tones were presented with delays of -2 to +10 msec between them.

A qualitative-quantitative sequence was used to identify the HFI sideband. The frequency of the second tone was roved between the highest excitatory frequency of the neuron and 50 kHz with 1-5 kHz resolution. Preliminary data indicated that inhibitory sidebands in most neurons lie just outside the excitatory tuning curve (consistent with (Razak and Fuzessery 2006; Wu et al. 2008). Therefore, the frequency of second tone

was varied with 1 kHz resolution near the high-frequency edge of the tuning curve, and with 5 kHz resolution further away. The frequency-delay combinations of the two tones that resulted in a clear decrease in response compared to CF tone alone were qualitatively noted as inhibitory sidebands.

Duration Tuning

The response of neurons to the CF tone with durations between 2-200 msec was recorded to determine duration tuning. Neurons were considered duration tuned if they demonstrated band-pass or short-pass characteristics (Fuzessery and Hall 1999; Fuzessery et al. 2006; Razak and Fuzessery 2006). Band-pass duration tuned neurons demonstrated at least 50% decline from maximum for durations shorter or longer than a preferred duration. The response of short-pass duration tuned neurons decreased below 50% of maximal response as durations increased.

Response variability

Response variability was quantified using the fano factor (fano Factor = [Variance/mean]) (Kara et al. 2000). Fano factor was calculated for three different measures of response to 20 repetitions of FM sweeps: the number of spikes per stimulus presentation (magnitude variability), the 1st spike latency for each presentation (latency variability), and the inter-spike interval for each presentation (ISI variability). For each neuron, multiple sweep rates were repeated 20 times to determine rate selectivity functions. For a given response variability measure (magnitude, latency, ISI), fano factor

was calculated for every sweep rate that elicited at least 3 spikes and averaged across sweep rates. Measures from all neurons within each age group were averaged for across group comparisons.

Data analysis

Unless otherwise noted, one-way ANOVA with post-hoc pairwise comparisons were used to compare response measures across age groups. $P<0.05$ was taken as statistically significant.

Results

The aim of this study was to compare FM sweep rate and direction selectivity in the core auditory cortex (A1/AAF) across three age groups in a presbycusis model. Direction selectivity was assessed in 53 middle age (M) neurons and 65 old (O) neurons. Rate selectivity for downward FM sweeps was assessed in 147 M and 163 O neurons. Previously published data (Trujillo et al., 2011) from the young (Y) group (84 neurons for direction selectivity and 194 neurons for rate selectivity) are used here for comparison.

Auditory brainstem response and other basic response properties

Figure 4.2 shows the average ABR thresholds from a subset of mice across the age groups. Note that Figure 4.2 plots 'threshold attenuation' (higher the attenuation, the lower the threshold). There was a significant hearing loss in the 'M' and 'O' groups

compared to the ‘Y’ group. A two-way ANOVA on threshold by age group by frequency revealed a significant main effect of age group $F(2, 559) = 429$, $p < 0.001$ and a significant main effect of frequency $F(9, 559) = 94$, $p < 0.001$. However, these effects were superseded by a significant interaction between age group and frequency $F(18, 559) = 5.18$, $p < 0.001$. A tukey post-hoc revealed that at <40 kHz, all three groups were different ($p < 0.01$). At >40 kHz, the ‘Y’ group had significantly lower threshold than the ‘M’ and ‘O’ groups. The ‘M’ and ‘O’ group were not different from each other at frequencies >40 kHz. These results imply that moderate presbycusis was observed in the ‘M’ group, and severe presbycusis was observed in the ‘O’ group. The intention was to utilize potential variability in ABR thresholds within age groups to determine if response measures were correlated with hearing loss. However, as can be seen in Figure 4.2, there was not much variability in ABR thresholds within age groups. Therefore, the ABR was only used to determine the degree of presbycusis in a subset of mice we used for electrophysiology.

Figure 4.3 represents the distribution of CFs (Figure 4.3A-C) and thresholds (Figure 4.3D-F). A one-way ANOVA of age group by CF revealed a significant main effect of CF distribution $F(2, 404) = 50.67$, $p < 0.001$. A tukey hsd post-hoc test revealed that the ‘O’ group had a significantly lower CF compared to the ‘Y’ and ‘M’ groups ($p < 0.01$). No difference was observed between ‘Y’ and ‘M’. Our distributions are similar to published tonotopic maps in the C57 (Willott et al. 1993). A one-way ANOVA of age group by threshold revealed a significant main effect of threshold distribution $F(2, 216) = 44.05$, $p < 0.001$. A tukey hsd post-hoc test revealed that, as expected, the ‘O’ group had

a significantly higher threshold compared to the 'Y' and 'M' groups. No difference was observed between 'Y' and 'M'. These data indicate that CF and threshold values were similar between Y and M mice and changed in the expected direction in the O group. All response properties identified below were obtained at intensities 10-20 dB above threshold. This indicates that M and Y neurons were tested at relatively similar absolute intensities, while O neurons were tested at higher absolute intensities. Because all neurons were tested at similar relative intensities above threshold, differences in neural detectability of excitatory sounds is unlikely to be a factor in the analysis below.

Effects of Presbycusis on Direction Selectivity

Direction selectivity was assessed at three FM sweep rate ranges: <1 kHz/msec, 1.1-3 kHz/msec and 3.1-10 kHz/msec. On average DSI was ~0, indicating poor direction selectivity in the mouse cortex across the three groups (Figure 4.4). For <1 kHz/msec range, a one-way ANOVA did not reveal a significant effect of age-group ($F(2, 201) = 0.43$, $p = 0.65$), indicating no presbycusis-related change in DSI at those FM sweep rate ranges. For 1.1-3 kHz/msec range, one-way ANOVA did not reveal a significant effect of age ($F(2, 201) = 0.94$, $p = 0.39$), indicating no presbycusis-related change in DSI at those FM sweep rate ranges. For the 3.1-10 kHz/msec. range, one-way ANOVA revealed a significant main effect of age on DSI ($F(2, 201) = 3.23$, $p < 0.05$). A tukey hsd post-hoc revealed that the 'O' and the 'M' group were significantly different, with the 'Y' group demonstrating a slight tendency toward upward sweeping FMs (-0.07) and the 'M' group demonstrating a slight tendency toward downward sweeping FMs (0.04). The 'O' group

was no different than the 'Y' or 'M' groups. These results suggest a subtle shift toward preferring downward FM sweeps in the middle age group. However, due to the rather small changes in DSI and a lack of difference between 'O' and both 'Y' and 'M', we interpret these results to indicate very little or no change in direction selectivity with presbycusis.

Neurons with DSI values >0.3 and <-0.3 were considered direction selective (Mendelson and Cynader 1985) and the prevalence of such direction selective neurons was compared across the three age groups. Across different rate ranges and groups, less than 25% of neurons were direction selective (collapsed across rate ranges: 'Y' = 20%, 'M' = 15%, 'O' = 23%) and the prevalence did not change with age ($\chi^2 = 4.382$, $p = 0.357$). Collectively, these results indicate weak FM sweep direction selectivity in the mouse auditory cortex which does not change with presbycusis.

Effects of Presbycusis on FM Sweep Rate Selectivity

Figure 4.1 shows the different types of rate selective neurons. Table 4.1 provides the distribution of tuning type by age. A majority of 'Y' neurons demonstrate BP and FP rate tuning. The percentage of BP and FP neurons decreased in the 'M' and 'O' groups ($\chi^2 = 14.46$, $p < 0.05$). There was a higher percentage of SP neurons in the 'M' and 'O' groups. This indicates a presbycusis-related decrease in neurons selective for fast and medium sweep rates.

Rate tuning index (RTI) is a quantitative measure that indicates the degree to which a neuron is FM sweep rate selective (Atencio et al. 2007; Brown and Harrison

2009; Trujillo et al. 2011). We compared RTI within each FM rate selectivity type (FP, BP, AP and SP) across age-groups. There was a significant reduction in RTI in BP neurons across age groups (Figure 4.5B, one-way ANOVA $F(2, 193) = 10.97$, $p < 0.001$). A tukey hsd post-hoc revealed that the O group had a significantly lower RTI than the Y group. There were no differences between the Y and M groups and M and O groups for BP neurons. There was no difference in RTI in the other three classes of neurons across age (One-way ANOVAs, $p < 0.05$). These results indicate that the degree of selectivity decreases with presbycusis in the most selective type of neurons in the auditory cortex.

Effects of Presbycusis on 50% cut-off rate

The 50% cutoff rates of fast-pass, band-pass, and slow-pass neurons as well as the best rate of band-pass neurons were quantified as measures of rate selectivity and compared across age groups. In BP neurons, both 50% cut-off (Figure 4.6A) and best-rate (Figure 4.6C) were significantly reduced with presbycusis: (One-way ANOVAs: 50% cut-off: $F(2, 193) = 15.94$, $p < 0.001$, best-rate: $F(2, 193) = 38.88$, $p < 0.001$). A tukey hsd post-hoc revealed that the O group had a significantly slower 50% cutoff and best-rate than the Y and M groups ($p < 0.05$). The 50% cut-off rate in FP neurons (Figure 4.6B) also showed a significant presbycusis-related reduction (One-way ANOVA, $F(2, 108) = p < 0.05$). A tukey hsd post-hoc test revealed that the O group had a significantly slower 50% cutoff than the Y group. There was no change in SP neurons (Figure 4.6D)

(One-way ANOVA, $p > 0.05$). These results indicate that neuronal selectivity in FP and BP neurons shift towards slower sweep rates with presbycusis.

Variability in response to FM sweeps with presbycusis

The fano factor is an indication of the variability in neuronal spiking in response to repetitions of the same stimulus. Figure 4.7 shows an example BP neuron to illustrate three measures of fano factor: response magnitude, response latency and inter-spike interval (ISI). For each measure, the fano factor was averaged across the different sweep rates tested for a given neuron. In figure 4.5, each fano factor measure is indicated in the raster plot for the sweep rate tested. This neuron had an average response magnitude fano factor of 2.03, a response latency fano factor of 11.4, and an ISI fano factor of 32.44.

Response magnitude variability increased for BP (One-way ANOVA, $F(2, 193) = 12.69$, $p < 0.001$) and FP neurons (One-way ANOVA, $F(2, 108) = 4.83$, $p < 0.01$), but not in AP and SP neurons, with presbycusis (Figure 4.8, One-way ANOVA). All three groups were different from each other for BP neurons (tukey hsd, $p < 0.05$). In fast-pass neurons, variability increased in the M group relative to the Y group (tukey hsd, $p < 0.05$) as well as increased in the O group relative to the Y group (tukey hsd, $p < 0.05$).

Response latency and ISI measures focus on temporal variability. Response latency variability was unaffected by presbycusis (Figure 4.9, One-way ANOVA, $F(2, 193) = 2.17$, $p = 0.117$). Inter-spike interval variability increases with presbycusis (Figure 4.10). This was significant in BP (Figure 4.10B, One-way ANOVA, $F(2, 193) = 4.99$, $p < 0.01$), FP (Figure 4.10C, One-way ANOVA, $F(2, 108) = 3.25$, $p < 0.05$) and SP (Figure

4.10D, One-way ANOVA, $F(2, 193) = 6.55$, $p < 0.01$) neurons, but not in AP neurons. A tukey hsd post-hoc revealed that the 'O' group was significantly more variable than the 'Y', and 'M' groups for BP neurons ($p < 0.05$) and the 'Y' group was significantly less variable than the 'M' and 'O' groups for FP and SP neurons. Taken together, the variability analysis indicates that cortical representation of FM sweeps becomes noisy with presbycusis. Both spike-rate and temporal representations are affected, with particularly consistent effects on neurons selective for fast and medium sweep rates.

Sideband inhibition decreases in presbycusis

The distribution of neurons with sideband inhibition and duration tuning by age group is provided in Table 4.2. A χ^2 test for independence revealed a decreased percentage of inhibitory sidebands and an increased percentage of duration tuning ($\chi^2 = 44.8$, $p < 0.001$).

Discussion

The main finding of this study is that cortical processing of FM sweeps is considerably altered by presbycusis. Specifically, the 50% cut-off and the best rate are significantly shifted towards slower rates in fast-pass and band-pass neurons. The 50% cut-off rate is approximately in the middle of the range of rates over which a neuron shows maximum decline in response magnitude. Thus, this is the rate near which each neuron is maximally informative about sweep rates (Harper and McAlpine 2004). The best-rate is a measure of the sweep rate that is best detected. This indicates that with

presbycusis, cortical neurons' range of best detection and discrimination rates shift towards slower rates. The fano-factor is a measure of how variable a neuron's response across repetitions of the same stimulus. Both response magnitude and ISI showed increased variability in response to FM sweeps with presbycusis. This suggests an overall increase in the noisiness of sweep rate representation. Once again this affected FP and BP neurons more.

We also see a reduction in inhibitory sidebands and increased duration tuning. Sideband and duration tuning are mechanisms of FP/BP rate selectivity in Y mouse cortex. Sideband inhibition is the dominant mechanism, and its loss in presbycusis may explain the decreased percentage of FP/BP neurons. Properties of sideband such as arrival time and bandwidth explain the 50% cut-off rate of FP/BP neurons. The shift in 50% rates towards slower rates may also be explained by the decrease in sideband inhibition. Despite the significant loss of sideband inhibition, neurons in the O group still exhibited BP/FP selectivity. This is likely due to the increased percentage of duration tuning in the O group. These data illustrate that plasticity in mechanisms may at least partially compensate for FM sweep rate selectivity changes in presbycusis.

Our data are supportive of the two dominant theories of processing declines with aging: the noisy processing theory (Mahncke et al. 2006a) and the speed of processing theory (Salthouse 1996). The noisy processing theory attributes processing declines to weakened, unreliable, and low-fidelity sensory processing that impairs cognitive function due to the difficulty in performing cognitive operations on a degraded sensory signal (Mahncke et al. 2006a; Mahncke et al. 2006b). In terms of FM processing, the increased

variability observed is suggestive of increased noise in processing. The speed of processing theory attributes processing decline to a reduction in the speed at which processing can be carried out, impairing an individual's ability to perform cognitive operations on stimuli that is rapidly changing (Salthouse 1996), such as the fast frequency transitions in human speech. The leftward shift in rate selectivity functions with presbycusis towards slower rates suggests that neurons integrate sweep spectra over a longer time course to generate robust responses. This suggested increase in integration time is a mechanism of slowing down of processing.

The fact that some of these changes occur in the middle age group indicates that hearing loss is a likely cause of the slowed and noisy processing because the middle age group, while suffering high frequency hearing loss, is not yet senescent. However, this suggestion can be validated only by comparison with a strain of mice that does not undergo accelerated hearing loss (e.g., CBA strain, (Walton et al. 2008; Walton 2010; Walton et al. 1995; Willott et al. 1993; Willott et al. 1991). Strain specific differences in response selectivity may confound this approach. More recently, the development of the C57 mouse strain that does not undergo accelerated hearing loss now provides an opportunity to disambiguate age and hearing loss in presbycusis-related change in auditory processing (Harding et al. 2005; Keithley et al. 2004)

FM sweeps processing with presbycusis

Our data are consistent with the only other study that examined FM processing with age (Mendelson and Ricketts 2001). This study used three different sweep rates

and showed that neurons in the aged cortex respond best to slow sweep rates compared to young rats. No age-related differences were found in the inferior colliculus and thalamus in the aging rat indicating that the plasticity was specific to the cortex and not inherited from subcortical change (Lee et al. 2002; Mendelson and Lui 2004; Mendelson and Ricketts 2001). One possible explanation for this cortex-specific change may lie in how FM rate selectivity is shaped. The primary mechanism of rate selectivity in pallid bat and mouse cortex is spectrotemporal interactions between the excitatory tuning curve and inhibitory sidebands. In both species, removal of sideband inhibitory frequencies from the sweep reduces or eliminates rate selectivity. At least some of the inhibition involved in sweep selectivity is generated at the level of the cortex (Razak and Fuzessery 2009; Zhang et al. 2003). This is consistent with Miller et al, who indicated that inhibitory responses are less faithfully transmitted from the thalamus to the cortex. There is also significant convergence in the thalamocortical inputs which may smear selectivity. This suggests that cortex refines some the inhibitory properties locally and does not simply inherit it (Nelken et al. 2003). Parvalbumin (PV) containing fast-spiking inhibitory interneurons shape inhibitory sidebands in the cortex and likely shape selectivity for rapid temporal features (Atencio and Schreiner 2008; Wu et al. 2008). Cortical PV expression declines with presbycusis. This decline in expression of PV can reduce inhibitory neurotransmission.(Ouda et al. 2008) As a result of declining PV expression and other identified sources of reduced cortical inhibitory markers (Burianova et al. 2009; O'Neill et al. 1997; Ouda et al. 2008), there will be an overall decline in sideband inhibition as observed in this study and a consequent decline in FM rate selectivity.

Variability of spiking with age

Neuronal spike variability has been explored in the visual cortex of aging monkeys. In areas V1 and MT, variability in spike count increases with age. Interestingly, their fano factor measure of spike count had means ~1.5 in the young cortex and ~2.5 in the old cortex. Here, we report values within that range that change by the same magnitude. The similarities indicate that the means and magnitude of change indicate that similar mechanisms may be at play. Weakened neuromodulatory systems have been implicated in noisy processing (Li et al. 2001). Balanced excitation and inhibition also regulates spike timing (Elhilali et al. 2004). If inhibition is weakened, the temporal interaction between excitation and inhibition may be altered, resulting in noisy spike timing.

Whereas our response magnitude variability was in line with published values of fano factor, our fano factor values for first spike latency and inter-spike interval are larger then published values. This may be due to 1) the naturally different spectrotemporal dynamics of FM sweeps of varying rates relative to the excitatory tuning curve, 2) the interaction of excitation and inhibition at different FM sweep rates, especially near the 50% cutoff for fast-pass and band-pass neurons, 3) the length of our spike window (300 msec from stimulus onset).

The amount of time an FM sweep spends inside a neurons excitatory tuning curve depends on the FM sweep rate and tuning curve excitatory and inhibitory bandwidths. A fast, short duration FM sweep will spend less time in the excitatory tuning curve than a long, slow FM sweep rate. The relative timing and bandwidth of the inhibitory sidebands

can shape FM rate selectivity (Gordon and O'Neill 1998; Razak and Fuzessery 2006; Trujillo et al. 2012). Specifically, it has been reported that the relative bandwidth and timing of inhibition that decrease a neurons response by 50% compared with control response can accurately predict the 50% cutoff for fast-pass and band-pass neurons (Razak and Fuzessery 2006; Trujillo et al. 2012). The 50% cutoff is a probabilistic measure, meaning that half the time inhibition reaches the neuron before excitation, thus suppressing its spike rate. This indicates that the interaction between the relative arrival times of excitation and inhibition is variable. This variability could lead to high fano factors for both 1st spike latency and inter-spike interval. If the inhibition suppresses half the spikes per 20 stimulus presentations, then the remaining spikes may have variable latencies and inter-spike intervals and this could account for the high fano factors observed in the present study.

Fano factor can increase with increase spike windows (Baddeley et al. 1997). Our spike window is 300msec relative to stimulus onset. For inter-spike interval, this could significantly increase inter-spike interval variability. If a neuron fires robustly to the onset of a stimulus, then trails off toward the end of the stimulus, the inter-spike intervals during the initial burst will be relatively small, on the order of milliseconds. Later spikes would likely occur tens or hundreds of milliseconds apart. An example of this phenomenon can be seen in Figure 4.7C.

Despite high variability in inter-spike interval, a significant increase in inter-spike variability was observed for band-pass, fast-pass, and slow-pass neurons. This is not observed for 1st spike latency. This may seem counterintuitive since both are measures of

relative spike timing. However, it has been reported that characteristics and dynamics are different for 1st spike latency and inter-spike intervals, indicating that different mechanisms may govern those properties (Phillips and Sark 1991).

In order to efficiently decode sensory stimuli, neurons must distinguish signal from noise (Bialek and Rieke 1992). Information about the signal can be coded by changes in the number of spikes as stimulus quality changes, i.e. as a sound becomes longer or shorter in duration the neuron may increase or decrease firing rate. The noise can be decoded by response variability. For example, a low noise signal may result in precise spike timing whereas a high noise signal may result in variable spike timing. According to the noisy processing theory of cognitive aging, if a neuron becomes more variable in its spiking with age, extracting signal from noise may be impaired and fidelity of sensory representation reduced. According to the speed of processing theory, if a neuron changes in its ability to modulate spike rate as a stimulus quality changes, it could miss information in rapidly changes stimuli, such as the frequency changes that occur in speech.

Conclusions

The present data suggest a presbycusis-related decreased in FM sweep selectivity and changes in underlying mechanisms. The decreased sideband inhibition is consistent with overall decrease in inhibition in the aging brain (Burianova et al. 2009; Ouda et al. 2008). Part of this decline may be related to PV expression. This contention is consistent with data from Merzenich that showed that behavioral training improves auditory

processing as well as increases PV expression (de Villers-Sidani et al. 2010). Perhaps the most surprising aspect of this study is the increased percentage of neurons selective for the duration of tones in presbycusis. Tone duration tuning also depends on precise temporal interactions between inhibition and excitation. This indicates that in some situations, there may be age-related increase in inhibitory function. Future studies need to address the mechanisms of increased duration tuning with presbycusis.

Figures:

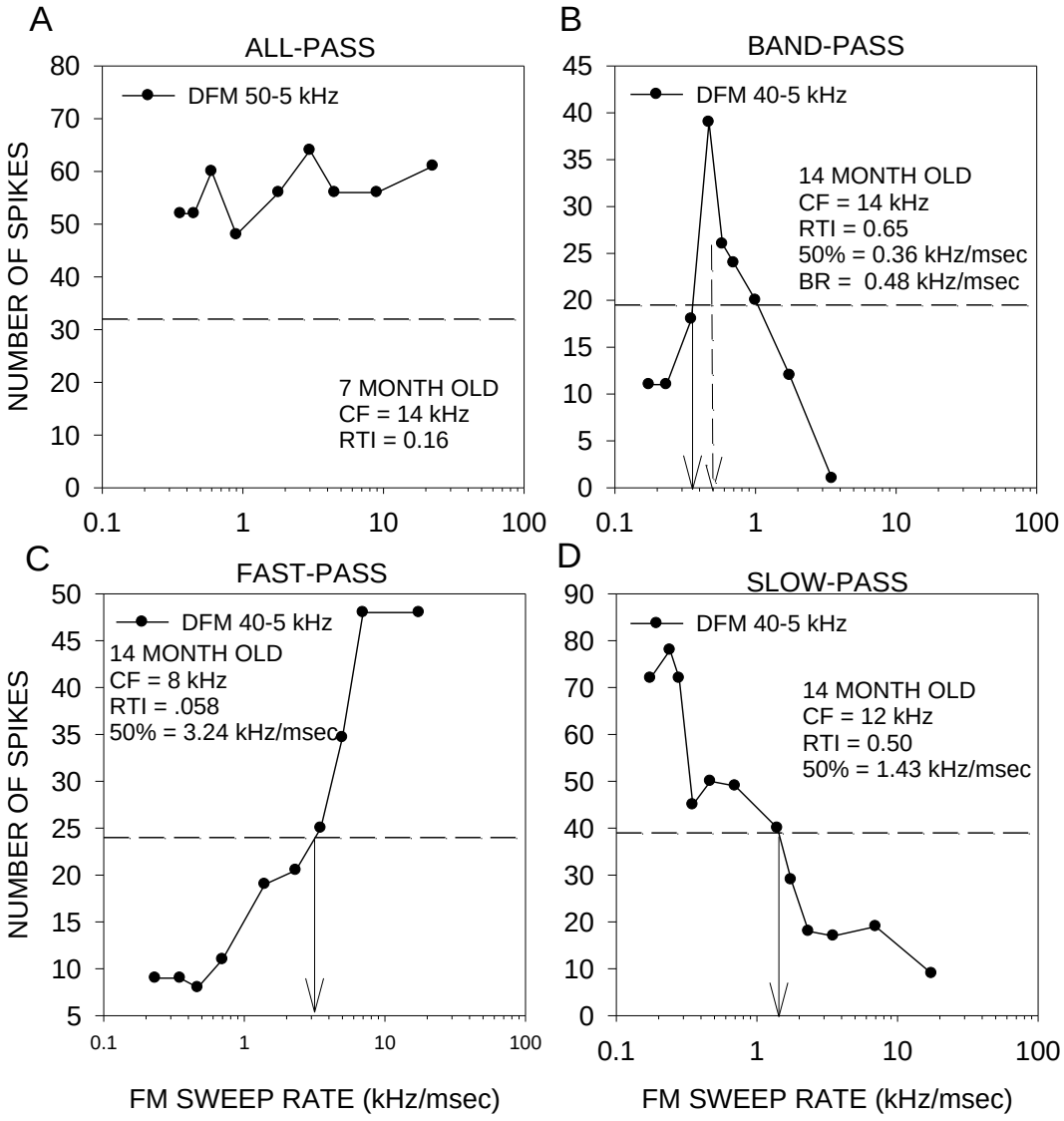

Figure 4.1: Classification of FM sweep rate tuning. (A) All-pass (B) Band-pass (C) Fast-pass (D) Slow-pass. The dashed line in each panel marks 50% of maximum response. The 'number of spikes' on the y-axis in this and all subsequent graphs are in response to 20 repetitions of each stimulus. The bandwidth of sweep used is indicated in each panel. CF: characteristic frequency, RTI-out: rate tuning index calculated for sweeps with bandwidths that extended well outside the excitatory tuning curve, BR: best rate for the band-pass neuron, 50%: the 50% cut-off rate for band-pass, fast-pass, and slow-pass. The solid arrows in A – C represents the 50% cutoff rate and the dashed arrow represents the best rate in B.

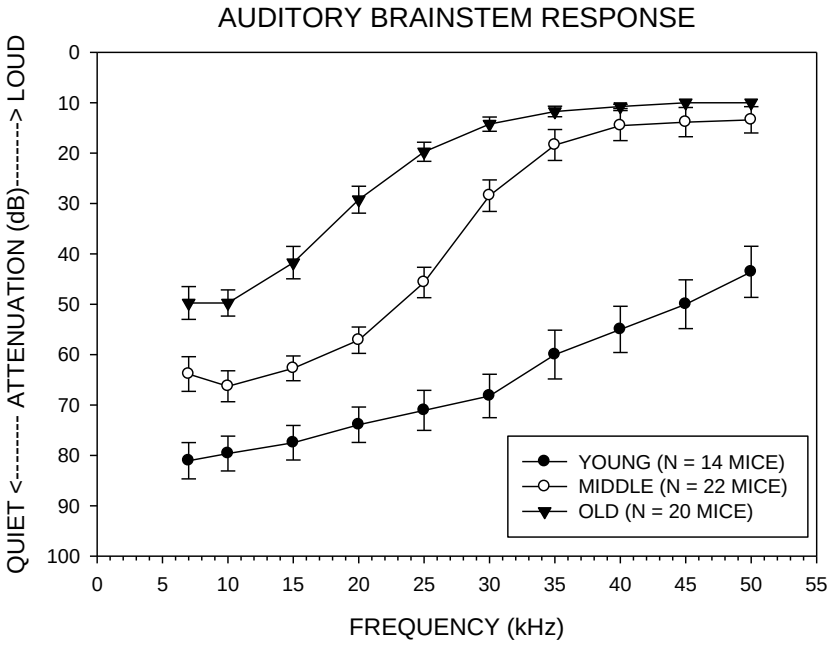

Figure 4.2: Auditory brainstem response decreases with presbycusis: Auditory brainstem response was assessed at frequencies between 7 – 50 kHz. The threshold for each frequency was defined as the attenuation at which a 5dB step eliminated the first peak of the ABR evoked response (Y – axis). The symbols represent mean +/- SEM for young (closed circles), middle (open circles), and old (triangle). A two-way ANOVA on threshold by age group by frequency revealed a significant main effect of age group $F(2, 559) = 429$, $p < 0.001$, a significant main effect of frequency $F(9, 559) = 94$, $p < 0.001$. However, these effects were superseded by a significant interaction between age group and frequency $F(18, 559) = 5.18$, $p < 0.001$. A tukey post-hoc revealed that below 40 kHz, all three groups are difference ($p < 0.01$).

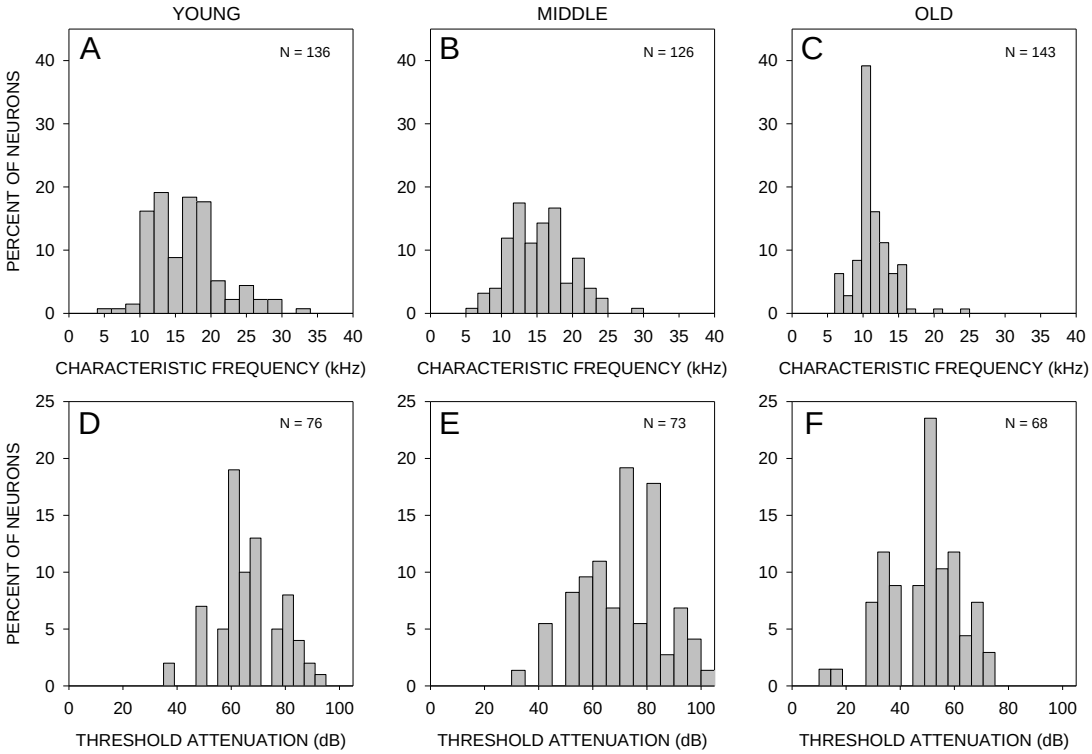

Figure 4.3: Distributions of characteristics frequency (A – C) and thresholds (D – E). A one-way ANOVA of age group by CF revealed a significant main effect of CF distribution $F(2, 404) = 50.67$, $p < 0.001$. A tukey hsd post-hoc test revealed that the 'O' group had a significantly lower CF compared to the 'Y' and 'M' groups ($p < 0.01$). No difference was observed between 'Y' and 'M'. A one-way ANOVA of age group by threshold revealed a significant main effect of threshold distribution $F(2, 216) = 44.05$, $p < 0.001$. A tukey hsd post-hoc test revealed that the 'O' group had a significantly less attenuated (louder) threshold compared to the 'Y' and 'O' groups. No difference was observed between 'Y' and 'M'

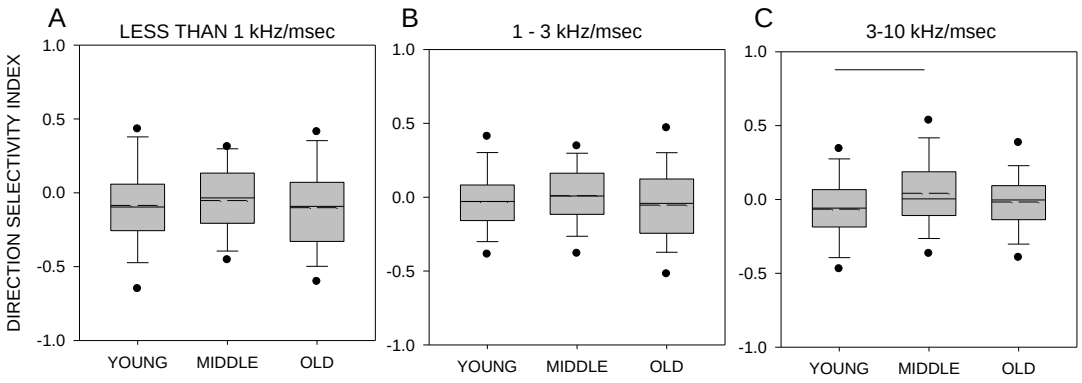

Figure 4.4: Direction selectivity with presbycusis. Neurons in the young adult mouse cortex are not, on average, selective for the direction of FM sweeps. (A) A boxplot of DSI by age-group for FM sweep rates less than 1 kHz/msec. (B) A boxplot of DSI by age-group for FM sweep rates less than 1-3 kHz/msec. (C) A boxplot of DSI by age-group for FM sweep rates less than 3-10 kHz/msec. The upper and lower edge of each box represents the 75^{th} and 25^{th} percentiles respectively. The vertical bars represent standard deviation around the mean. The horizontal bar within each plot represents the median and the hashed line represents the mean. A one-way ANOVA did not reveal a significant effect of age-group for less than 1 kHz/msec (A) $F(2, 201) = 0.43$, $p = 0.65$, or 1.1-3 kHz/msec range (B) $F(2, 201) = 0.94$, $p = 0.39$, indicating no presbycusis-related change in DSI at those FM sweep rate ranges. For the 3.1-10 kHz/msec. range, one-way ANOVA revealed a significant main effect of age on DSI (C) $F(2, 201) = 3.23$, $p < 0.05$.

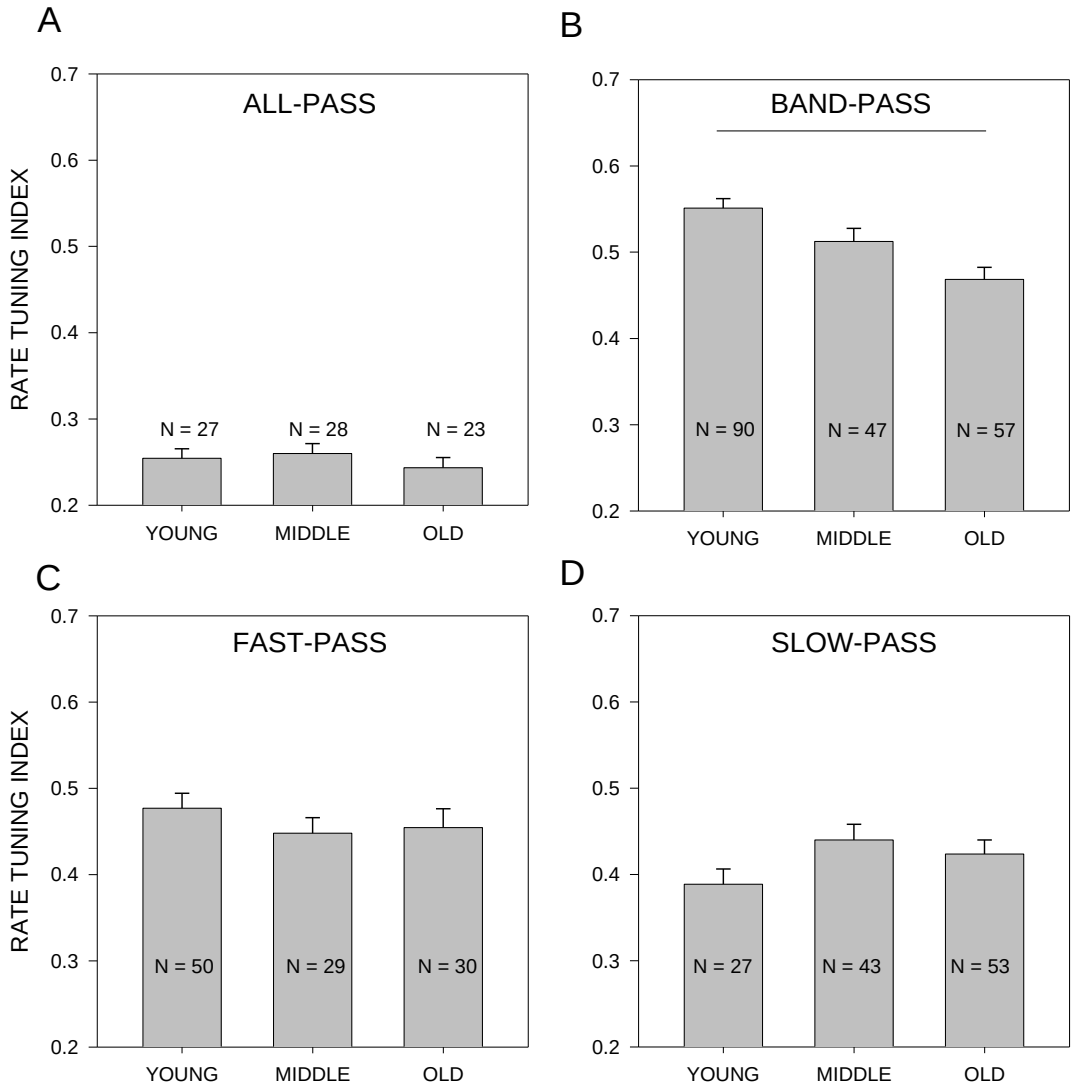

Figure 4.5: Rate tuning is decreased in presbycusis. Rate tuning index plotted by tuning type: all-pass (A), band-pass (B), fast-pass (C), and slow-pass (D). Each bar represents mean + SEM for the young, middle, and old age groups. The horizontal lines represent differences as revealed by a tukey hsd post hoc test. Band-pass neurons decrease in degree of selectivity as a function of age.

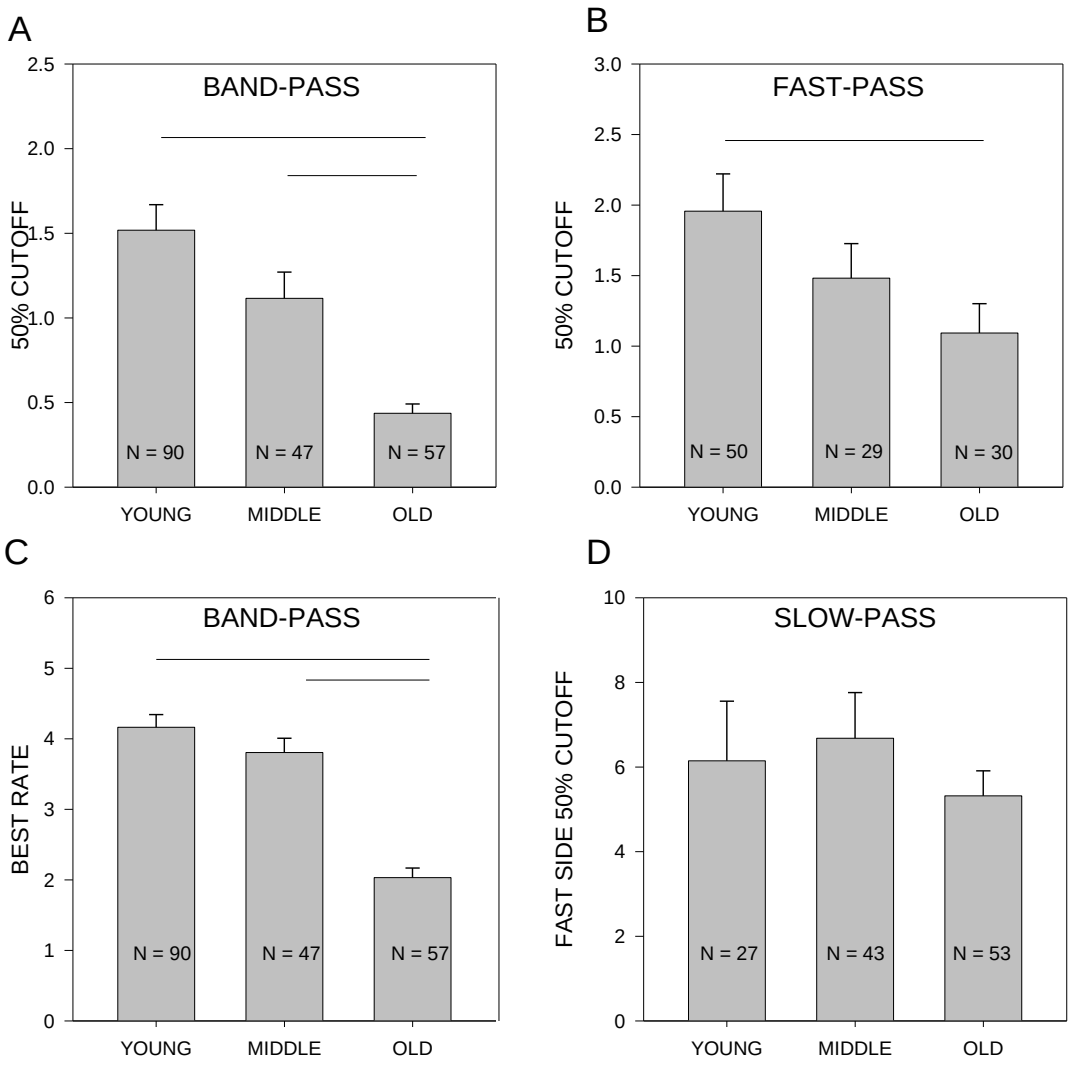

Figure 4.6: FM rate selectivity slows with presbycusis FM rate selectivity plotted by tuning type: all-pass (A), band-pass (B), fast-pass (C), and slow-pass (D). Each bar represents mean + SEM for the young, middle, and old age groups. The horizontal lines represent differences as revealed by a tukey hsd post hoc test. In BP neurons, both 50% cut-off (A) and best-rate (C) were significantly reduced with presbycusis:

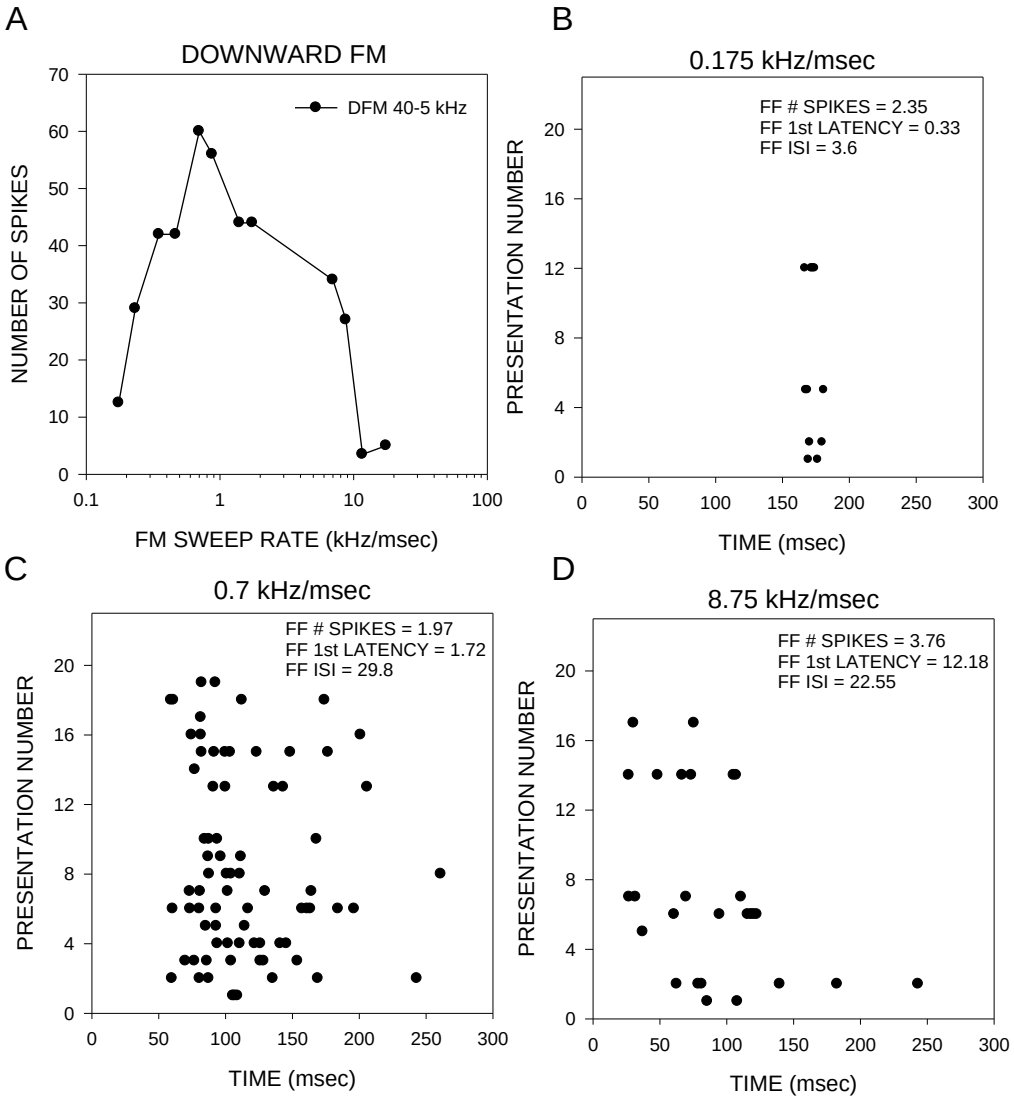

Figure 4.7: Example of Fano factor: An example of fano factor for a band-pass neuron (A). Fano factor is calculated from the raster plot at each rate of each FM sweep rate tested for each neuron. Each stimulus was repeated for 20 consecutive trials. Each line of the y-axis of the raster plots in (B – D) represents one stimulus presentation. Fano factor was calculated for trial to trial variability (FF # SPIKES), response latency variability (FF 1st LATENCY), and inter-spike interval variability (FF ISI). Fano factors were calculated for each FM sweep tested for each neuron. (B) represents the raster and fano factors (inset) for 0.175 kHz/msec. (C) represents the raster and fano factors (inset) for 0.7 kHz/msec. (D) represents the raster and fano factors (inset) for 8.75 kHz/msec. For each neuron, the fano factors were averaged for each FM sweep rate tested. The average fano factors for the neuron depicted in the figure were: trial to trial variability: 2.03, response latency variability: 11.4, and inter-spike interval variability: 32.44.

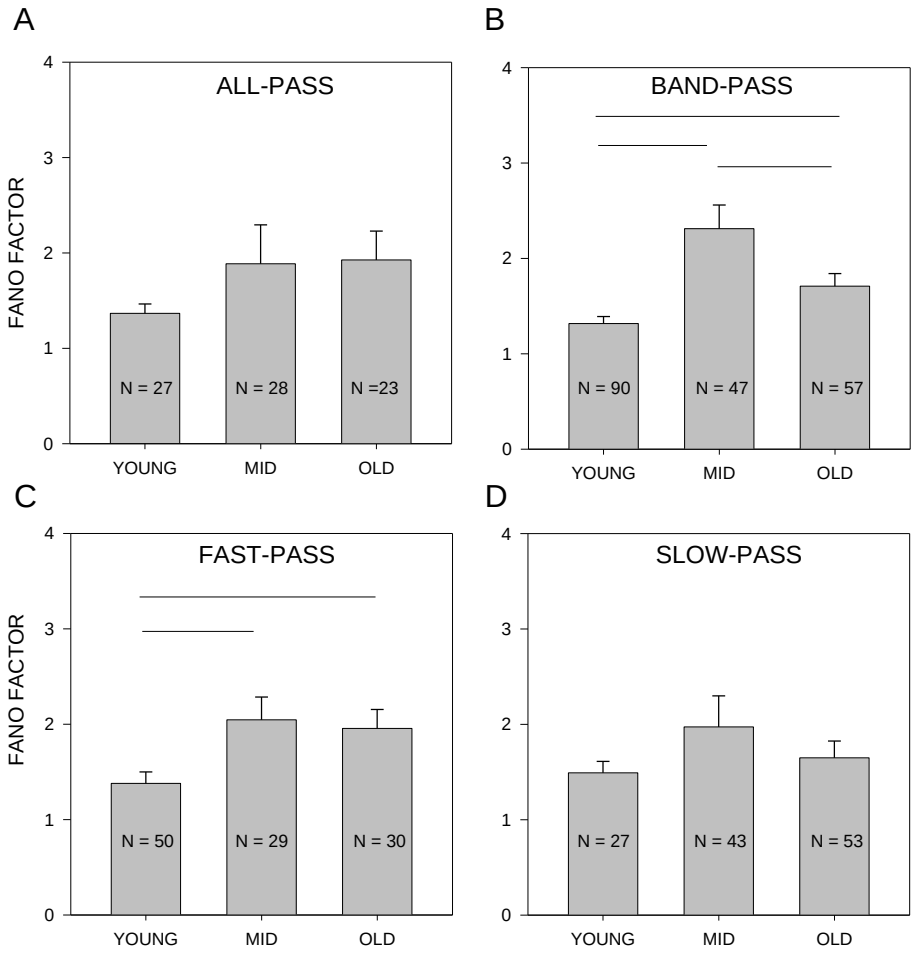

Figure 4.8: Trial to trial variability increases with presbycusis: The trial to trial variability for all-pass (A), band-pass (B), and fast-pass (C), and slow-pass (D). Each bar represents mean + SEM for the young, middle, and old age groups. The horizontal lines represent differences as revealed by a tukey hsd post-hoc test. As depicted in (B), in band-pass neurons variability increased from the 'Y' to 'M'. Interestingly, 'M' has increased variability relative to 'O'.

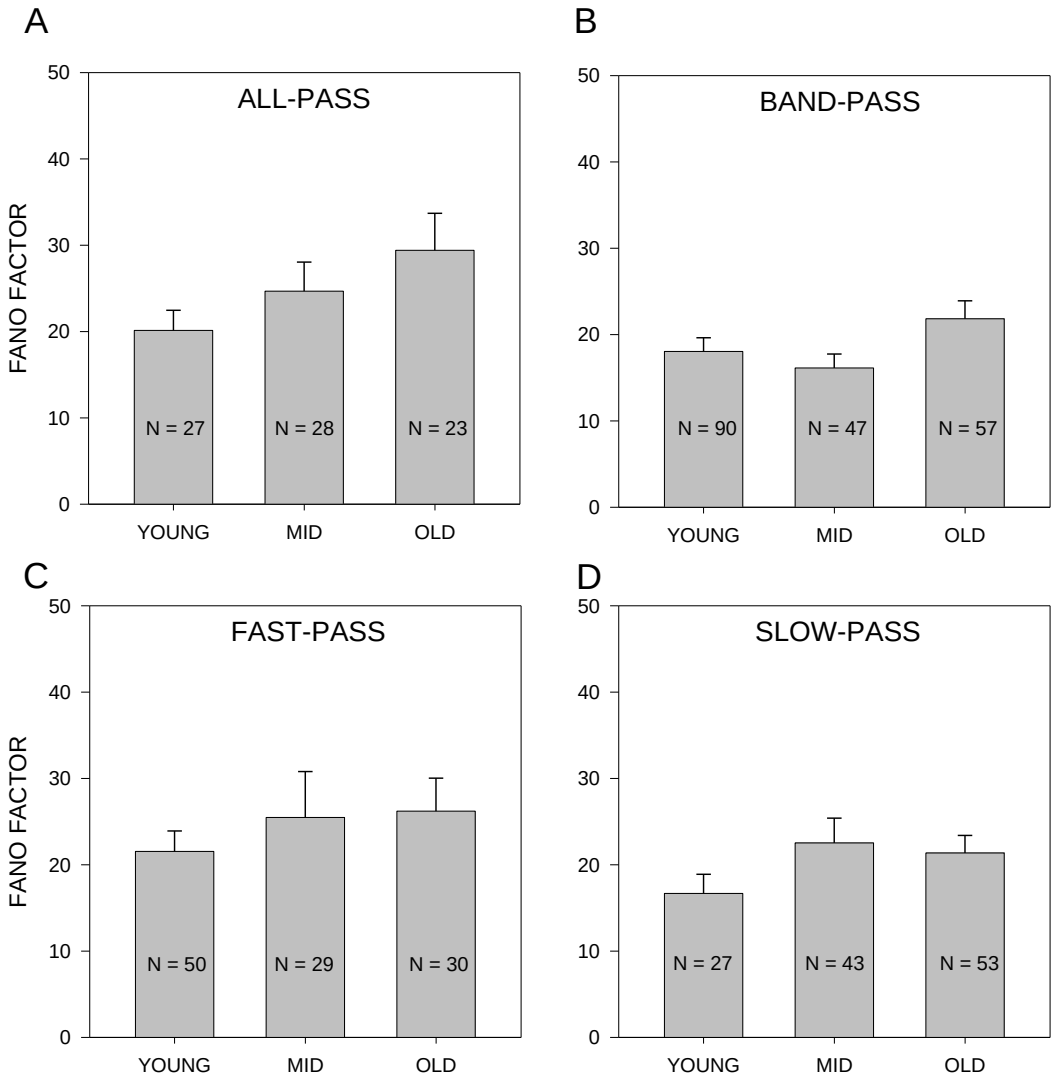

Figure 4.9: Variability in first spike latency does not change with presbycusis: The response latency variability for all-pass (A), band-pass (B), and fast-pass (C), and slow-pass (D). Each bar represents mean + SEM for the young, middle, and old age groups. No differences were observed in all-pass neurons (A), band-pass neurons (B), fast-pass neurons (C)or slow-pass neurons (D).

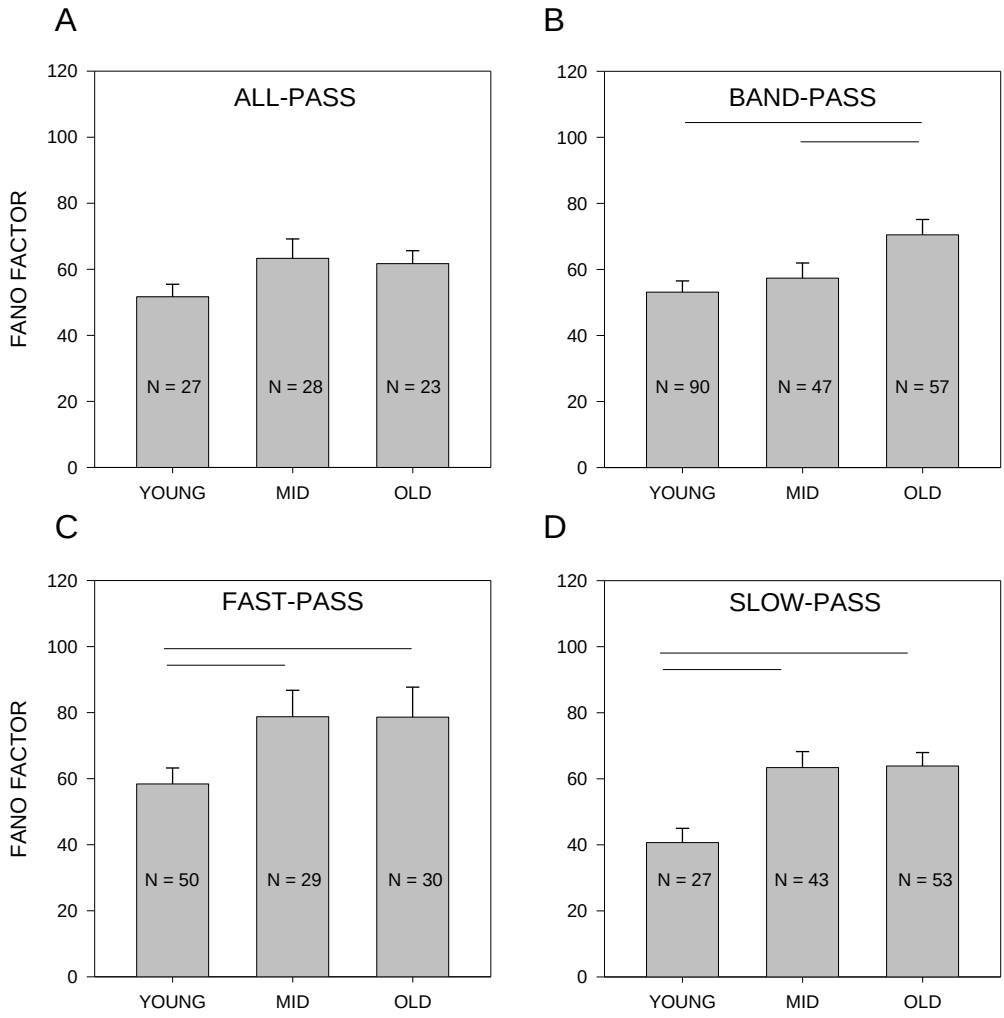

Figure 4.10: Inter-spike intervals become more variable with presbycusis: The inter-spike interval variability for all-pass (A), band-pass (B), and fast-pass (C), and slow-pass (D). Each bar represents mean + SEM for the young, middle, and old age groups. The horizontal lines represent differences as revealed by a tukey hsd test. As depicted in (B), inter-spike interval variability increased in band-pass neurons from young to old, and also increased from middle to old. As depicted in (C), spike interval variability increased in fast-pass neurons from young to old, and also increased from young to old. As depicted in (D), interval variability increased in slow-pass neurons from young to old, and also increased from young to old (D). No differences were observed in all-pass neurons (A).

Table 4.1: Distribution of FM sweep rate tuning type:

TUNING TYPE	YOUNG (N = 194)	MID (N = 147)	OLD (N = 163)
ALL-PASS	14%	19%	14%
BAND-PASS	46%	32%	35%
FAST-PASS	26%	20%	18%
SLOW-PASS	14%	29%	33%

Table 4.2: Distribution of mechanisms:

Age Group	HFI Present	Duration Tuning Present
Young	88%, n=53	34%, n = 97
Middle	34% , n = 29	44%, n = 47
Old	12%, n = 51	46%, n = 60

Chapter 5: Conclusions

I began investigating the effects of aging on FM sweeps processing seven years ago. In a study conducted while a Neuroscience Research Associate at Posit Science Corporation, I determined that FM sweep discrimination begins to decline at age 40 and profound deficits set in around age 70. Those results mimic, in a way, the results I have reported in this dissertation. While the theme of the dissertation is changes in cortical processing of FM sweeps in a mouse model of presbycusis, there are several other findings that stand out. The first is that I reported that the mouse auditory cortex is selective for a narrow range of FM sweep rates, and there are depth effects, indicating that additional computations may occur at the level of the cortex. The second finding was that the mechanisms that govern FM sweep rate selectivity are similar to what is reported in the pallid bat. In fact, other than the pallid bat, this is the only study to report multiple mechanisms shaping FM sweep rate selectivity in the auditory cortex. Lastly, I report that some deficits exist in the middle age group of the mouse model of presbycusis, which matches what is seen in the human study on FM sweep discrimination.

The mouse is a useful tool to explore neural dysfunction due to the power of genetic engineering tools available (Barkat et al. 2011; Linden et al. 2003; Linden and Schreiner 2003; Liu 2006; Mataga et al. 2001; Morishita et al. 2010; O'Connor et al. 2009; Portfors 2007; Portfors et al. 2009; Sugiyama et al. 2008). Due to the known etiology of presbycusis in the C57, my results will complement future studies on mice that do not have the specific mutations that cause high frequency hearing loss in the C57. One available mouse strain, the CAST mouse, has the same genetic background as the

C57 but has the wildtype Cdh23 gene. Comparisons with that mouse would elucidate the contribution of the Cdh23 mutation in cortical processing of FM sweeps. Another possible comparison is the mouse strain that is commonly compared to the C57, the CBA mouse.

The studies reported in this dissertation are not without limitation. Specifically, studying neural processing in an anesthetized mouse creates an artificial experiment where certain response properties and neuromodulatory systems are enhanced or suppressed. In order to adequately address the response properties of the cortex, experiments are needed in awake and perhaps behaving animals.

To conclude, I hope that my research lives on and provides a framework for creating therapeutic remedies to treat presbycusis, thus improving the lives of tens of millions of people.

Bibliography:

Atencio Ca, Blake DT, Strata F, Cheung SW, Merzenich MM, and Schreiner CE. Frequency-modulation encoding in the primary auditory cortex of the awake owl monkey. ***J Neurophysiol*** **98: 2182-2195, 2007.**

Atencio Ca, and Schreiner CE. Laminar diversity of dynamic sound processing in cat primary auditory cortex. ***J Neurophysiol*** **103: 192-205, 2010.**

Atencio CA, and Schreiner CE. Spectrotemporal Processing Differences between Auditory Cortical Fast-Spiking and Regular-Spiking Neurons. ***J Neurosci*** **28: 3897-3910, 2008.**

Baddeley R, Abbott LF, Booth MCA, Sengpiel F, Freeman T, Wakeman EA, and Rolls ET. Responses of neurons in primary and inferior temporal visual cortices to natural scenes. ***Proceedings of the Royal Society of London Series B: Biological Sciences*** **264: 1775-1783, 1997.**

Barkat T, Polley D, and Hensch T. A critical period for auditory thalamocortical connectivity. ***Nat Neurosci*** **14: 1189-1194, 2011.**

Bialek W, and Rieke F. Reliability and information transmission in spiking neurons. ***Trends in Neurosciences*** **15: 428-434, 1992.**

Brand A, Urban R, and Grothe B. Duration tuning in the mouse auditory midbrain. ***J Neurophysiol*** **84: 1790-1799, 2000.**

Brosch M, and Schreiner CE. Time Course of Forward Masking Tuning Curves in Cat Primary Auditory Cortex. ***J Neurophysiol*** **77: 923-943, 1997.**

Brown Ta, and Harrison RV. Responses of neurons in chinchilla auditory cortex to frequency-modulated tones. ***J Neurophysiol*** **101: 2017-2029, 2009.**

Burianova J, Ouda L, Profant O, and Syka J. Age-related changes in GAD levels in the central auditory system of the rat. ***Exp Gerontol*** **44: 161-169, 2009.**

Calford MB, and Semple MN. Monaural inhibition in cat auditory cortex. ***J Neurophysiol*** **73: 1876-1891, 1995.**

Casseday JH, Ehrlich D, and Covey E. Neural Measurement of Sound Duration: Control by Excitatory-Inhibitory Interactions in the Inferior Colliculus. ***J Neurophysiol*** **84: 1475-1487, 2000.**

Casseday JH, Ehrlich D, and Covey E. Neural tuning for sound duration: role of inhibitory mechanisms in the inferior colliculus**.** ***Science*** **264: 847-850, 1994.**

Chen G-D. Effects of stimulus duration on responses of neurons in the chinchilla inferior colliculus. ***Hear Res*** **122: 142-150, 1998.**

Christensen K, Doblhammer G, Rau R, and Vaupel JW. Ageing populations: the challenges ahead. ***The Lancet*** **374: 1196-1208, 2009.**

Coughlin M, Kewley-Port D, and Humes LE. The relation between identification and discrimination of vowels in young and elderly listeners. ***J Acoust Soc Am*** **104: 3597-3607, 1998.**

Cruikshank SJ, Killackey HP, and Metherate R. Parvalbumin and calbindin are differentially distributed within primary and secondary subregions of the mouse auditory forebrain. ***Neuroscience*** **105: 553-569, 2001.**

Davis AC. Epidemiological profile of hearing impairments: the scale and nature of the problem with special reference to the elderly. ***Acta Otolaryngol Suppl*** **476: 23-31, 1990.**

de Villers-Sidani E, Alzghoul L, Zhou X, Simpson KL, Lin RCS, and Merzenich MM. Recovery of functional and structural age-related changes in the rat primary auditory cortex with operant training. ***PNAS*** **107: 13900-13905, 2010.**

Duysens J, Orban GA, Cremieux J, and Maes H. Velocity selectivity in the cat visual system. III. Contribution of temporal factors. ***J Neurophysiol*** **54: 1068-1083, 1985a.**

Duysens J, Orban GA, Cremieux J, and Maes H. Visual cortical correlates of visible persistence. ***Vis Res*** **25: 171-178, 1985b.**

Duysens J, Schaafsma SJ, and Orban GA. Cortical Off Response Tuning for Stimulus Duration. ***Vis Res*** **36: 3243-3251, 1996.**

Ehrlich D, Casseday JH, and Covey E. Neural tuning to sound duration in the inferior colliculus of the big brown bat, eptesicus fuscus. ***J Neurophysiol*** **77: 2360-2372, 1997.**

Elhilali M, Fritz JB, Klein DJ, Simon JZ, and Shamma SA. Dynamics of Precise Spike Timing in Primary Auditory Cortex. ***J Neurosci*** **24: 1159-1172, 2004.**

Erway LC, Willott JF, Archer JR, and Harrison DE. Genetics of age-related hearing loss in mice: I. Inbred and F1 hybrid strains. ***Hear Res*** **65: 125-132, 1993.**

Felsheim C, and Ostwald J. Responses to exponential frequency modulations in the rat inferior colliculus. ***Hear Res*** **98: 137-151, 1996.**

Feng AS, Hall JC, and Gooler DM. Neural basis of sound pattern recognition in anurans. ***Prog Neurobiol* 34: 313-329, 1990.**

Fitzgibbons PJ, and Gordon-Salant S. Age effects on discrimination of timing in auditory sequences. ***J Acoust Soc Am* 116: 1126-1134, 2004.**

Fitzgibbons PJ, and Gordon-Salant S. Aging and temporal discrimination in auditory sequences. ***J Acoust Soc Am* 109: 2955-2963, 2001.**

Fitzgibbons PJ, Gordon-Salant S, and Friedman SA. Effects of age and presentation rate on temporal order recognition. ***J Acoust Soc Am* 120: 991-999, 2006.**

Francis HW, Ryugo DK, Gorelikow MJ, Prosen CA, and May BJ. The functional age of hearing loss in a mouse model of presbycusis. II. Neuroanatomical correlates. ***Hear Res* 183: 29-36, 2003.**

Frisina DR, and Frisina RD. Speech recognition in noise and presbycusis: relations to possible neural mechanisms**.** ***Hear Res* 106: 95-104, 1997.**

Fuzessery ZM, and Hall JC. Role of GABA in shaping frequency tuning and creating FM sweep selectivity in the inferior colliculus**.** ***J Neurophysiol* 76: 1059-1073, 1996.**

Fuzessery ZM, and Hall JC. Sound duration selectivity in the pallid bat inferior colliculus. ***Hear Res* 137: 137-154, 1999.**

Fuzessery ZM, Razak KA, and Williams AJ. ***Multiple mechanisms shape selectivity for FM sweep rate and direction in the pallid bat inferior colliculus and auditory cortex*. Heidelberg, ALLEMAGNE: Springer, 2011.**

Fuzessery ZM, Richardson MD, and Coburn MS. Neural mechanisms underlying selectivity for the rate and direction of frequency-modulated sweeps in the inferior colliculus of the pallid bat. ***J Neurophysiol* 96: 1320-1336, 2006.**

Galazyuk AV, and Feng AS. Encoding of sound duration by neurons in the auditory cortex of the little brown bat, Myotis lucifugus. ***J Comp Physiol A Neuroethol Sens Neural Behav Physiol* 180: 301-311, 1997.**

Gates GA, and Mills JH. Presbycusis. ***The Lancet* 366: 1111 - 1120, 2005.**

Gittelman JX, and Li N. FM velocity selectivity in the inferior colliculus is inherited from velocity-selective inputs and enhanced by spike threshold. ***J Neurophysiol* 106: 2399-2414, 2011.**

Gittelman JX, and Pollak GD. It's about time: how input timing is used and not used to create emergent properties in the auditory system. ***The Journal of Neuroscience*** **31: 2576-2583, 2011.**

Godey B, Atencio CA, Bonham BH, Schreiner CE, and Cheung SW. Functional Organization of Squirrel Monkey Primary Auditory Cortex: Responses to Frequency-Modulation Sweeps. ***J Neurophysiol*** **94: 1299-1311, 2005.**

Gooler DM, and Feng AS. Temporal coding in the frog auditory midbrain: the influence of duration and rise-fall time on the processing of complex amplitude-modulated stimuli. ***J Neurophysiol*** **67: 1-22, 1992.**

Gordon-Salant S. Hearing loss and aging: New research findings and clinical implications. ***J Rehab Res Dev*** **42: 9-24, 2005.**

Gordon-Salant S, and Fitzgibbons PJ. Profile of auditory temporal processing in older listeners. ***J Speech Hear Res*** **42: 300-311, 1999.**

Gordon-Salant S, and Fitzgibbons PJ. Sources of age-related recognition difficulty for time-compressed speech. ***Journal of Speech, Language, and Hearing Research*** **44: 709-719, 2001.**

Gordon-Salant S, and Fitzgibbons PJ. Temporal factors and speech recognition performance in young and elderly listeners. ***J Speech Hear Res*** **36: 1276-1286, 1993.**

Gordon-Salant S, Yeni-Komshian GH, Fitzgibbons PJ, and Barrett J. Age-related differences in identification and discrimination of temporal cues in speech segments. ***J Acoust Soc Am*** **119: 2455-2466, 2006.**

Gordon M, and O'Neill WE. Temporal processing across frequency channels by FM selective auditory neurons can account for FM rate selectivity**.** ***Hear Res*** **122: 97-108, 1998.**

Griffiths TD, Rees A, and Green GGR. Disorders of human complex sounds processing. ***Neurocase*** **5: 365-378, 1999.**

Grimsley JMS, Monaghan JJM, and Wenstrup JJ. Development of Social Vocalizations in Mice. ***PLoS ONE*** **6: e17460, 2011.**

Hall DA, Haggard MP, Akeroyd MA, Summerfield AQ, Palmer AR, Elliott MR, and Bowtell RW. Modulation and task effects in auditory processing measured using fMRI. ***Human Brain Mapping*** **10: 107-119, 2000.**

Happel MFK, Jeschke M, and Ohl FW. Spectral Integration in Primary Auditory Cortex Attributable to Temporally Precise Convergence of Thalamocortical and Intracortical Input. ***J Neurosci*** **30: 11114-11127, 2010.**

Harding GW, Bohne BA, and Vos JD. The effect of an age-related hearing loss gene (Ahl) on noise-induced hearing loss and cochlear damage from low-frequency noise. ***Hear Res*** **204: 90-100, 2005.**

Harper NS, and McAlpine D. Optimal neural population coding of an auditory spatial cue. ***Nature*** **430: 682-686, 2004.**

He J, Hashikawa T, Ojima H, and Kinouchi Y. Temporal Integration and Duration Tuning in the Dorsal Zone of Cat Auditory Cortex. ***J Neurosci*** **17: 2615-2625, 1997.**

He N-j, Dubno JR, and Mills JH. Frequency and intensity discrimination measured in a maximum-likelihood procedure from young and aged normal-hearing subjects. ***J Acoust Soc Am*** **103: 553 - 565, 1998.**

He N-j, Mills JH, and Dubno JR. Frequency modulation detection: Effects of age, psychophysical method, and modulation waveform. ***J Acoust Soc Am*** **122: 467-477, 2007.**

He W, Segupta M, Velkoff V, and DeBarros K. 65+ in the United States: 2005. Current Population Reports, Special Studies. **Washington DC: 2005.**

Heil P, Rajan R, and Irvine DR. Sensitivity of neurons in cat primary auditory cortex to tones and frequency-modulated stimuli. I: Effects of variation of stimulus parameters. ***Hear Res*** **63: 108-134, 1992a.**

Heil P, Rajan R, and Irvine DRF. Sensitivity of neurons in cat primary auditory cortex to tones and frequency-modulated stimuli. II: Organization of response properties along the [`]isofrequency' dimension**.** ***Hear Res*** **63: 135-156, 1992b.**

Henry KR, and Chole RA. Genotypic differences in behavioral, physiological and anatomical expressions of age-related hearing loss in the laboratory mouse. ***Audiology*** **19: 369-383, 1980.**

Holmstrom LA, Eeuwes LBM, Roberts PD, and Portfors CV. Efficient Encoding of Vocalizations in the Auditory Midbrain. ***J Neurosci*** **30: 802-819, 2010.**

Hunter KP, and Willott JF. Aging and the auditory brainstem response in mice with severe or minimal presbycusis. ***Hear Res*** **30: 207-218, 1987.**

Ison J, Allen P, and O'Neill W. Age-Related Hearing Loss in C57BL/6J Mice has both Frequency-Specific and Non-Frequency-Specific Components that Produce a Hyperacusis-Like Exaggeration of the Acoustic Startle Reflex. ***JARO* 8: 539-550, 2007.**

Johnson KR, Erway LC, Cook SA, Willott JF, and Zheng QY. A major gene affecting age-related hearing loss in C57BL/6J mice. ***Hear Res* 114: 83-92, 1997.**

Johnson KR, Yu H, Ding D, Jiang H, Gagnon LH, and Salvi RJ. Separate and combined effects of Sod1 and Cdh23 mutations on age-related hearing loss and cochlear pathology in C57BL/6J mice. ***Hear Res* 268: 85-92, 2010.**

Johnson KR, Zheng QY, and Erway LC. A Major Gene Affecting Age-Related Hearing Loss Is Common to at Least Ten Inbred Strains of Mice. ***Genomics* 70: 171-180, 2000.**

Kara P, Reinagel P, and Reid RC. Low Response Variability in Simultaneously Recorded Retinal, Thalamic, and Cortical Neurons. ***Neuron* 27: 635-646, 2000.**

Kaur S, Rose HJ, Lazar R, Liang K, and Metherate R. Spectral integration in primary auditory cortex: Laminar processing of afferent input, in vivo and in vitro. ***Neuroscience* 134: 1033-1045, 2005.**

Kazmierczak P, Sakaguchi H, Tokita J, Wilson-Kubalek EM, Milligan RA, Muller U, and Kachar B. Cadherin 23 and protocadherin 15 interact to form tip-link filaments in sensory hair cells. ***Nature* 449: 87-91, 2007.**

Keithley EM, Canto C, Zheng QY, Fischel-Ghodsian N, and Johnson KR. Age-related hearing loss and the ahl locus in mice**.** ***Hear Res* 188: 21-28, 2004.**

Lee HJ, Wallani T, and Mendelson JR. Temporal processing speed in the inferior colliculus of young and aged rats. ***Hear Res* 174: 64-74, 2002.**

Leigh-Paffenroth ED, and Elangovan S. Temporal Processing in Low-Frequency Channels: Effects of Age and Hearing Loss in Middle-Aged Listeners. ***J Am Acad of Audiol* 22: 393-404, 2011.**

Leventhal AG, Wang Y, Pu M, Zhou Y, and Ma Y. GABA and Its Agonists Improved Visual Cortical Function in Senescent Monkeys. ***Science* 300: 812-815, 2003.**

Li S-C, Lindenberger U, and Sikstrom S. Aging cognition: from neuromodulation to representation. ***Trends in Cognitive Sciences* 5: 479-486, 2001.**

Linden JF, Liu RC, Sahani M, Schreiner CE, and Merzenich MM. Spectrotemporal structure of receptive fields in areas AI and AAF of mouse auditory cortex. ***J Neurophysiol* 90: 2660-2675, 2003.**

Linden JF, and Schreiner CE. Columnar Transformations in Auditory Cortex? A Comparison to Visual and Somatosensory Cortices. ***Cerebral Cortex*** **13: 83-89, 2003.**

Liu RC. Prospective contributions of transgenic mouse models to central auditory research. ***Brain Res*** **1091: 217-223, 2006.**

Liu RC, Miller KD, Merzenich MM, and Schreiner CE. Acoustic variability and distinguishability among mouse ultrasound vocalizations. ***J Acoust Soc Am*** **114: 3412-3422, 2003.**

Lopez-Torres Hidalgo J, Gras CB, Lapeira JT, Verdejo MÃL, del Campo del Campo JM, and Rabadan FE. Functional status of elderly people with hearing loss. ***Arch Gerontol Ger*** **49: 88-92, 2009.**

Mahncke HM, Bronstone A, and Merzenich MM. Brain plasticity and functional losses in the aged: Scientific bases for a novel intervention. ***Progress in Brain Research*** **157: 81-109, 2006a.**

Mahncke HW, Connor BB, Appelman J, Ahsanuddin ON, Hardy JL, Wood RA, Joyce NM, Boniske T, Atkins SM, and Merzenich MM. Memory enhancement in healthy older adults using a brain plasticity-based training program: A randomized, controlled study. ***PNAS*** **103: 12523-12528, 2006b.**

Martin JS, and Jerger JF. Some effects of aging on central auditory processing**.** ***J Rehab Res Dev*** **42: 25-44, 2005.**

Mataga N, Fujishima S, Condie BG, and Hensch TK. Experience-Dependent Plasticity of Mouse Visual Cortex in the Absence of the Neuronal Activity-Dependent Markeregr1/zif268. ***J Neurosci*** **21: 9724-9732, 2001.**

McMullen NT, and de Venecia RK. Thalamocortical patches in auditory neocortex. ***Brain Res*** **620: 317-322, 1993.**

Mendelson JR, and Cynader MS. Sensitivity of cat primary auditory cortex (Al) neurons to the direction and rate of frequency modulation. ***Brain Research*** **327: 331-335, 1985.**

Mendelson JR, and Lui B. The effects of aging in the medial geniculate nucleus: a comparison with the inferior colliculus and auditory cortex. ***Hearing Research*** **191: 21-33, 2004.**

Mendelson JR, and Ricketts C. Age-related temporal processing speed deterioration in auditory cortex. ***Hear Res*** **158: 84-94, 2001.**

Mendelson JR, Schreiner CE, Sutter ML, and Grasse KL. Functional topography of cat primary auditory cortex: responses to frequency-modulated sweeps. ***Exp Brain Res*** **94: 65-87, 1993.**

Merzenich MM, Jenkins WM, Johnston P, Schreiner C, Miller SL, and Tallal P. Temporal Processing Deficits of Language-Learning Impaired Children Ameliorated by Training. ***Science*** **271: 77-81, 1996.**

Michalon A, Sidorov M, Ballard TheresaÂ M, Ozmen L, Spooren W, Wettstein JosephÂ G, Jaeschke G, Bear MarkÂ F, and Lindemann L. Chronic Pharmacological mGlu5 Inhibition Corrects Fragile X in Adult Mice. ***Neuron*** **74: 49-56, 2012.**

Middlebrooks JC, and Zook JM. Intrinsic organization of the cat's medial geniculate body identified by projections to binaural response-specific bands in the primary auditory cortex. ***J Neurosci*** **3: 203-224, 1983.**

Mikaelian DO. Development and degeneration of hearing in the C57/b16 mouse: relation of electrophysiologic responses from the round window and cochlear nucleus to cochlear anatomy and behavioral responses. ***Laryngoscope*** **89: 1-15, 1979.**

Miller LM, Escabi MA, Read HL, Schreiner CE Functional convergence of response properties in the auditory thalamocortical system. **Neuron 32: 151–160, 2001.**

Mittmann DH, and Wenstrup JJ. Combination-sensitive neurons in the inferior colliculus. ***Hear Res*** **90: 185-191, 1995.**

Moore BCJ, Glasberg BR, and Hopkins K. Frequency discrimination of complex tones by hearing-impaired subjects: Evidence for loss of ability to use temporal fine structure. ***Hear Res*** **222: 16-27, 2006.**

Morishita H, Miwa JM, Heintz N, and Hensch TK. Lynx1, a Cholinergic Brake, Limits Plasticity in Adult Visual Cortex. ***Science*** **1238: 1-4, 2010.**

Nelken I, Fishbach A, Las L, Ulanovsky N, and Farkas D. Primary auditory cortex of cats: feature detection or something else? ***Biol Cybernetics*** **89: 397-406, 2003.**

Nelken I, and Versnel H. Responses to linear and logarithmic frequency-modulated sweeps in ferret primary auditory cortex. ***Eur J Neurosci*** **12: 549-562, 2000.**

Noben-Trauth K, Zheng QY, and Johnson KR. Association of cadherin 23 with polygenic inheritance and genetic modification of sensorineural hearing loss. ***Nat Genet*** **35: 21-23, 2003.**

O'Connor DH, Huber D, and Svoboda K. Reverse engineering the mouse brain. ***Nature*** **461: 923-929, 2009.**

O'Neill WE, Zettel ML, Whittemore KR, and Frisina RD. Calbindin D-28k immunoreactivity in the medial nucleus of the trapezoid body declines with age in C57BL/6, but not CBA/CaJ, mice. ***Hear Res*** **112: 158-166, 1997.**

Ouda L, Druga R, and Syka J. Changes in parvalbumin immunoreactivity with aging in the central auditory system of the rat. ***Experimental Gerontology*** **43: 782-789, 2008.**

Patel HH, and Sillito AM. Inhibition and velocity tuning in the cat visual cortex ***J Physiol*** **284: 113P - 114P, 1978.**

Pearl R. ***The Rate of Living, Being an Account of Some Experimental Studies on the Biology of Life Duration.*** **New York: Alfred A. Knopf, 1928.**

Phillips DP, and Sark SA. Separate mechanisms control spike numbers and inter-spike intervals in transient responses of cat auditory cortex neurons. ***Hear Res*** **53: 17-27, 1991.**

Poon PWF, Chen X, and Hwang JC. Basic determinants for FM responses in the inferior colliculus of rats. ***Exp Brain Res*** **83: 598-606, 1991.**

Popelar J, Groh D, PelÃ¡novÃ¡ J, Canlon B, and Syka J. Age-related changes in cochlear and brainstem auditory functions in Fischer 344 rats. ***Neurobiology of Aging*** **27: 490-500, 2006.**

Portfors CV. Types and Functions of Ultrasonic Vocalizations in Laboratory Rats **and Mice.** ***J Amer Assoc Lab An Sci*** **46: 28-34, 2007.**

Portfors CV, Roberts PD, and Jonson K. Over-representation of species-specific vocalizations in the awake mouse inferior colliculus. ***Neuroscience*** **162: 486-500, 2009.**

Razak KA, and Fuzessery ZM. Facilitatory Mechanisms Underlying Selectivity for the Direction and Rate of Frequency Modulated Sweeps in the Auditory Cortex. ***J Neurosci*** **28: 9806-9816, 2008.**

Razak KA, and Fuzessery ZM. GABA shapes selectivity for the rate and direction of frequency-modulated sweeps in the auditory cortex. ***J Neurophysiol*** **102: 1366-1378, 2009.**

Razak KA, and Fuzessery ZM. Neural Mechanisms Underlying Selectivity for the Rate and Direction of Frequency-Modulated Sweeps in the Auditory Cortex of the Pallid Bat. ***J Neurophysiol*** **96: 1303-1319, 2006.**

Razak KA, and Pallas SL. Neural Mechanisms of Stimulus Velocity Tuning in the Superior Colliculus. ***Journal of Neurophysiology*** **94: 3573-3589, 2005.**

Ricketts C, Mendelson JR, Anand B, and English R. Responses to time-varying stimuli in rat auditory cortex. ***Hear Res*** **123: 27-30, 1998.**

Ries PW. Prevalence and characteristics of persons with hearing trouble: United States, 1990–91. ***Vital Health Stat*** **10: 1 - 75, 1994.**

Rotschafer SE, Trujillo MS, Dansie LE, Ethell IM, and Razak KA. Minocycline treatment reverses ultrasonic vocalization production deficit in a mouse model of Fragile X Syndrome. ***Brain Res*** **1439: 7-14, 2012.**

Sadagopan S, and Wang X. Contribution of Inhibition to Stimulus Selectivity in Primary Auditory Cortex of Awake Primates. ***J Neurosci*** **30: 7314-7325, 2010.**

Sadagopan S, and Wang X. Nonlinear spectrotemporal interactions underlying selectivity for complex sounds in auditory cortex. ***J Neurosci*** **29: 11192-11202, 2009.**

Salthouse TA. The processing-speed theory of adult age differences in cognition. ***Psych Rev*** **103: 403-428, 1996.**

Schmiedt R. The Physiology of Cochlear Presbycusis. In: ***The Aging Auditory System*****2010.**

Schneider BA, Daneman M, and Pichora-Fuller K. Listening in aging adults: From discourse comprehension to psychoacoustics. ***Canadian Journal of Experimental Psychology*** **56: 139-152, 2002.**

Schuknecht HF. Presbyacusis. In: ***Pathology of the Ear*****. Cambridge, MA: Harvard, University Press, 1974.**

Smith GE, Housen P, Yaffe K, Ruff R, Kennison RF, Mahncke HW, and Zelinski EM. A Cognitive Training Program Based on Principles of Brain Plasticity: Results from the Improvement in Memory with Plasticity-based Adaptive Cognitive Training (IMPACT) Study. ***Journal of the American Geriatrics Society*** **57: 594-603, 2009.**

Spongr VP, Flood DG, Frisina RD, and Salvi RJ. Quantitative measures of hair cell loss in CBA and C57BL/6 mice throughout their life spans. ***J Acoust Soc Am*** **101: 3546-3553, 1997.**

Stevens KN, and Klatt DH. Role of formant transitions in the voiced-voiceless distinction for stops. ***The Journal of the Acoustical Society of America*** **55: 653-659, 1974.**

Stiebler I, Neulist R, Fichtel I, and Ehret G. The auditory cortex of the house mouse: left-right differences, tonotopic organization and quantitative analysis of frequency representation. ***J Comp Physiol A Neuroethol Sens Neural Behav Physiol*** **181: 559-571, 1997.**

Suga N. Analysis of frequency-modulated sounds by auditory neurones of echo-locating bats. ***J Physiol*** **179: 26-53, 1965.**

Sugiyama S, Di Nardo Aa, Aizawa S, Matsuo I, Volovitch M, Prochiantz A, and Hensch TK. Experience-dependent transfer of Otx2 homeoprotein into the visual cortex activates postnatal plasticity. ***Cell*** **134: 508-520, 2008.**

Sutter ML, and Loftus WC. Excitatory and Inhibitory Intensity Tuning in Auditory Cortex: Evidence for Multiple Inhibitory Mechanisms. ***J Neurophysiol*** **90: 2629-2647, 2003.**

Syka J, Suta D, and Popel J. Responses to species-specific vocalizations in the auditory cortex of awake and anesthetized guinea pigs. **Hear Res 206: 177-184, 2005.**

Taberner AM, and Liberman MC. Response properties of single auditory nerve fibers in the mouse. ***J Neurophysiol*** **93: 557-569, 2005.**

Tian B, and Rauschecker JP. Processing of Frequency-Modulated Sounds in the Cat ’s Anterior Auditory Field. ***Surgery*** **71: 1994.**

Tian B, and Rauschecker JP. Processing of frequency-modulated sounds in the lateral auditory belt cortex of the rhesus monkey. ***J Neurophysiol*** **92: 2993-3013, 2004.**

Trujillo M, Measor K, Carrasco MM, and Razak KA. Selectivity for the rate of frequency-modulated sweeps in the mouse auditory cortex. ***J Neurophysiol*** **106: 2825-2837, 2011.**

Trujillo MS, Razak KA, and Carrasco MM. Mechanisms underlying selectivity for the rate of frequency modulated sweeps in the core auditory cortex of the mouse. ***Under Review*** **2012.**

Ulanovsky N, Las L, Farkas D, and Nelken I. Multiple Time Scales of Adaptation in Auditory Cortex Neurons. ***J Neurosci*** **24: 10440-10453, 2004.**

Walton J, Barsz K, and Wilson W. Sensorineural Hearing Loss and Neural Correlates of Temporal Acuity in the Inferior Colliculus of the C57bl/6 Mouse. ***JARO*** **9: 90-101, 2008.**

Walton JP. Timing is everything: Temporal processing deficits in the aged auditory brainstem. ***Hear Res*** **264: 63-69, 2010.**

Walton JP, Frisina RD, and Meierhans LR. Sensorineural hearing loss alters recovery from short-term adaptation in the C57BL/6 mouse. ***Hear Res*** **88: 19-26, 1995.**

Washington SD, and Kanwal JS. DSCF Neurons Within the Primary Auditory Cortex of the Mustached Bat Process Frequency Modulations Present Within Social Calls. ***J Neurophysiol*** **100: 3285-3304, 2008.**

Weinstein BE, and Ventry IM. Hearing Impairment and Social Isolation in the Elderly. ***J Speech Hear Res*** **25: 593-599, 1982.**

Welsh LW, Welsh JJ, and Healy MP. Central presbycusis. ***The Laryngoscope*** **95: 128-136, 1985.**

Willott J, Parham K, and Hunter K. Comparison of the auditory sensitivity of neurons in the cochlear nucleus and inferior colliculus of young and aging C57BL/6J and CBA/J mice. ***Hear Res*** **53: 78-94, 1991.**

Willott JF. Effects of aging, hearing loss, and anatomical location on thresholds of inferior colliculus neurons in C57BL/6 and CBA mice. ***J Neurophysiol*** **56: 391-408, 1986.**

Willott JF, Aitkin LM, and McFadden SL. Plasticity of auditory cortex associated with sensorineural hearing loss in adult C57BL/6J mice. ***J Comp Neurol*** **329: 402-411, 1993.**

Willott JF, Carlson S, and Chen H. Prepulse inhibition of the startle response in mice: Relationship to hearing loss and auditory system plasticity. ***Behav Neurosci*** **108: 703-713, 1994.**

Willott JF, Parham K, and Hunter KP. Comparison of the auditory sensitivity of neurons in the cochlear nucleus and inferior colliculus of young and aging C57BL/6J and CBA/J mice. ***Hear Res*** **53: 78-94, 1991b.**

Wu GK, Arbuckle R, Liu B-h, Tao HW, and Zhang LI. Lateral Sharpening of Cortical Frequency Tuning by Approximately Balanced Inhibition. ***Neuron*** **58: 132-143, 2008.**

Zeng F-G, Nie K, Stickney GS, Kong Y-Y, Vongphoe M, Bhargave A, Wei C, and Cao K. Speech recognition with amplitude and frequency modulations. ***PNAS* 102: 2293-2298, 2005.**

Zhang LI, Tan AYY, Schreiner CE, and Merzenich MM. Topography and synaptic shaping of direction selectivity in primary auditory cortex. ***Nature* 424: 201-205, 2003.**

Zheng QY, Johnson KR, and Erway LC. Assessment of hearing in 80 inbred strains of mice by ABR threshold analyses. ***Hear Res* 130: 94-107, 1999.**

Zurita P, Villa AEP, de Ribaupierre Y, de Ribaupierre F, Rouiller EM (1994) Changes of single unit activity in the cat's auditory thalamus and cortex associated to different anesthetic conditions**. Neurosci Res 19:303–316.**